The Effects of Biomedical Signal Compression in Wireless Ambulatory Healthcare

A thesis presented by

Garreth Higgins

To

The College of Engineering and Informatics

National University of Ireland Galway

Galway, Ireland

In fulfilment of the requirements for the degree of

Doctor of Philosophy

In the subject of

Electrical & Electronic Engineering

Professor in Discipline: Prof. G. Ó Laighin

Supervisors: Dr. E. Jones & Dr. M. Glavin

October 2013

Table of Contents

Declaration of Authorship

I herby declare that the work contained in this thesis is my own except where otherwise indicated, and it has not been submitted by me in pursuance of any other degree.

Signature: _____ Date: _____

Garry Higgins

Acknowledgments

I'd like to start by thanking my supervisors, Dr. Edward Jones and Dr. Martin Glavin, for all their guidance, help and patience. They provided constant advice and motivation to see this doctorate through to the end. I'd also like to thank all the other staff of Electronic Engineering in NUI Galway for their direct and indirect help. Particularly Mary Costello, Martin Burke, Myles Meehan, Dr. Fearghal Morgan and Prof. Gearóid Ó Laighin. Also to all those in Electrical & Electronic Engineering past and present (in Nuns Island and in the New Engineering Building). There are too many to name specifically but my thanks to all those I met and worked with.

I would also like to thank Science Foundation Ireland (SFI) for providing my funding under the Efficient Embedded DSP for Mobile Digital Health (EEDSP) Strategic Research Cluster programme (grant number SRC/07/I1169). My thanks go to all the members of the EEDSP research cluster who I have met and worked with over the course of my research. Specific thanks go to Dr. Stephen Faul, Dr. Robert McEvoy and Dr. Liam Marnane in University College Cork for their invaluable help in EEG based research, and in providing the REACT software. Above all I'd like to thank Dr. Brian McGinley, post-doctoral researcher in the EEDSP research cluster at NUI Galway, for always being willing to provide assistance and steer me in the right direction.

A special thanks to my parents Anne and Tim. Without their unwavering love and support I would not be where I am today. They are always there to do whatever they can. Not forgetting my brother David whose love and support was felt from across whatever distance happens to be separating us at any given time.

Finally, to Eibhlín and Leo. Their love has kept me sane and their patience has seen me through. I could not have achieved this without them.

Abstract

This thesis seeks to contribute to the field of ambulatory healthcare by examining methodologies to minimise the size of bioelectric signals, whilst preserving the quality of the diagnostic information contained within them. It begins by examining two compression algorithms using JPEG2000 and SPIHT based approaches. At low levels of fidelity loss, it was found that these algorithms could compress EEG data up to a Compression Ratio (CR) of 9. This level of fidelity loss was found to have little impact on the diagnostic information in the signals. Higher levels of compression were then tested, employing an automated seizure detection algorithm to analyse the loss in seizure detection levels. It was found that high levels of seizure detection performance were maintained with CRs of up to 90. An alternative approach to SPIHT-based EEG compression is presented whereby the level of quantisation is used to control the level of fidelity loss and SPIHT is employed as an entropy encoder. This approach was found to achieve substantial benefits in compression gains, achieving a CR of 100. It was also observed that this approach preserved the energy envelope of the signal more faithfully than other approaches.

The final portion of this thesis focuses on protecting SPIHT compressed ECG signals from the impact of bit errors. The importance of the location of the error is first examined and it is found that the earlier an error occurs in a signal, the larger the impact on the reconstructed signal. This result is extended to determine the percentage of the compressed bit stream that needs to be protected to preserve signal quality at two operating points: *"good"* and *"very good"*. This was found to correspond to 12.5% and 50% respectively. Finally, a methodology to provide this level of protection at Bit Error Ratios (BERs) of up to 10^{-2} is presented.

List of Figures

List of Tables

List of Appendices

Appendix A: Journal Publications Arising from this Thesis

Garry Higgins, Brian McGinley, Edward Jones, Martin Glavin, "An evaluation on the effects of wavelet coefficient quantisation in transform based EEG compression", *Computers in Biology and Medicine*, 43, pp. 661-669, July 2013.

Garry Higgins, Brian McGinley, Stephen Faul, Robert P. McEvoy, Martin Glavin, William P. Marnane, Edward Jones, "The Effects of Lossy Compression on Diagnostically Relevant Seizure Information in EEG Signals", *IEEE Journal of Biomedical and Health Informatics*, Vol. 17, Issue 1, pp. 121-127, Jan. 2013.

Garry Higgins, Brian McGinley, Noel Walsh, Martin Glavin, Edward Jones, "Lossy Compression of EEG Signals using SPIHT", *Electronics Letters*, Issue Vol. 47, Issue 18, pp 1017-1018, Sept. 2011.

List of Abbreviations

AC	Arithmetic Coder
ACC	American College of Cardiology
ACP	American College of Physicians
ACSC	Ambulatory Care-Sensitive Conditions
AEEG	Ambulatory EEG
AECG	Ambulatory ECG
AHA	American Heart Association
ASIM	American Society of Internal Medicine
AUC	Area Under the ROC Curve
BCH	Bose-Chaudhuri-Hocquenghem cyclical codes
BER	Bit Error Ratio
CAD	Computer Aided Diagnosis
CDF	Cumulative Density Function
CDF9/7	Cohen-Daubechies-Feavueau 9/7 wavelet filter
CR	Compression Ratio
DCT	Discrete Cosine Transform
DSP	Digital Signal Processing
DWT	Discrete Wavelet Transform
ECG	Electrocardiography
EEG	Electroencephalography
EZW	Embedded Zero-tree Wavelet
FEC	Forward Error Correction codes
FN	False Negative
FP	False Positive
HF	High Frequency
HRV	Heart Rate Variability

LE	Low Energy
LIS	List of Insignificant Sets
LIP	List of Insignificant Points
LSB	Least Significant Bit
LSP	List of Significant Points
LSS	Least Significant Section
MAC	Media Access Control
MATLAB	MATrix LABoratory
MLT	Modulated Lapped Transform
MSB	Most Significant Bit
MSS	Most Significant Section
PDF	Probability Distribution Function
PRD	Percentage Root mean squared Distortion
PRD1	Means adjusted PRD
PSD	Power Spectral Density
REACT	Real-time EEG Analysis for event deteCTion
RMS	Root Mean Square
ROC	Receiver Operating Characteristic
RR	Interval between successive R complexes of ECG signals
RS	Reed Solomon
SDNN	Standard Deviation between all NN intervals of ECG signals
SPIHT	Set Partitioning in Hierarchical Trees
SVM	Support Vector Machine
TN	True Negative
TP	True Positive
NN	Normalised intervals between adjacent QRS complexes

WLAN	Wireless Local Area Network
WT	Wavelet Transform

List of Mathematical Notation

$\mathbf{L^2}(\mathbb{R})$	The space of measurable, square-integral functions $f(x)$
$\mathbb{R}$	The set of real numbers
$\langle .,. \rangle$	Inner product
z^*	The complex conjugate of z
$\{a, b\}$	Set containing a and b
$P(a)$	The probability of a occurring
$[a, b)$	Right open interval, greater than or equal to a but less than b
$\|.\|$	Euclidean or l^2 norm
$P(X \leq x)$	The probability that X is less than or equal to x
$\lfloor x \rfloor$	Largest integer number not greater than x
$\|x\|$	Absolute value of x

Chapter 1 Introduction

1.1 Motivation

"Ambulatory healthcare" is generally defined as care delivered on an outpatient basis; that is, where the patient is required to stay in hospital for less than one calendar day. It is the primary method of healthcare service availed of by much of the population in developed countries, such as the United States of America [1]. Increasing levels of lifestyle-style related diseases and the need for long-term monitoring of chronic disorders creates an increased need for ambulatory healthcare monitoring devices [2]. Access to ambulatory care can be seen to reduce hospital and emergency room admissions for a wide number of medical disorders [3]. Reduction of hospital admission for non-essential reasons has been identified as a key objective to reduce cost and minimise disruption to elective healthcare [4]. One effective method of doing this is to reduce the number of admissions for Ambulatory Care-Sensitive Conditions (ACSCs), defined as conditions that should not require hospital admission with sufficient application of preventative and primary care. A recent survey suggests that emergency admissions for ACSCs costs the National Health Service in the UK stg£1.42 billion annually [5]. Affordance of appropriate primary care can greatly reduce this expenditure. Effective ambulatory and telemedical

monitoring of patients can improve the quality of care of patients with long-term illness and ACSCs [6], [7]. True wearable ambulatory monitoring devices present an effective means of providing healthcare to patients in a timely manner, while minimising the time they are required to spend in an in-patient facility. In the case of this research, the term "ambulatory" is used to refer to healthcare systems that employ a wearable device, allowing at-home or remote monitoring of a patient, to aid in the diagnosis of medical conditions.

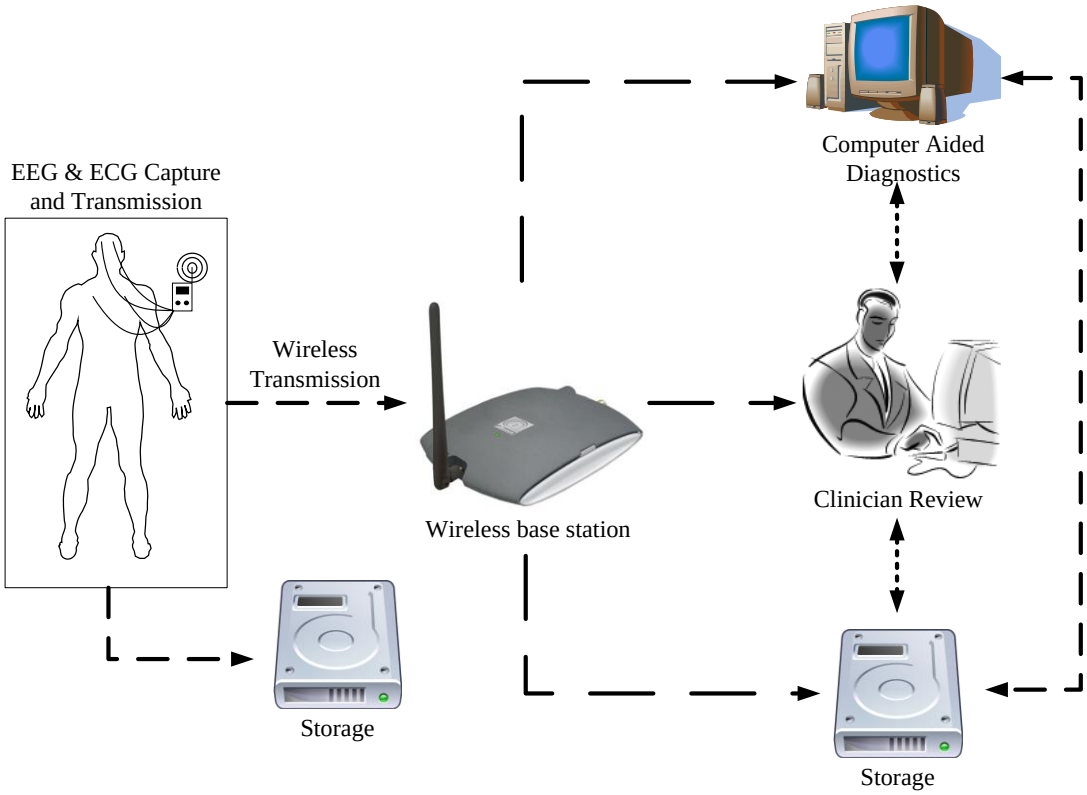

Figure 1.1: Diagram of typical setup for ambulatory biomedical signal capture.

This research was primarily motivated by the design of an ambulatory healthcare monitoring device to remotely monitor a variety of medical conditions. The work described in this thesis was carried out as part of a larger multi-institutional project relating to the development of low-power DSP technologies for wearable healthcare devices. This thesis focuses on the compression of biomedical signals, while maintaining diagnostic integrity. Specifically, it looks at first maximising signal compression while maintaining diagnostic information and secondly, protecting the compressed signals from the damaging effects of bit errors.

Figure 1.1 shows a diagram of a proposed ambulatory biomedical signal capture system based around the concept of wireless transmission to a remote base station. In this architecture, the signals are captured on-board the wearable device. These signals are compressed using one of the algorithms used in this research. Error protection is added to the compressed data using the research presented in the latter portion of this thesis. From here, the data can either be stored for future review, or wirelessly transmitted for off-site processing. Off-site processing allows for a number of uses for the captured data: Computer Aided Diagnosis (CAD) uses software algorithms to automatically process the captured data, clinicians can review or monitor the data as it arrives, or the data can be stored for future review. Several or all of these outcomes may occur together. For instance, CAD is rarely relied on completely for diagnosis and so is used to aid clinicians in analysis. Similarly, it may be used to trigger alerts for suspected events of interest (e.g. seizure events) which can be passed immediately to a clinician for analysis. Finally, all received data are likely to be stored for future review.

This thesis investigates methods for compressing biomedical signals for use on an ambulatory monitoring device. The objective is to maximise compression gains while preserving the integrity of the signal's diagnostic information from the effects of 1) fidelity loss due to increased compression, and 2) random bit errors on the compressed bit stream during wireless transmission. Two biomedical signal types are considered: electroencephalogram (EEG) and electrocardiogram (ECG). EEG data capture in particular generates large amounts of data [8]. Wireless communication is suitable for ambulatory system design as it allows better device mobility and remote monitoring; however, wireless transmission is a large consumer of device power [9], [10]. Minimising the amount of time that wireless transmission is active can greatly improve the duration of the battery life. Similarly, despite the cost per-Megabyte for data storage steadily declining over time [11], it can still be a significant factor in mobile system design. Data compression offers a means of reducing the size in bits of the biomedical signal.

Data compression can be divided into two types: lossless and lossy. Lossless compression allows the data to be compressed and decompressed with no loss in signal information. Lossy compression allows some loss in signal information by representing the original coefficients in a reduced form. Decompression is required at the receiver in order to reconstruct the original signal for display or diagnostic

purposes. While lossless compression ensures faithful reconstruction of the original signal, the requirement to represent all data coefficients in compressed form limits the compression gains that can be achieved. Lossy compression allows for far greater levels of compression at the expense of some loss in fidelity. If the level of loss is carefully selected, compression gains can be maximised without impacting on the important information in the data.

During transmission, bit errors can result in any given bit of the compressed data being inverted. This can result in an unpredictable impact on the signal when the stream is reconstructed. At best, this error may have no discernable impact on the signal, at worst it could result in complete signal corruption, which may in turn result in misdiagnosis. Error correction codes offer a means to protect against bit errors. The encoder adds redundant information to the data stream to protect against a specified number of errors.

The initial part of this thesis focuses on attempting to maximise the compression of EEG signals, while maintaining diagnostic information relevant to seizure events. The JPEG2000 [12] and SPIHT [13] image compression algorithms were identified as suitable algorithms due to their good compression abilities and the fact that it is possible to implement them on low-powered devices [14], [15]. Epilepsy and seizure events were chosen due to the possible improvement to care ambulatory monitoring might offer [16]. Classification of the effects of compression on these events was identified as an area that needed attention. Several approaches to handling this problem are presented. Analysis of the potential power savings of using data compression is also performed.

After a signal has undergone compression, the importance of the remaining bits to the signal's structure increases. That is to say, there is an increased likelihood of a bit error having a more significant impact on the signal than if a bit error occurred in an uncompressed signal. An analysis on the effects of bit errors on compressed biomedical signals and proposing methods to protect against them is presented. ECG signals were used for this portion of the research. The signals are first encoded with SPIHT compression due to its good compression ability and bit-ordering properties. Before a protection scheme could be designed, the effects of the location of the bit error first had to be examined. Using this knowledge, it is possible to target key portions of the compressed bit stream that are needed to maintain diagnostic integrity. A methodology to protect these key bit stream portions was developed with

Reed-Solomon codes. This allows for integrity preservation without undue overhead in the compressed bit-steam.

1.2 Contributions and Publications

1.2.1 Contributions

The primary contributions of this thesis can be summarised as:

1. Analysis and comparison of two compression algorithms suitable for an ambulatory EEG device.
2. Determining the maximum level of signal fidelity loss for EEG compression using JPEG2000 and SPIHT in order to maintain diagnostic information for seizure events.
3. Analysis of computational and energy requirements for embedded implementation of compression, and quantification of potential energy savings in an ambulatory device.
4. Examining the benefits of lowering the quantisation level in transform based compression of EEG signals.
5. Classifying the impact of bit errors in relation to their location in the bit stream of SPIHT-compressed ECG signals, and determining the proportions of the bit stream that needs to be protected from errors to preserve a range of diagnostic measurements for SPIHT-compressed ECG.
6. Proposal of a methodology to design RS codes to achieve these levels of protection and testing their functionality with selected performance targets.

1.2.2 Journal Publications

The publications that have resulted from this research are as follows:

Published

- Garry Higgins, Brian McGinley, Edward Jones, Martin Glavin, "An evaluation on the effects of wavelet coefficient quantisation in transform based EEG compression", *Computers in Biology and Medicine*, 43, pp. 661-669, 2013.
- Garry Higgins, Brian McGinley, Stephen Faul, Robert P. McEvoy, Martin Glavin, William P. Marnane, Edward Jones, "The Effects of Lossy Compression on Diagnostically Relevant Seizure Information in EEG

Signals", *IEEE Journal of Biomedical and Health Informatics*, Vol. 17, Issue 1, pp. 121-127, 2013

- Garry Higgins, Brian McGinley, Noel Walsh, Martin Glavin, Edward Jones, "Lossy Compression of EEG Signals using SPIHT", *Electronics Letters*, Issue Vol. 47, Issue 18, pp 1017-1018, 2011,
- Brian McGinley, Martin O'Halloran, Raquel Conceicao, Garry Higgins, Edward Jones, Martin Glavin, "The Effects of Compression on Ultra Wideband Radar Signals", *Progress in Electromagnetics Research*, Vol. 117, pp. 51-65, 2011

Under Review/In Preparation

- Garry Higgins, Brian McGinley, Martin Glavin, Edward Jones, "The Effects of Bit Errors on Compressed ECG Signals in Mobile Healthcare", Submitted to *IEEE Signal Processing Letters*, July 2013
- Richard Mc Sweeney, Brian McGinley, Stephen Faul, Garry Higgins, Martin Glavin, Edward Jones, William Marnane, Emanuel Popovici, "Context Aware Adaptive EEG Data Compression".

1.2.3 Conference Papers

Published

- Garry Higgins, Stephen Faul, Robert P. McEvoy, Brian McGinley, Martin Glavin, William P. Marnane, Edward Jones, "EEG Compression Using JPEG2000: How Much Loss Is Too Much?", *32nd Annual International Conference of the IEEE EMBS*, Buenos Aires, Argentina, August 31 - September 4, 2010
- Garry Higgins, Brian McGinley, Edward Jones and Martin Glavin, "Efficient EEG Compression using JPEG2000 with Coefficient Thresholding" *IET Irish Signals and Systems Conference (ISSC 2010)*, 23-24 June, 2010
- Garry Higgins, Brian McGinley, Martin Glavin, Edward Jones, "Low Power Compression of EEG Signals Using JPEG2000", *2010 4th International Conference on Pervasive Computing Technology for Healthcare (PervasiveHealth)*, 22-25 March, 2010

1.3 Thesis Structure

The remainder of this thesis is structured as follows.

Chapter 2 - Background Information and Relevant Literature

This chapter provides background on the biomedical signals considered in this research as well as their diagnostic use. It also examines previous research into ambulatory biomedical signal monitoring devices, as well as justification and methodologies for signal compression on these devices. The compression algorithms used within this research and alternative approaches used in similar research are also briefly discussed. Background and discussion of the error-protection scheme employed in this thesis is presented.

Chapter 3 – EEG Compression Methodology

This chapter outlines the detailed operation of the compression algorithms used in the course of this research. Secondly, the common performance metrics used in this thesis are discussed. Finally, the primary EEG database used for testing is presented, with justification for its selection.

Chapter 4 - Compression of EEG Signals

This chapter presents the methodology used for compressing EEG signals with the JPEG2000 and SPIHT algorithm. The intial part of this chapter focusses on examining the compression performance at low signal distortion levels, in order to preserve signal fidelity for visual display, and verifies that diagnostic integrity is maintained using a seizure detection algorithm. Next, the chapter considers the possibility of increasing compression levels by allowing higher levels of signal distortion. An automated seizure detection algortihm is employed to determine the maximum acceptable level of loss, and thus the maximum achievable compression level. Finally, an analysis is performed on the potential benefits of implementing compression in a wireless AEEG system. The computational cost of compression in hardware and the potential power savings from compressing the data prior to transmission is analysed and presented.

Chapter 5- The Effects of Wavelet Coefficient Quantisation in EEG Compression

An alternative approach to SPIHT based EEG compression is examined in this chapter. EEG data are compressed by reducing the bit level available to the quantisation block, employing SPIHT as an entropy encoder. The resulting signals are evaluated for compression gains and levels of fidelity loss in comparison to the original signals. These results are directly compared to the results of compressing the same signals with the standard SPIHT approach of bit stream truncation.

Chapter 6 - ECG Compression with SPIHT in the Presence of Bit Errors

This chapter seeks to examine the impact of bit errors on compressed signals. In this case, compression and transmission of ECG data are considered. Performance metrics for evaluating the impact of lossy compression on ECG data are examined and the ECG database used for testing is introduced. The importance of the location of the error within the compressed stream is first investigated. The impact of bit errors is then examined at compression levels ranging from low to high.

Chapter 7 - Preservation of Quality in SPIHT-Compressed ECG Signals in the Presence of Bit Errors

The results of the previous chapter are built-on to present a methodology on how to protect SPIHT-compressed ECG data from random bit errors. Properties of SPIHT compression are exploited to minimise the amount of data needing to be protected, thus reducing the overhead required from the error protection scheme. Increased levels of compression are evaluated to determine the impact on diagnostic information, and to preserve the research goal of minimising the size of the data to be transmitted.

Chapter 8 - Conclusions

This final chapter revisits the work presented throughout this thesis and summarises the main results and conclusions reached. It concludes by listing the main contributions this thesis has made and outlines some potential future work that could build upon them.

Chapter 2 Background Information and Relevant Literature

2.1 Introduction

This chapter outlines the relevant background underlying the research described in this thesis. Firstly, a brief explanation of the different bioelectric signals used in the work is given. A background on epilepsy and the use of EEG data to aid in diagnosis is presented. Next, this chapter examines mobile healthcare systems as used for ECG and EEG based diagnostic purposes. Information on the use of computer aided diagnosis is provided, as well as the benefits of wireless transmission and advantages to using mobile devices for ambulatory monitoring in general. This chapter also looks at the general compression of biomedical signals and specifically at the algorithms used during this research. Finally, it deals with the protection of compressed biomedical signals from bit errors, dealing specifically with the error protection scheme used in this research.

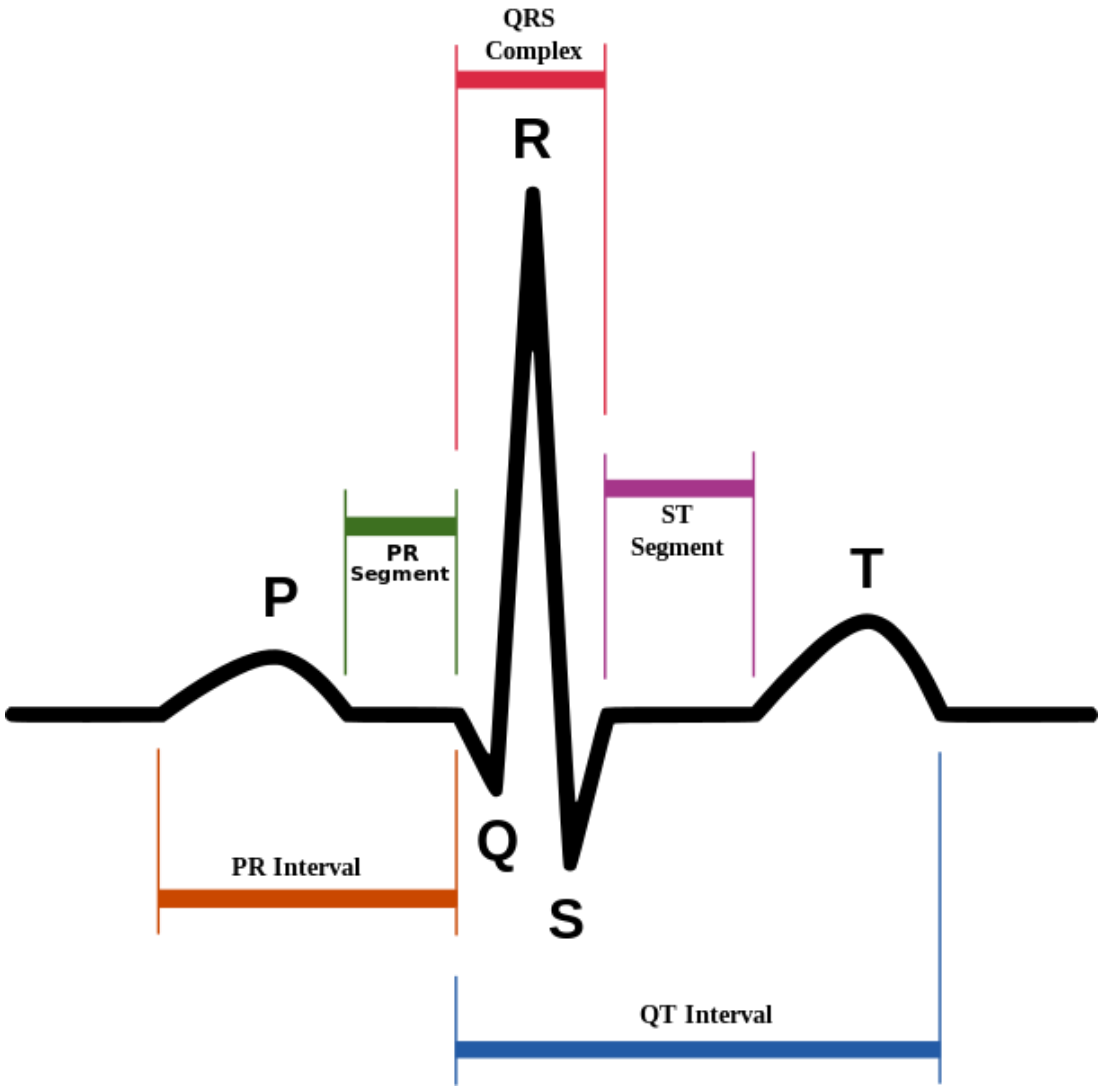

Figure 2.1: Normal ECG sinus rhythm.

2.2 Diagnostic Use of Bioelectric Signals

The ability to monitor non-invasively the operation of organs inside the human body by measuring their bioelectric output was first discovered at the end of the 19th century [17], when it was found that electrodes placed on the skin could produce a graphical representation of the activity of internal organs, such as the heart or brain. Analysis of these signals aid clinicians in diagnoses of a variety of conditions that could otherwise prove problematic. This section discusses two such signals that form the basis of the applications considered in this thesis:

- Electrocardiogram (ECG)
- Electroencephalogram (EEG)

2.2.1 ECG

Electrocardiography describes the electrical activity of the heart. It is recorded by placing electrodes on the surface of the body [17]. The voltage variations between electrodes produces a waveform whose morphology and timing conveys information on the physical activity of the heart at any given time. By monitoring these waveforms, clinicians are able to diagnose a range of cardiac related conditions such as arrhythmias, ischemias and myocardial infarction that may otherwise prove problematic [17]. Figure 2.1 shows the QRS complex for a normal sinus rhythm of ECG data. The various waveform components reflect the activity of the heart at each point in time. The P wave reflects right and left atrial depolarization, the QRS complex reflects depolarization of the right and left ventricles and the T wave reflects ventricular repolarization. Variation from this normal sinus rhythm is called arrhythmia. Arrhythmias are problematic as they are indicative of improper firing of the pacemaker cells of the heart, which is in turn indicative of underlying cardiac abnormalities.

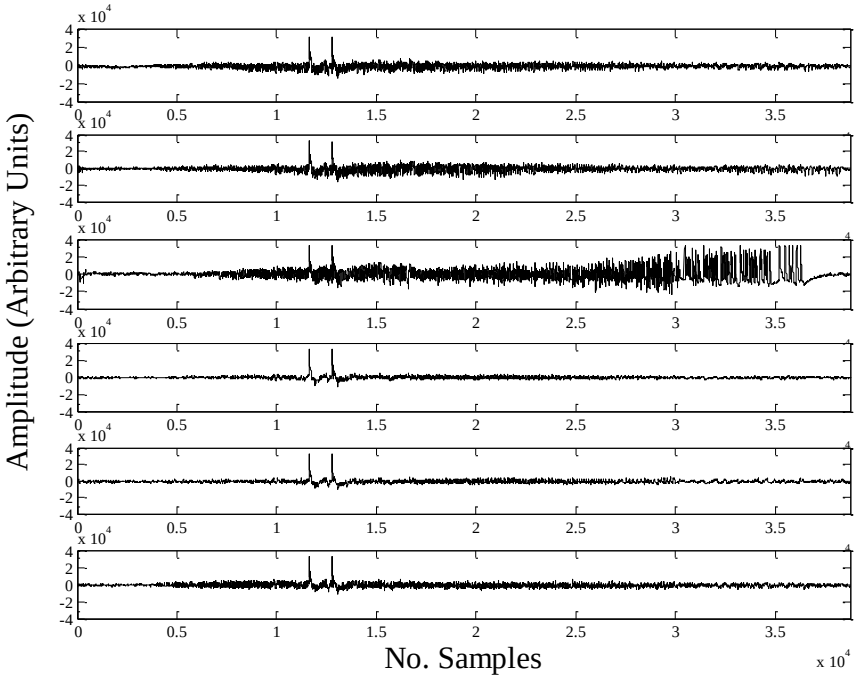

Figure 2.2: 6-Channel EEG data with seizure event sampled at 256Hz.

2.2.2 EEG

Electroencephalography (EEG) is the recording of the electrical activity of the brain. It provides an important clinical tool for analysing the operation of the brain, providing a method for real-time monitoring of neural activity. EEG is used to aid in the diagnosis of a variety of diseases such as epilepsy, sleep disorders and dementia [17]–[19]. Unlike ECG waveforms, EEG does not follow a clear, easily distinguished, repetitive waveform. The diversity of rhythms it can produce is wide, depending on not just neurological conditions, but also the current mental state of the patient [17]. EEG itself measures the electrical field caused by the firing of millions of neurons. It is usually measured on the scalp, but intracranial recording also occurs in some cases where prolonged inpatient monitoring is required. Figure 2.2 shows a sample plot of multi-channel EEG rhythm containing a seizure event, recorded intracranially. While there are many applications for EEG monitoring, this research focuses on the use of EEG to aid in the diagnosis of epilepsy.

Epilepsy is a neurological condition that affects approximately 1% of the population, but is difficult to diagnose [20], [21]. The gold-standard diagnosis requires long-term EEG and video monitoring (video EEG) in an attempt to capture a seizure on both video and EEG telemetry [19]. Epileptiform activity shows on EEG recordings as a sudden change in spectral content, often with a rhythmic, spiky waveform. These periods are known as ictal EEG. The occurrence of these events can vary greatly from individual to individual. Some individuals may experience only a few over the course of their lifetime, whereas extreme cases may experience numerous seizures daily. The duration of the event can also vary greatly, from a few seconds to a few minutes [17].

2.3 Mobile Healthcare and Computer Aided Diagnosis

In 1947 a self-contained ECG monitoring device was developed by Norman Jeff Holter, with practical ambulatory implementations being produced a few years later [22], [23]. The use of these devices for ambulatory ECG (AECG) monitoring became so ubiquitous that the term "Holter Monitor" is synonymous with all AECG monitors, and often ambulatory monitors for other bioelectric signals. Ambulatory monitoring of ECG signals has become commonplace in the diagnosis of a multitude of cardiac related conditions [24], [25]. In 1999 a joint task force between the

American College of Cardiology (ACC) and American Heart Association (AHA) published AECG guidelines to ensure proper usage [26].

Recent years have seen an increased interest in AEEG. EEG proved more problematic to record than ECG due to need for signal amplification and multi-channel recording [19]. A practical AEEG device was presented by Ives and Woods in 1975 in [27]. Due to technological constraints, this was limited to 4 channels and was cumbersome to wear. As technology advanced, practical implementation of 32-channel ambulatory devices was possible by the 1990s. The use of AEEG to aid in the diagnosis of epilepsy has long been noted. Gotman reports on the benefits of its use in [28]. In [29], a retrospective study found AEEG clinically useful in 75% of cases. It is also shown to be useful in documenting seizures that were not recognized by patients [30].

Computer Aided Diagnosis (CAD) involves the use of computers to aid in the interpretation of biomedical signals or images. CAD systems are generally employed to assist doctors in situations where large amounts of data are being monitored from one or more sources. The CAD system can highlight suspected areas of interest for review by medical professionals. In [31], the author provides a review of CAD systems for use in medical imaging and potential future avenues of research. This paper identifies the use of CAD systems as being complementary to the physician, providing a "second opinion" on diagnostic interpretation. An analysis of CAD based publications in the five years prior to this publication identified the chest, breast and colon as the primary areas of research, but found other organs such as brain, skeletal and vascular systems also of interest.

While CAD systems initially focussed on cardiovascular diseases, lung cancer and breast cancer ([31]), the benefits of its use in other areas of medicine should also be apparent. AEEG monitoring is often combined with CAD systems, particularly in cases of seizure activity or suspected epilepsy. In [32], Liporace *et al.* compared the use of CAD analysis of 24hr AEEG data from epilepsy patients to the more traditional approach of sleep-deprived EEG, for the purpose of seizure detection. They concluded that CAD based analysis offered significant advantages, including detection of seizure events not noticed by the patient. The authors conclude by advocating the use of CAD systems with AEEG devices, to improve clinical information due to increased seizure detection. An analysis of AEEG devices

coupled with CAD is performed by Waterhouse in [19]. The author foresees the benefits of so called "closed loop systems" which combine AEEG and CAD systems on a mobile device to both monitor and anticipate seizure events. Another review of benefits of AEEG devices is presented in [33]. In it the authors analyse the benefits of using AEEG in clinical practice. The advantage of combining AEEG devices with CAD based analysis is noted in several papers. One such paper analyses the use of long-term AEEG monitoring in children [34]. This system employed CAD based analysis to monitor children and adolescents with known or suspected epilepsy. The authors conclude that AEEG systems with CAD analysis provides an additional benefit for the diagnosis of epileptic and non-epileptic events. In a recent paper by Acharya *et al.,* the authors present a review of CAD approaches for analysis of epilepsy in EEG data [35]. They identify the difficulties in a fully automated CAD based epilepsy detection system and review previous approaches to seizure detection and classification. It is concluded that accuracies of more than 99% have been achieved by such systems.

2.3.1 Wireless transmission

The use of wireless transmission is of benefit to ambulatory monitoring devices. Wire-free operation improves user comfort and wear-ability. It also allows immediate transmission of data to a clinician or base-station, which may provide automated analysis of the signals. In [16], Casson *et al.* report that wireless transmission on AEEG devices is preferable to a wired system. The benefits they list include comfort to user and real-time access to the data. The latter is important both in providing real-time monitoring and the ability to check signal quality remotely. This is advantageous as any errors in the recording process can be identified immediately and addressed. In [10], Yates *et al.* analyse the power trade-off in the design of wireless EEG headsets. They suggest that wireless architectures are key to the design of longer term monitoring with AEEG devices. Martin *et al.* examined the issues involved in wearable ECG monitoring devices in [9]. They state that wireless medical sensors are the ultimate goal in order to provide "continuous real-time feedback and monitoring of a user's condition". While their work focused on ECG monitoring, they also identify EEG monitoring as a future goal.

2.3.2 Benefits and Approaches to Ambulatory Monitoring

As previously mentioned, the advantages of AECG devices have long been perceived and leveraged for diagnostic purposes. More recent times have seen increased interest in AEEG devices as the benefits of its use become more apparent. While video EEG is the gold-standard for epilepsy diagnosis, there is still a chance that no epileptiform activity will be experienced within the period of evaluation. Although accurate figures for the general population are difficult to determine, one study has shown that for EEGs taken from 308 patients with epilepsy, 18% never exhibited epileptiform discharges over several months of recordings and only 55% displayed discharges during their first examination [36]. It is conceivable therefore, that a patient displaying potential signs of epilepsy may display no seizure activity during a single in-patient monitoring session. Misdiagnosis is also a significant issue due to limitations in the data available to the clinician. Smith *et al.* [37] report that elongating the period of EEG observation would have the effect of reducing the number of false positives, and increasing the detection rate of epileptiform activity. Binnie *et al*. [38] report that long-term monitoring may be required in as many as 5% of people diagnosed with epilepsy, and 13-20% of adult tertiary referrals and up to 40% of child referrals with potential cases of epilepsy. Clearly, in these situations, long-term in-patient monitoring is less than ideal in terms of expense, resource allocation and patient inconvenience. This situation is exacerbated where the availability of trained clinicians with the skills to analyse long term EEG data for seizure activity is limited. Ambulatory monitoring allows for prolonged periods of monitoring without the costs generally associated with it.

Casson and Rodriguez-Villegas have provided a number of research papers on the benefits of AEEG and on possible methods of implementation. In [16] they present feedback from medical professionals on the possible benefits of AEEG to aid in diagnosis. They identify epilepsy diagnosis, sleep studies and brain computer interfaces as areas that could benefit from AEEG devices. Within a survey conducted with 17 neurologists in the UK, 88% said they thought AEEG recordings would be more common in the future and 76% said it would be a "major improvement" to their practice if AEEG devices were available. In [39] the same authors present research on the feasibility of AEEG monitoring and conclude it is possible to process the data on a wearable device without impacting on performance. They also present a number

of techniques for wirelessly transmitting EEG data from a mobile device in [40]–[42]. These techniques are based on discontinuous transmission of data. On-board seizure detection algorithms detect seizure events and only transmit these events to a receiver.

In [43], Avila *et al.* present an AEEG device using wireless transmission. It includes a compression block to reduce the size of the data to be transmitted, to minimise power consumption. They find that their approach suggests that wireless transmission of EEG data is possible on a low power ambulatory device. Prilutskiy *et al.* examines the transmission of ECG and EEG data wirelessly using a microprocessor and the IEEE 802.15.4 (Zigbee) standards [44]. The system design is presented with a reported 15hr battery life with support for single channel ECG and four channel EEG recording. Kang *et al.* propose a method of wireless ECG monitoring based on a modified MAC layer in the WLAN [45]. The authors report the benefits of remote ECG data monitoring in providing real-time data to medical personnel, with wireless networks being used to transmit the data. They propose their modified MAC layer is necessary to enable real-time monitoring and quality of service guarantees over the IEEE802.11 protocol. Huang and Miaou present research based on transmitting SPIHT-compressed ECG data over a 3G network [46]. They identified the benefits of being able to transmit the data wirelessly for remote monitoring of patient health. The use of the SPIHT compression was proposed to minimise the amount of ECG data to be transmitted. It was argued in [46] that compression is necessary to overcome the bandwidth limitations of wireless transmission for real-time monitoring, in spite of continually improving network speeds. Finally, they report that their proposed system is robust up to bit error ratios (BERs) of 10^{-5}.

2.4 Compression

Data compression is the process of encoding a set of data such that the size of the encoded set is smaller than the size of the original, unencoded data. It exists in all forms of digital communications, where maximising the amount of data that can be transmitted with a limited bandwidth is important. Compression algorithms involve two components; the compression algorithm which is used to create a representation of the data in its reduced form, and the reconstruction (or decompression) algorithm

that is used to convert the compressed signal back to its original form. Data compression can be divided into two types: lossless and lossy [47]. Lossless compression involves no loss of information between the original data set and the one created after the compressed data has been decompressed/reconstructed, i.e. perfect reconstruction. Lossy compression involves some loss of signal information such that the reconstructed data is not exactly equal to that of the original. While lossless compression may seem like the best choice from the perspective of signal fidelity, the compression gains that can be achieved are generally quite limited. Lossy compression on the other hand allows for an inexact reconstruction of the data set. This allows the algorithm to discard elements of the signal it deems unnecessary to preserve the reconstructed data set or represent them in reduced form. The amount of loss allowed is usually application-specific and set by the system designer. Generally speaking, the greater the acceptable levels of loss, the higher the compression gains that can be achieved. This aspect is examined in some depth in Chapter 4 and Chapter 5 of this thesis.

It should be noted that some authors suggest the inclusion of a third class of compression dubbed “near lossless” (e.g. [48]–[50]). This term has been applied to lossy compression techniques that seek to keep the loss of data fidelity to a minimum, such that the reconstructed data may superficially appear identical to the original. This term has not been used in this research however, as the distinction between lossy and “near lossless” is arbitrary, and all “near lossless” compression can be considered as lossy.

Biomedical signal compression techniques can be broadly divided into three categories: 1) Direct Data 2) Transform based compression and 3) Other compression methods [51], [52]. Direct Data methods are generally time domain based approaches that exploit redundancies in signal data to increase compression. Compression efficiency is therefore limited if the signal is not sparse in the time domain, e.g. EEG data. Memon *et al.* present an evaluation of a number of direct data compression techniques in [8]. In it they note that traditional direct data techniques do not work well on EEG signals due to the lack of reoccurring, exact patterns.

Methods in category 3) include compression methods such as non-linear prediction, neural network based compression and subband coding (other than those used in

transform based approaches). Sriraam *et al.* present a number of recent papers on EEG compression using neural networks [48], [53]. In both papers, the authors make use of predictors as part of an approach to give near-lossless compression of EEG data. This is combined with quantisation and entropy encoding schemes to maximise compression gains. In [54], Bazán-Prieto *et al.* present a compression technique based on cosine modulated filter banks, with 7 bit quantisation. They examine the use of their proposed compression algorithm on EEG data at low levels of loss, known *a priori* by the encoder. A similar approach is used for ECG compression in [52]. In this paper, the authors note that despite the similarity between the subband decomposition employed by their algorithm and those frequently employed by transform based compression, it is not in actuality a transform method.

Transform-based compression includes methods that transform the time domain signal into the frequency, or other domain prior to compression. Examples of these transform operations include the Fourier Transform (FT) and Wavelet Transform (WT) which exploit signal sparsity in a particular domain [55], [56]. The research presented here falls into category 2). Specifically, it examines compression of biomedical signals based on wavelet transforms.

The basis for all compression algorithms explored in this research is the Discrete Wavelet Transform (DWT). The work in [57] presents the use of the family of wavelets known as the Cohen-Daubechies-Feavueau (CDF) biorthogonal wavelets. In [57], the coefficients for a selection of biorthogonal wavelets were given. In particular, the biorthogonal wavelet, CDF9/7 (biorthogonal4.4) has been adopted as the mother wavelet of choice for a wide variety of applications. It has often been used in research related to image compression and bioelectric signal compression [58], [59]. The JPEG2000 image compression algorithm uses CDF9/7 as the mother wavelet for lossy image compression in Part 1 of the standard [12].

Since the inception of the DWT and biorthogonal wavelet, there has been a growing increase in their use in signal compression methods, including in biomedical applications. These are often paired with various entropy encoding algorithms, such as SPIHT or arithmetic coding (AC), to maximise compression. Cárdenas-Barrera *et al.* present a wavelet and wavelet packet based EEG compression algorithm in [55]. This paper is of particular interest as it uses a lossy compression scheme and makes a recommendation for an acceptable level of loss based on an application independent

metric. The proposed methodology involves applying a threshold level to the wavelet coefficients, setting all coefficients below this level to zero. The remaining coefficients are quantised and coded using run-length coding. Dehkordi *et al.* present an EEG compression approach based on WT and Embedded Zero-tree Wavelet (EZW) encoding [60]. They seek to exploit the intra-channel redundancy present in EEG signals by using differential encoding to maximise compression. An ECG compression approach is outlined by Manikandan *et al.* in [61]. Their methodology is based on a novel approach to thresholding wavelet coefficients, with Huffman entropy encoding. The CDF9/7 biorthogonal filter is used for the DWT. The authors report that they achieve results slightly better than corresponding SPIHT based compression.

JPEG2000 is a compression algorithm designed for both lossless and lossy compression of image files. It was designed to replace the older JPEG file format with more advanced features, such as superior low bit-rate performance, lossy and lossless compression and good error resilience [62]. Part 1 of the specification contains the core components of the codec and was the first part ratified by the Joint Photographic Experts Group [12]. These core components include the Discrete Wavelet Transform (DWT), quantisation and an Arithmetic Coder (AC).

A pre-processing stage involves partitioning the image into rectangular tiles of equal size. Each of these partitions is then compressed independently with its own compression parameters. This step is specific to image compression and seeks to exploit some properties of the image for the following compression steps.

The DWT replaces the Discrete Cosine Transform (DCT) of the original JPEG format. While DCT performs well at low compression ratios, it deteriorates quickly as compression ratios increases above 30:1. DWT meanwhile, has a much more gradual degradation [58]. The JPEG2000 Part 1 standard includes two types of DWT. As well as the previously mentioned CDF9/7, it also includes the Le Gall 5/3 integer-to-integer DWT. This makes use of integer coefficients for the lifting steps so that there is no loss of information due to the forward and inverse transform. CDF9/7, in contrast, uses floating-point arithmetic in the lifting steps. This causes a slight loss in the values between the forward and inverse transform due to the rounding affect of the floating-point numbers. Analysis of this impact shows it to be negligible.

The adaptive binary Arithmetic Coder (AC) replaces the Huffman coder of JPEG as the entropy coder for JPEG2000. AC is a lossless entropy coder, that can be seen as a generalization of the Huffman coder [63]. The AC can perform near optimal entropy coding on a given data set [64]. The AC operates by representing a message by an interval of real numbers between 0 and 1. Huffman coding, in contrast, uses integer values to represent each symbol in the message. This causes inefficiency problems when the probability of a symbol approaches one [65]. In general, as the sophistication of source models increases, the better the performance of AC in comparison to Huffman coding [66]. The operation of AC is controlled by *states*, where the information from encoding one symbol is brought forward to influence the next [67].

A large number of variations on the internal operation of the AC have been proposed. Although first proposed in the 1960's [68], it was not initially possible to implement at that time as the arithmetic accuracy needed for the AC increases with the length of the message, hence limitations in processing power of computers at the time precluded effective implementation. The first obstacle was overcome in [69] when it was observed that coding could be carried out using finite precision arithmetic. While this work proved it was possible, the algorithm was still not efficient enough for real-world operation. In 1979, both Rissanen [70] and Langdon [71] proposed a more efficient coder for binary sequences. Moffat *et al.* presented an improved algorithm in [72] seeking to improve efficiency and support large alphabet sizes.

Some prior research on the use of JPEG2000 in compression of bioelectric signals also exists. In [73], Bilgin *et al.* applied JPEG2000 compression to ECG signals, using a normalised matrix of ECG periods, to allow two-dimensional (2D) compression of the signals. By aligning intra-beat periods of successive waveforms, they sought to maximise the redundancy present in the matrix, to allow for greater compression gains. They found JPEG2000 compared favourably to other algorithms, but misdetection of ECG periods could result in inefficiencies. In [74], JPEG2000 is used in lossless mode by Srinivasan *et al.* to compress EEG signals. It is one of three algorithms used to losslessly compress in EEG signals in one and two dimensions. This work also used AC independently as a compression algorithm. The results

suggest that DWT prior to AC enables the AC to achieve more efficient compression.

Set Partitioning In Hierarchical Trees (SPIHT) is an image compression algorithm first proposed by Said and Pearlman in [13]. Although initially designed for image compression, it has since been applied to a range of signal compression applications with good results [75]–[77]. The core principles of SPIHT are a generalization of the Embedded Zerotree Wavelet (EZW) coder proposed by Shapiro in [78]. Both algorithms are based on the concept of compression by grouping samples of smaller size and encoding them at a lower bit rate. Compression is achieved when the information to encode the group's location, size and threshold is smaller than the number of bits required to preserve the unencoded data [79]. Naturally occurring data sets rarely contain samples of smaller size in grouped locations, thus the bits required to preserve location information exceed the savings made by encoding these smaller samples at a lower bit rate. It is for this reason that SPIHT is often paired with the WT (as outlined in [13]), where wavelet coefficients in different subbands have a temporal relationship with each other. If the sizes of the subbands differ, a single coefficient in the smaller subband may represent the same spatial location as multiple coefficients in the other subbands, thus creating the potential for large compression gains. SPIHT achieves high compression gains by keeping insignificant coefficients in large subsets.

The authors of [77] proposed using SPIHT with a Modulated Lapped Transform (MLT) to give a scalable audio encoder. This allowed the encoded audio to scale from lossless to any level of lossy compression to accommodate bandwidth requirements. SPIHT has also been used for compression of bioelectric signals, which is of interest in this thesis. Compression of ECG signals using the standard SPIHT algorithm has yielded impressive results [80], [81]. Other authors have sought to improve on these results by incorporating two-dimensional compression to exploit ECG's periodicity [82]–[84]. All three of these papers incorporate a beat detection algorithm as a pre-processing step to create and align a two dimensional array of successive beats. A DWT operation is then applied to maximise correlation and improve compression performance. The robustness of SPIHT to transmission over wireless interfaces has also been examined. In [46] Huang and Miaou examine transmission of SPIHT-compressed ECG signals over a 3G-based wireless testbed.

They discovered that SPIHT-compressed ECG signals could cause a 95% reduction in transmission time with no perceivable loss in quality. They also discovered that BERs of 10^{-5} or lower caused no perceivable impact on the received signal, as evaluated by analysing the ECG waveform complex.

EEG compression using SPIHT has also been examined, albeit to a lesser degree. Srinivasan *et al.* investigated SPIHT, JPEG2000 and other algorithms for lossless compression of EEG data in two dimensions [74], [85]. They sought to maximise compression gains by exploiting redundancies in the EEG signals while preserving all the signal data. As previously mentioned, lossless compression severely limits the compression gains that can be achieved. In [86], Daou and Labeau present a 2-D SPIHT based EEG compression methodology using EEG data obtained from Montreal Neurological Institute. They propose a pre-processing technique to exploit the correlation between EEG channels to maximise compression and employs two transform operations: a DWT and Discrete Cosine Transform (DCT). DCT is applied here to de-correlate the 2D EEG data. They suggest this results in a better compression gain to fidelity loss ratio than using standard (1D) SPIHT.

Further details on the operation and implementation of SPIHT in this research are outlined in Chapter 3.

2.5 Reed-Solomon Codes

A bit error is said to have occurred in data transmission if a given bit at the receiver is not equal to the corresponding bit sent by the transmitter. The impact of these errors can vary greatly, depending on factors such as the location of the error and the nature of data being transmitted. Broadly speaking, there are two approaches to dealing with bit errors; 1) error detection and 2) error correction. Both approaches involve the addition of redundant information to the data packet being transmitted. This redundant information is then used by the decoder to analyse the received packet to detect errors (in approach 1) and to fix errors (in approach 2). In the case of 1), if the decoder detects a bit error in the received packet, it can either ignore the error or discard the whole packet. An extension of this scheme can see the decoder request retransmission of the packet containing errors. However, this requires the existence of a back channel, whereby the receiver can communicate with the transmitter to request retransmission. Approach 2) involves the addition of redundant

data in the form of forward error correction (FEC) codes. These codes allow the receiver to identify errors and recover the information into a packet "most likely" to match the original.

Reed-Solomon (RS) codes are a form of FEC codes first proposed by Irving S. Reed and Gustave Solomon in the 1960s [87]. Since their introduction, they have become some of the most commonly used error correcting codes in communications and storage systems. They have been included in system standards such as Compact Discs [88], Digital Subscriber Line [89] and Blu-ray [90]. In [91], Nayak *et al.* proposed a method of transmitting medical images with concealed patient information in a noisy environment. To do so they proposed interleaving digital images with text data or one dimensional data such as ECG, while also encrypting the data to be transmitted. They proposed the use of RS codes to protect the data from bit errors. They concluded that the RS codes protected the encoded data from corruption, as long as the number of errors did not exceed the capabilities of the RS code. Only (15,3) and (15,5) codes were tested.

In [45], Kang *et al.* propose a system to remotely monitor ECG signals in real-time. The proposed system is based on the IEEE 802.11 WLAN standard, with a modified MAC layer to provide for real-time telecardiology. RS codes are used for FEC in this modified MAC layer. The aim of the paper was to design a system to provide strict quality of service maintenance, in real-time. The authors conclude that their proposed architecture improves wireless network performance and satisfies the objectives they set out to achieve. No information on the data overhead involved in the modified system design is given.

McSweeney *et al.* presented a number of papers that incorporate the usage of RS codes in wireless sensors for medical applications [92]–[94]. These works focus on losslessly compressing ECG and EEG signals prior to wireless transmission. In [93], an analysis of the possibility of low-powered RS implementation for use on ambulatory devices is presented. It is observed that the decoding operation requires far greater computational resources than the encoding operation, due to the encoder employing a linear feedback shift register. This is an important observation for a portable implementation as the encoding operation would most likely take place on a platform with a limited power budget, while the decoding operation would take place on a platform that may have greater computational resources.

Other authors have investigated methods of protecting compressed bioelectric signals from the effects of bit errors with error protection schemes other than RS. In [95], Ma *et al.* investigate a method of protecting EZW compressed ECG signals using an error protection approach based on convolutional codes. Their objective was to reduce the energy cost of transmitting ECG data by reducing wireless antenna activation time through signal compression and unequal protection of the bit stream. Portions of the compressed stream deemed most important for reconstructed signal fidelity are targeted for higher levels of error protection. The authors conclude that there is significant benefit to applying an unequal approach to error protection when compared to approaches where equal protection is applied to all bits. A similar approach was by the authors of [96]. In it, Miaou *et al.* investigate a methodology to transmit ECG data using a Bluetooth device. The data are first compressed using the SPIHT algorithm and a variety of error protection schemes are then applied based on the perceived importance of the bits. The highest level of protection is provided by BCH (Bose-Chaudhuri-Hocquenghem) cyclic codes, with the ability to detect and correct a maximum of seven errors. The authors again conclude that compression prior to transmission is key to reducing power consumption in a wireless device and an unequal approach to error protection is necessary to preserve the power saving benefits of compression, while providing protection from bit errors.

2.6 Summary

This chapter has presented an overview of the main literature relevant to the research present in this thesis. A review of ECG and EEG signals and capture was given along with a review of ambulatory capture and ambulatory capturing devices and the advantages and difficulties they create. Finally, this chapter dealt with the signal processing techniques specific to this thesis; looking at biomedical signal compression in general, the signal compression techniques used in this thesis and error correction codes.

The next chapter will describe specific details of the compression algorithms used. It will outline the algorithmic implementation of the compression algorithms introduced in this chapter and the evaluation metrics common to the majority of this research. Details on the main EEG database used in this research will also be given.

Chapter 3 EEG Compression Methodology

3.1 Introduction

This chapter outlines the approach taken to implement the algorithms used during the course of this research. It begins by outlining the original compression algorithms on which this research is based, then discusses the modifications made to these algorithms in the course of this work, why they were made, and their advantages. It also presents the main database used for EEG testing and why it was chosen. Finally, the primary metrics used to measure performance are given. Figure 3.1 shows a block diagram of a possible system that employs the EEG compression research as part of a seizure detection system.

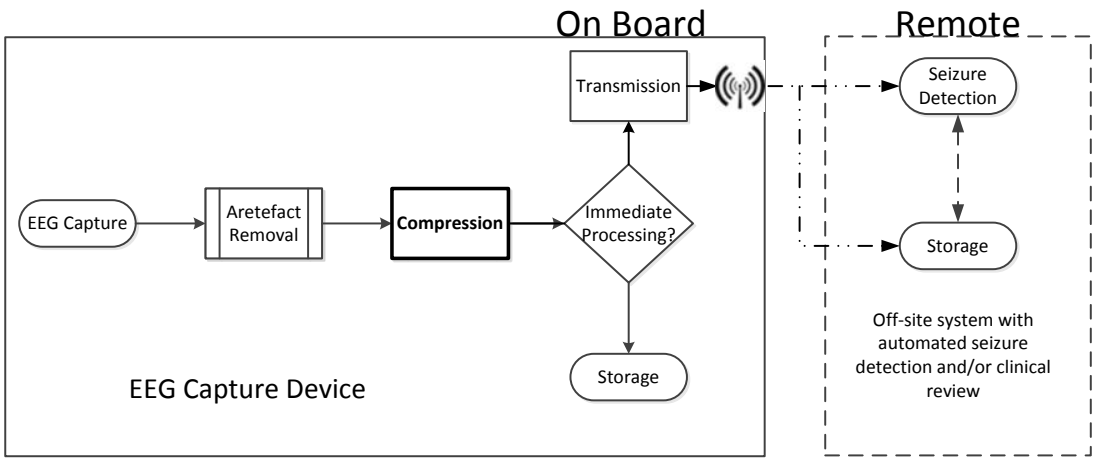

Figure 3.1: Block diagram of a possible seizure detection system architecture, consisting of a low-power wearable device communicating wirelessly with a remote server.

3.2 Common Elements of Compression Algorithms

This section will detail compression components common to both the compression algorithms described later in this chapter.

3.2.1 DWT

The Wavelet Transform (WT), gives a two-dimensional representation of a one-dimensional signal f. A wavelet (ψ) is a function of zero average:

$$\int_{-\infty}^{+\infty} \psi(t)dt = 0 \tag{1}$$

and ψ is often referred to as the *mother wavelet*. This mother wavelet is then used to create other wavelets by means of dilating and shifting. Dilation (compression and expansion of the wavelet, changing its frequency) is done with a scaling parameter s, and shifting (in time) is done by translating by u:

$$\psi_{u,s}(t) = \frac{1}{\sqrt{2}}\psi\left(\frac{t-u}{s}\right) \tag{2}$$

The WT of $f \in \mathbf{L^2}(\mathbb{R})$ at time u and scale s is

$$Wf(u,s) = \langle f, \psi_{u,s} \rangle = \int_{-\infty}^{+\infty} f(t) \frac{1}{\sqrt{s}} \psi^* \left(\frac{t-u}{s} \right) dt \quad (3)$$

where $\langle .,. \rangle$ is the inner product and $*$ is the complex conjugate. Wavelets are of interest in compression as many real-world signals are found to be sparse when expressed in a wavelet basis, thus facilitating compression [97]. The DWT reveals that a signal's energy is often focused in a small number of coefficients, with the others tending towards zero. By exploiting this redundancy, it is possible to represent the signal in a more compact form by setting coefficients below a threshold value to zero [98]. In 1910, Alfréd Haar proposed a simple piecewise constant function whose dilation and translations generate an orthonormal basis in $\mathbf{L^2}(\mathbb{R})$ [99]. In 1988 Ingrid Daubechies published her seminal work on orthonormal wavelets of compact support [100]. This led to the development of filter bank based transforms [101] and biorthogonal wavelet bases [57], [102].

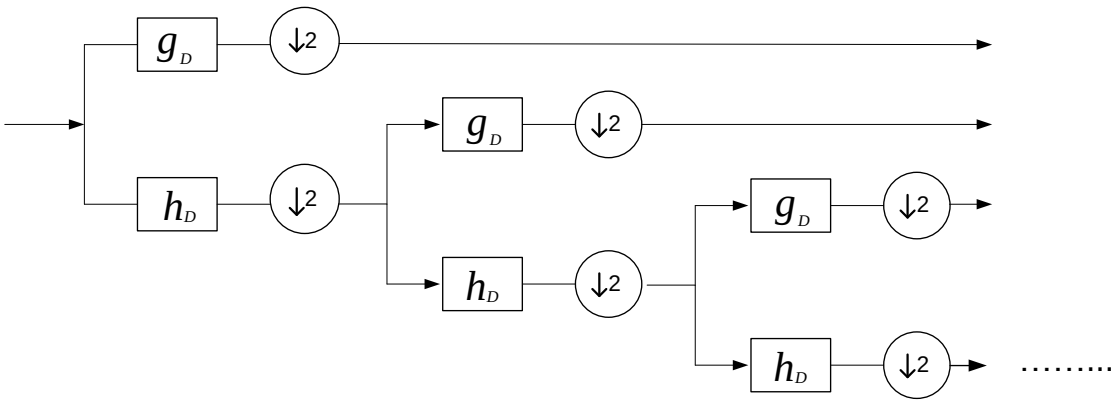

Figure 3.2: Example of DWT operation showing three step decomposition.

The DWT can be viewed as a collection of spatially-oriented trees. The signal coefficients are divided into subbands based on their frequency. The roots of the tree are the coefficients in the lowest frequency subband, which branches successively into higher frequency bands at the same spatial orientation [79]. Figure 3.2 shows an example of a three step DWT operation. Here, g_D signfies the high pass decomposition while h_D signifies low pass decomposition. The original JPEG2000 standard incorporates two DWTs: the Le Gall 5/3 integer to integer transform for lossless compression and the CDF9/7 floating point transform for lossy compression.

As one of the objectives of this research was to focus on lossy signal compression to maximise compression gains, only the CDF9/7 transform was implemented. The CDF9/7 transform was implemented using a lifting scheme as outlined in [101], [103]. The advantages of using a lifting scheme to constructing biorthogonal wavelets are outlined in [104] and includes faster operation and in-place calculation of the transform. The full properties of this wavelet filter can be found in papers such as [105]. This transform was common to all compression performed in this research.

3.2.2 Quantisation

After the DWT operation, a quantisation step is performed. Quantisation is a nonlinear and noninvertible method of mapping a large, finite sequence of numbers, $x(n)$, onto a smaller scale, $\hat{x}(n)$. The range $x(n)$ is divided into a number of equal intervals and then each interval is mapped to a codeword. It is worth noting that the codeword refers only to the interval and not to the original value. All input values are then expressed in terms of the interval they fall within. Figure 3.3 shows a graphical example of the quantisation process. The decoding process attempts to convert the $\hat{x}(n)$ values back to the original scale.

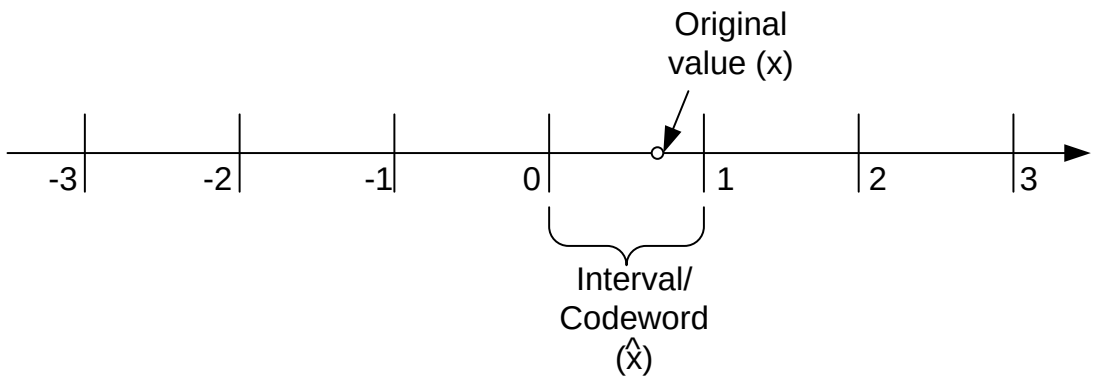

Figure 3.3: Example of input sequence of quantiser.

For this research a simple quantisation scheme was implemented where the wavelet coefficients were quantised using a standard integer quantisation approach. This approach was common to JPEG2000 and SPIHT. Quantisation provides an opportunity to vary the level of compression in the algorithm. By lowering the selected bit-rate of the quantiser, greater compression can be achieved. However, the lower the bit-rate available to the quantiser, the less information is retained in the

quantised coefficients. This results in a greater level of loss when the signal undergoes the inverse encoding operation. Research into the effects of varying this bit level is presented in Chapter 5 of this thesis.

3.3 JPEG2000

JPEG2000 is an image compression algorithm first ratified by the Joint Photographic Experts Group in 2000 [62]. It was designed to replace the original JPEG file format with more sophisticated compression components to give greater compression gains and improved image quality. Figure 3.4 shows a block diagram of the algorithm as implemented in this work, including the changes made as outlined below.

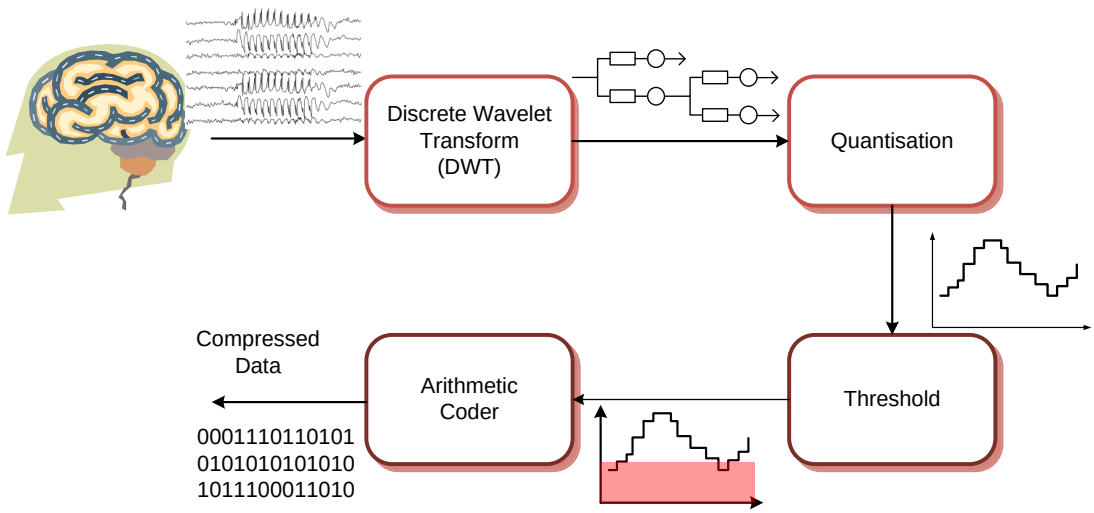

Figure 3.4: Modified JPEG2000 based compression approach as implemented in this research.

3.3.1 Thresholding

In addition to the basic JPEG2000 algorithm, a thresholding step was added to the encoding operation. Coefficients below a selected threshold level were deemed to be insignificant and set to zero. The greater the number of zero values, the higher the efficiency of the entropy encoder. It was noted during the implementation of the JPEG2000 algorithm that the addition of a thresholding step would allow for greater control of the achievable level of compression gains. By selecting the appropriate threshold level, larger compression gains can be achieved with minimal impact on the level of fidelity loss in the resulting signal. Future chapters investigate the

appropriate threshold level to select to achieve an optimum trade-off between compression and loss. Initially, the threshold step was placed after the DWT step and before the quantisation step. However, this was found to give unpredictable results, where the loss in signal information at a given threshold could vary greatly from signal-to-signal. This made it difficult to choose an appropriate threshold level for a desired level of information loss. For this reason, the thresholding step was moved to after the quantisation step. In this way, the threshold values were being applied to coefficients that had been normalised, giving more predictable levels of information loss and more consistent results across a range of signals.

3.3.2 Arithmetic Coder

The adaptive binary AC is the entropy encoder used in JPEG2000 Part 1. The AC reduces the symbols to be encoded into a single, unique binary fraction based on the Probability Distribution Function (PDF) of the symbols. To understand its operation, take an example of a source A, that generates symbols from an alphabet of size 4,

$$A = \{a_1, a_2, a_3, a_4\}$$

Assume these symbols have probabilities:

$$P(a_1) = 0.5, \qquad P(a_2) = 0.25, \qquad P(a_3) = 0.125, \qquad P(a_4) = 0.125$$

which all lie on the interval $[0,1)$.

Table 3.1: Probabilities and Ranges For Symbols a_n in Example.

Symbol	Probability	Range
a_1	0.5	[0,0.5)
a_2	0.25	[0.5,0.75)
a_3	0.125	[0.75,0.875)
a_4	0.125	[0.875,1)

The encoder begins with the interval [0,1), which is divided up into ranges for each symbol based on the probability of them occurring. These probabilities are given in Table 3.1. When the first symbol is encoded, the total range is updated to correspond

to the range of the symbol being encoded. The updated range is again divided based on the probabilities given in Table 3.1. This process is repeated until all symbols are encoded, with the range being updated with respect to each symbol being encoded, as it is encountered. A graphical example of this operation can be seen in Figure 3.5.

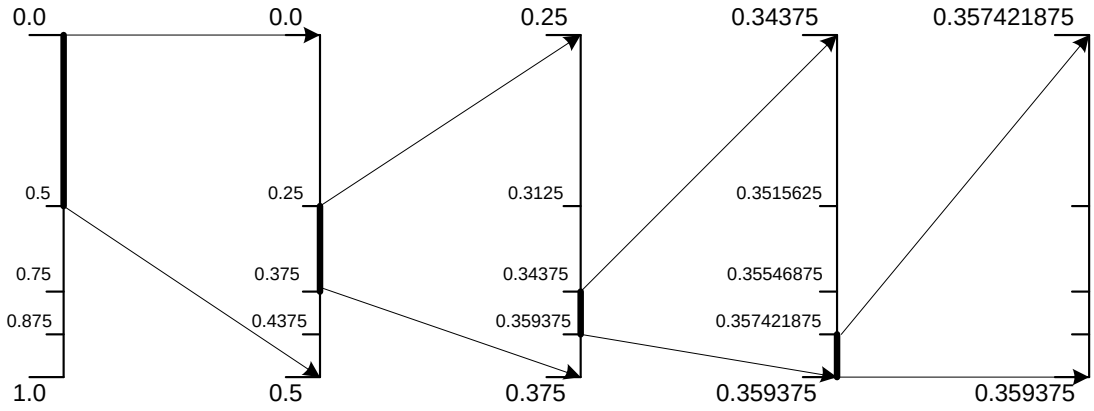

Figure 3.5: Graphical representation of example Arithmetic Coder.

To decode the message, the decoder accepts the fractional value as input and again compares it to the range values from Table 3.1. The value falls between the lower and upper bound of a_x and so a_x is the output. The encoder then must update the encoded value to remove the effects of the first symbol. A new range is calculated by taking the lower bound of the decoded symbol from the upper bound. The encoded value is calculated by taking the lower bound of the first symbol from the initial encoded value and dividing by the upper bound. The process continues until all symbols are decoded. It should be noted that the decoder will continue to decode unless the length of the original signal is passed as an argument or a predetermined escape character is received.

It can be seen from this example that the standard AC requires that the decoder has prior knowledge of the distribution of symbols in the original message. This would require transmission of the PDF with the encoded message for use by the decoder, or would require an assumed fixed PDF at both transmitter and receiver. With the Adaptive AC approach, the encoder and decoder initially assume a unity PDF. After each symbol is encountered and encoded, the PDF is dynamically updated to reflect the new probability of occurrence. This allows the encoder and decoder to operate

with no prior knowledge of the distribution of the messages symbols. It does however, result in reduction in efficiency in the encoding process.

Initial research focused on using the Adaptive AC as outlined in [47]. Signals were split into frames of size 1024 samples for compression, which corresponds to a length of 4s per frame at a sampling rate of 256 Hz. Each frame was treated independently. It was noticed however, that the compression gains of the encoder quickly levelled off, i.e. as the level of fidelity loss was increased, the CR did not significantly improve. Analysis of these observations suggested the efficiency of the AC was being limited by the PDF needing to be rebuilt for each frame being encoded, i.e. with the AC operating in adaptive mode. It therefore seemed logical to add some prior knowledge of the symbol PDFs to improve efficiency. Analysis of the PDF of the messages being encoded suggested a general Gaussian distribution to the symbols derived from the EEG database used for the research. While the AC can encode a message with a PDF that is not equal to the actual PDF of the message, the greater the difference between the actual PDF and the PDF used, the less efficiently it will encode. It was therefore decided to build an overall PDF of the EEG database and use this PDF for all frames being compressed. This allowed a single PDF to be used by the encoder and decoder, thus making it independent of the distribution of the symbols in any given frame. This was found to greatly improve the compression gains of the encoder. If a frame does not follow this generalised PDF, the AC will not encode as efficiently but will still offer significant compression gains.

3.4 SPIHT

SPIHT is an coding technique that operates by ordering coefficients in order of perceived importance through use of recursive analysis based on specified thresholds. While SPIHT can be paired with a variety of transform operations with good results, it is most often seen paired with a DWT operation [79]. The DWT arranges coefficients into groups of subbands where successive bands display a temporal relationship with each other due to the downsampling operation that occurs during the transform operation. These subbands form a non-overlapping spatial orientation tree structure, with each node branching into higher frequency subbands at the same spatial orientation. In layer i, each coefficient corresponds to two coefficients in layer $i + 1$ (Figure 3.6). If the sizes of the subbands differ, a single

coefficient in the smaller subband may represent the same spatial location as multiple coefficients in the other subbands. This creates the potential for large compression gains. SPIHT achieves high compression gains by keeping insignificant coefficients in large subsets

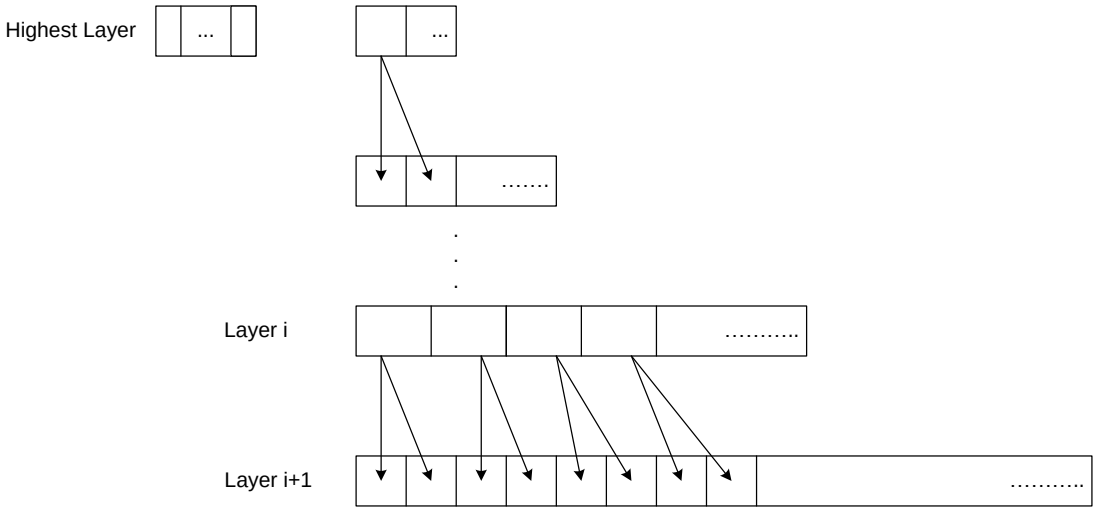

Figure 3.6: Temporal orientation tree showing relationship between coefficients on different subbands.

After the transform operation, SPIHT encodes the coefficients by recursively checking their significance against threshold levels. The thresholds used are powers of two, creating a binary representation of the integer value of the wavelet coefficients. The SPIHT encoding operation can be broken down into two passes: the Sorting Pass and the Refinement Pass. To describe the operation of the algorithm, it is first necessary to define some terms:

- **LIS** List of Insignificant Sets: contains sets of wavelet coefficients which are defined by tree structures, and which have been found to have magnitude smaller than a threshold (i.e. are "insignificant"). The sets exclude the coefficient corresponding to the tree or all subtree roots, and have at least four elements.
- **LIP** List of Insignificant Points: contains individual coefficients that have magnitude smaller than the threshold.
- **LSP** List of Significant Points: points found to have magnitude larger that the threshold (are significant).

- $\mathcal{O}(c_i)$ in the tree structures, the set of offspring (direct descendants) of a tree node defined by point location(i).
- $\mathcal{D}(c_i)$ set of descendants of node defined by pixel location(i).
- $\mathcal{L}(c_i)$ set defined by $\mathcal{L}(c_i) = \mathcal{D}(c_i) - \mathcal{O}(c_i)$.
- $\mathcal{H}$ the set of all root nodes
- A Type A entry: the entry i represents $\mathcal{D}(c_i)$ in the LIS
- A Type B entry: the entry i represents $\mathcal{L}(c_i)$ in the LIS

The operation of the algorithm is originally outlined for two dimensional images in [13] and in [75] is modified for one dimensional signals. It can be described as:

1. **Initialization**: Set the significance threshold 2^n with $n = \lfloor log_2(c_{max}) \rfloor$; set the LSP as an empty list; set the roots of similarity trees in the LIP and LIS;
2. **Sorting Pass:**

2.1. for each entry (i) in the LIP do:

2.1.1. output $S_n(i)$;

2.1.2. if $S_n(i) = 1$ then move (i) to the LSP and output the sign of c_i;

2.2. for each entry (i) in the LIS do:

2.2.1. if the entry is of Type A then

- output $S_n\big(\mathcal{D}(i)\big) = 1$ then
  - ♦ for each $(k) \in \mathcal{O}(i)$ do:
    - output $S_n(k)$;
    - if $S_n(k) = 1$ then add (k) to the LSP and output the sign of c_k;
    - if $S_n(k) = 0$ then add (k) to the end of the LIP;
  - ♦ if $\mathcal{L}(i) \neq 0$ then move (i) to the end of the LIS, as an entry of type B, and go to Step 2.2.2; otherwise, remove entry from (i) from the LIS;

2.2.2. if the entry is of Type B then

- output $S_n\big(\mathcal{L}(i)\big)$;
- if $S_n\big(\mathcal{L}(i)\big) = 1$ then
  - ♦ add each $(k) \in \mathcal{O}(i)$ to the end of the LIS as an entry of type A;
  - ♦ remove (i) from the LIS.

3. **Refinement Pass:** for each entry (i) in the LSP, except those included in the last sorting pass, output the nth most significant bit of $|c_i|$;
4. **Quantisation-Step Update:** decrement n by 1 and go to Step 2.

This process continues until $n = 0$ or the desired compression level is reached. As the encoder has prior knowledge of the length of the original data being compressed, it is possible to specify a desired compression level prior to encoding.

SPIHT orders the bit stream from Most Significant Bit (MSB) to Least Significant Bit (LSB). This "embedded" encoding allows the encoder to terminate encoding at a desired compression level. The bits encoded at this level are those deemed most important to reconstruct the original message, given the allotted bit budget (determined by the desired compression level). This more direct control over the compression level is in contrast to JPEG2000, where direct control of the compression level is not possible; instead, the compression level was calculated after compression and was estimated as an average of the compressed length of all the signals processed. The formula for calculating compression ratio (CR) is given in equation (4) in Section 3.6.1.

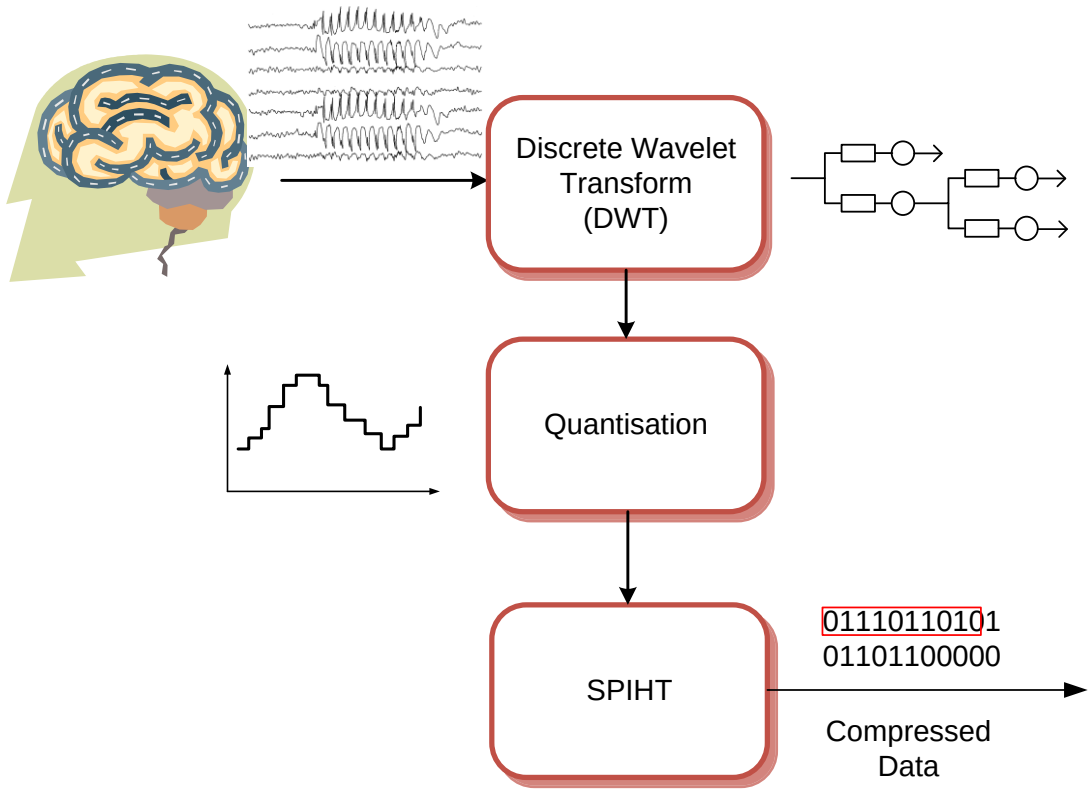

Figure 3.7: Block diagram of SPIHT compression approach as implemented in this research.

SPIHT is most often employed in lossy mode with a specified compression level, but it can also be employed where all the input coefficients are represented in the compressed bit stream and they can be perfectly reconstructed into their original form. While SPIHT itself is operating without truncation of the encoded bit stream (i.e. no explicit compression), the CDF9/7 DWT and quantisation blocks preceding it still cause a minor loss of fidelity between the original signal and signal reconstructed after compression. For this reason, it may not be strictly appropriate to refer to compression using this approach as "Lossless SPIHT". Instead the term "Non-Truncated SPIHT" has been employed in this thesis in reference to the fact that the full encoded bit stream is saved. Even without truncation of the encoded bit stream, SPIHT introduces an inherent compression on the signal in relation to the original signal length, because of the list structure it imposes on the signal. Empirical review of the data examined here shows that this inherent compression results in reduction of the bit stream length by around 50%. The impact of this inherent compression ability on system design is explored further in Chapter 6. A high-level block diagram of the SPIHT algorithm can be seen in Figure 3.7.

3.5 EEG Database

A database of EEG signals from patients with medically intractable focal epilepsy is maintained by the University of Freiburg [106], [107]. It contains seizure and non-seizure EEG data for 21 patients ranging in age from 13 to 50, sampled at 256 Hz with 16 bit resolution. This database was used for the majority of experiments reported in this thesis. It was chosen due to (i) its public availability, (ii) the 6-channel EEG recordings provided are likely to be close to what would be recorded by an AEEG device [108] and (iii) the intracranial recordings minimise the artefacts present in the recordings. While AEEG signals would normally include artefacts due to e.g. movement, eye blinks, this is not considered in this research. Artefact removal is typically carried out prior to compression in an AEEG device [109]–[111].

3.6 Performance Metrics

3.6.1 Compression Ratio (CR)

Compression Ratio (CR) is one of the key performance measures of a compression algorithm, and is defined as the ratio of the size of the compressed data to the size of the original data. It is used to quantify the data size savings from using the compression algorithm. It can be defined mathematically as:

$$CR = \frac{L.r}{\hat{b}} \tag{4}$$

where L is the length of the input signal in samples, r is the quantisation (bit resolution) of each original sample and $\hat{b}$ is the number of bits representing the compressed signal. The original bit-resolution (r) is given in the description of the file databases and L is specified by the user during algorithm setup. In the case of JPEG2000, $\hat{b}$ can be found by examining the length of the bit stream after the compression operation. For SPIHT, due to its embedded encoding property, the CR can be specified and controlled as part of the compression operation, thus allowing the algorithm to determine the desired $\hat{b}$ and terminate encoding when it is reached.

3.6.2 PRD and PRD1

Percentage Root-mean squared Distortion (PRD) is a measure of the difference between two signals. The standard metric can be defined as:

$$PRD = \left(\frac{\|x - \hat{x}\|}{\|x\|}\right) \times 100 \tag{5}$$

where x and $\hat{x}$ are the original and reconstructed signals, respectively, and $\| \ \|$ represents the Euclidean or l^2 norm. While this definition is the most frequently used version of this metric, a second definition also exists that removes the signal mean. This is frequently referred to as PRD1 and is defined as:

$$PRD1 = \left(\frac{\| \ x - \hat{x} \ \|}{\| \ x - \ \bar{x} \ \|}\right) \times 100 \tag{6}$$

where $\bar{x}$ is the mean of the signal. In [112], Blanco-Velasco *et al.* investigated the use of PRD and PRD1 to measure the quality loss in compressed ECG signals. They concluded that despite the prolific use of PRD, PRD1 gave results that more accurately represented the level of fidelity loss, especially in signals that contain a DC component. The authors of [54] found that PRD1 values could be as much as four times as high as PRD values for a given set of compressed EEG data due to the mean signal value biasing the PRD results. PRD1 was therefore selected as the preferred metric for measuring signal fidelity degradation in this research.

While PRD and PRD1 are widely-used and intuitively simple measures of distortion, they have well-known limitations; in particular, they give only a general measure of fidelity loss and cannot determine specific impact on the *diagnostic* content of a signal. This latter point is particularly important in the case of biomedical signals where the intention is to carry out some form of diagnosis on the signal.

3.7 Summary

This chapter has described the compression algorithms used throughout this thesis. It details the constituent components of the algorithms, how they were implemented and, where applicable, the reasons why implementation decisions were made. The

DWT and quantisation steps were introduced first as they are common to both algorithms. The operation of the DWT and reasons for the choice of CDF9/7 as the transform of choice were given. The operation of the quantisation step was presented, as well as the reasons for it being placed after the DWT in both algorithms. Following this, the general JPEG2000 algorithm was introduced. Coefficient thresholding was added to the JPEG2000 algorithm after the quantisation step to allow further control over the level of lossy compression in the signal. Arithmetic coding is used as an entropy encoder for the final data. An alternative method of building the PDF for compression was used as it was found to provide gains in compression. The SPIHT algorithm is the second compression algorithm used in this research. The initial components of the algorithm were the same as JPEG2000: DWT and quantisation. The quantised wavelet coefficients were then encoded using the SPIHT compression algorithm, adapted for use in 1D signals. The operation of this algorithm and its key properties were given.

The primary EEG database used in this research was the Freiburg epilepsy database. A description of this database and the reasons for selecting it as the primary database were given. Finally, the primary performance metrics were explored. These metrics are common through all the research in this thesis and are used to measure 1) the compression gain and 2) the fidelity loss. These are given as CR and PRD1 respectively.

With the exception of the EEG database and JPEG2000, these components are common to all the research in this thesis. The next two chapters address methods of EEG compression where maximum compression is desirable, without loss of information necessary to diagnosis. Chapter 4 will examine the compression of the Freiburg database using the two compression algorithms outlined in this chapter. It will seek to determine which is more efficient at compressing EEG data without losing diagnostic information and if compression on a mobile device is practical.

Chapter 4 Compression of EEG Signals with JPEG2000 and SPIHT

4.1 Introduction

Lossy compression of ECG signals has long been investigated. EEG research however, has primarily focussed on lossless compression [113]–[115]. While lossless compression is an ideal outcome, the requirement to preserve all signal components severely limits the compression gains that can be reached, which is disadvantageous in the context of achieving desirable power savings in ambulatory systems. Lossless compression generally focuses on exploiting the redundancy in the signal and efficiently encoding correlated coefficients to minimise the bits needed to represent them. However, by allowing a measure of loss, the compression gains can be greatly improved. EEG signals contain information not required for diagnostic purposes. By minimising these coefficients, large gains in compression can be achieved. Efficient lossy compression involves identifying these coefficients and removal of those deemed not necessary to reconstruct the signal to the desired fidelity level. This chapter presents a method of compressing EEG signals using two DWT based compression approaches; JPEG2000 and SPIHT. It begins by briefly outlining the overall approach taken to compression. The compression algorithms

have already been described in some detail in Chapter 3. The chapter then presents the results of CR versus PRD1 for low levels of fidelity loss. Next, this chapter discusses the problem of quantifying the impact of lossy compression on EEG data. The REACT automated seizure detection algorithm is presented as an alternative method of quantifying this loss through use of CAD. The signals compressed at low levels of loss are examined with REACT to ensure diagnostic integrity is maintained. Once this is established, maximising compression levels is explored by allowing higher levels of loss and verifying seizure information retention with REACT. Finally, this chapter looks at the benefits of compressing EEG data on an ambulatory device by investigating if compression prior to wireless transmission would provide a net decrease in energy expenditure.

As outlined in Chapter 3, compression was applied to the database of EEG data from 21 patients with medically intractable focal epilepsy provided by the University of Freiburg [106], [107]. The compression algorithms were applied to the database at varying levels of loss, and the signals then reconstructed to examine the impact on signal quality. The compressed bit stream can be used for either transmission or storage, depending on the application required.

4.2 EEG Compression at Low Compression Ratios

Initial research focused on the compression of EEG signals using the JPEG2000 algorithm as outlined in Chapter 3. The thresholding step was used to control the level of loss in the algorithm, which in turn controls the level of compression. By increasing the threshold level, a greater number of coefficients were set to zero, thus increasing the compression efficiency of the AC. However, the greater the threshold level, the greater the level of loss in the resulting signal. The number of wavelet decompositions and the quantisation level were selected based on the results found in [116]. An 8-level DWT and 10-bit quantisation of the DWT output coefficients were chosen for the original 16-bit signals. Each signal was divided into windows of size 1024, i.e. 4s. These windows were compressed and reconstructed using 5 different threshold values. Threshold values were chosen to give a range of PRD1 values from very low (<1%) to above 10%. The CR and PRD1 values were averaged for each patient, and an overall average was calculated for all patients in the database, at each threshold level.

The SPIHT algorithm was also applied to the Freiburg database at a range of compression levels chosen to result in PRD1 values over the same range up to 10%. As outlined in the description of the SPIHT algorithm, the desired CRs can be readily controlled prior to compression; this is a significant advantage of SPIHT over JPEG2000. The compressed bit streams were then reconstructed to create an approximation of the original signal, so the PRD1 could be calculated. A plot of PRD1 versus CR for JPEG2000 and SPIHT can be seen in Figure 4.1.

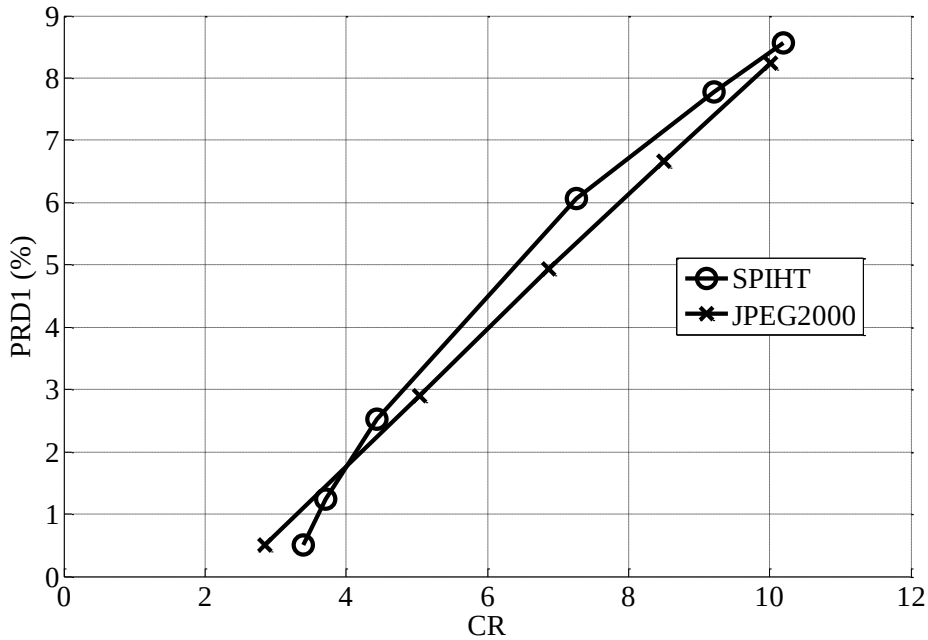

Figure 4.1: CR vs. PRD1 for EEG signals compressed with SPIHT and JPEG2000 for CRs lower than 11.

At very low CRs, SPIHT provides better performance than JPEG2000, in terms of lower distortion for a given CR. As CR increases, SPIHTs PRD1 values increase faster than JPEG2000, exceeding JPEG2000s PRD1 when the CR passes 4. It remains this way until the CR approaches 10 where these values begin to converge again. The PRD limit suggested in [55] of 7% was selected as the maximum allowable level of fidelity for visual inspection of the reconstructed signal. From Figure 4.1, it can be seen that a PRD1 of 7% corresponds to an average CR of approximately 8.3 for SPIHT and almost 9 for JPEG2000.

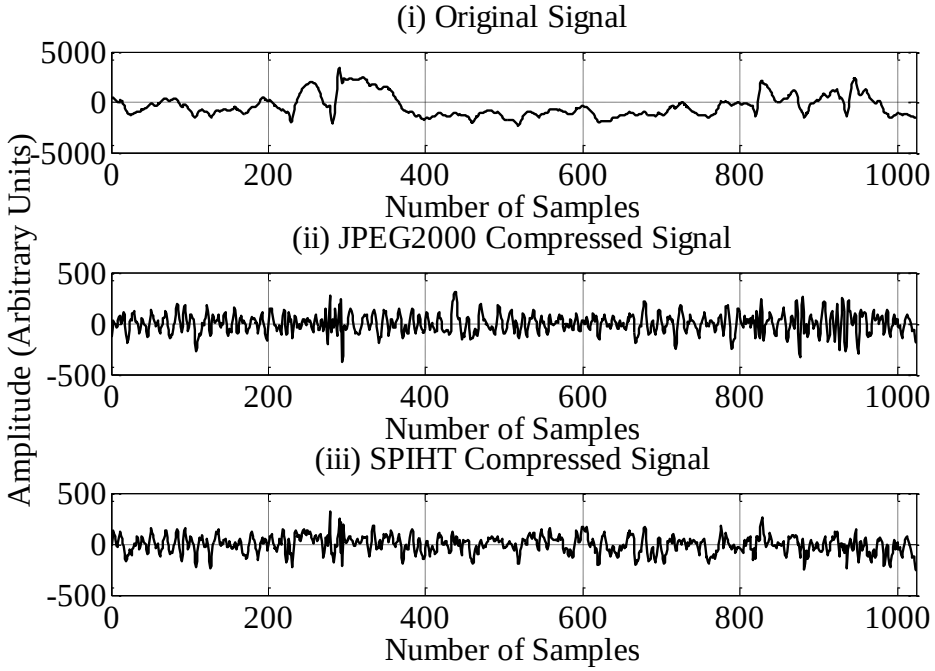

Figure 4.2: Plot of example of (i) original EEG signal, and the resulting error signals after compression with (ii) JPEG2000 and (iii) SPIHT at ~7% PRD1.

Figure 4.2 shows a plot of a sample of a signal selected at random from the Freiburg database versus the same sample after compression with approximately a 7% PRD1. It is clear from this comparison that very little of the signal information is lost at 7% PRD1. It is worth remembering however, that PRD1 only gives an average indication of loss in signal fidelity relative to the original signal. It does not directly measure the impact of signal degradation on diagnostically relevant information. This gives rise to two important questions:

1) Is the diagnostically relevant information being retained at this PRD1 level?
2) If it is, can a higher level of loss be tolerated?

While 1) can be predicted to hold true due to 7% PRD1 maintaining 99.5% of the signals energy [55], it was necessary to further investigate the effects of this compression on the EEG signals to verify this prediction and to address 2).

4.3 Preservation of Diagnostic Information

Initial verification of the data integrity was performed by visual inspection of the data post compression. However, due to the nature of the data being evaluated, a trained clinician would be necessary to fully verify that the important diagnostic information is being maintained. Unlike ECG ([25], [117], [118]), no standardised metrics have so far been proposed to measure the loss of signal information in EEG signals with respect to the impact on diagnostically relevant information. The use of Computer Aided Diagnosis (CAD) systems was briefly discussed in Chapter 2. In the context of healthcare, the use of CAD provides a means to rapidly and consistently analyse large volumes of data. In the context of this research, using an effective CAD system to analyse the lossy compressed EEG signals makes it possible to determine the impact of compression on diagnostic information.

REACT (Real-time EEG Analysis for event deteCTion) is an automated epileptic seizure detection system [119]–[121]. The REACT algorithm operates on EEG data by extracting a rich set of features from the time, energy and spectral domains. In total, fifty-five features are extracted [122]. Frequency domain features extracted include total power, wavelet coefficients and total spectral power. Time domain features include curve length, number of maxima and minima and RMS amplitude. Finally, some of the information theory features included are Shannon entropy and spectral entropy. A full list of the features used can be found in [123].

At REACTs core lies a Support Vector Machine (SVM) classifier which uses rules that have been automatically derived using machine learning and pattern recognition techniques. These rules are used to classify the extracted EEG features as seizure or non-seizure. Full details on the structure and operation of REACT can be found in [121], [122], [124]–[126]. The algorithm has been shown to give very accurate seizure detection performance, as verified by clinical review of its performance [122], [126]. In [122], Temko *et al.* report detection rates as high as 100% with four false detections per hour for neonatal EEG.

Although REACT was initially designed for use in neonatal seizure detection, subsequent research has demonstrated that it can also achieve very high seizure detection performance on adult EEG [119]. In this research it was employed as a method of evaluating the retention of diagnostically-important data in EEG signals after lossy compression. The impact of compression on seizure detection

performance was also evaluated with respect to PRD1, which quantifies loss of fidelity in the signal. REACT was used in order to quickly evaluate many hours of EEG data. This was important as each variation of compression parameters creates a whole new instance of the database. If a trained clinician was required to review this data, it would take many hours of work to classify each instance of the database. This quickly becomes impractical when multiple compression parameters are tested, to establish a range of fidelity loss in the compressed signals. The use of REACT is not necessarily intended to replace a clinician in diagnosis, but in this research is used as a tool to monitor the impact of compression on the diagnostically relevant information on the signals. REACT was initially run on the original database to establish baseline performance. Performance of the algorithm is evaluated by use of the Receiver Operator Characteristic (ROC) curve. This is a graphical representation of the relationship between the sensitivity and specificity of the classifier. Sensitivity (Se) is defined as the percentage of seizure epochs correctly classified and specificity (Sp) is defined as the percentage of non-seizure epochs correctly classified. They are defined mathematically as:

$$Se = \frac{TP}{TP + FN} \tag{7}$$

$$Sp = 1 - \frac{FP}{TN + FP} \tag{8}$$

where TP is the total number of seizure events detected correctly (true positives), FN is the number of missed seizure events (false negatives), FP corresponds to seizures detected by the algorithm that do not exist in the original signal (false positives) and TN corresponds to non-seizure events correctly classified by the algorithm (true negatives).

The Area Under the Curve (AUC) is calculated for the ROC and gives a numerical evaluation of the classifier's performance. An AUC of unity implies perfect classification, with the classifier identifying all seizure events correctly, with no false positive or false negative events. The AUC results in the research were reported as a Percentage of Total AUC. This is given mathematically as

$$Percentage\ Total\ AUC = AUC \times 100 \quad (9)$$

where 100% corresponds to an AUC of unity. In practice, a classifier is unlikely to achieve this result. Moreover, there are often some discrepancies even among trained clinicians in the identification and location of seizure events.

In research making use of REACT for automated seizure detection, a subset of the Freiburg database was used for testing. This subset was chosen due to the quality criteria outlined in [119]. Specifically, 15 patients were selected from the 21. Three patients (1, 18 and 19) were discarded due to the length of seizure events being less than 10 seconds and three others (5, 8 and 10) were removed due to the large amount of artefact data present. The remaining 15 patients' EEG recordings comprise 132.7 hours of data with approximately 120 mins of seizure activity over 61 seizure events. For test purposes the EEG data are processed on a frame-by-frame basis, with frames of duration 4 seconds. Therefore, the total number of frames is 119430, with 1800 frames containing seizures. Pre-filtering was not applied to the signals prior to compression.

For each patient in the dataset, the REACT system was loaded with an SVM classifier built specifically for that patient. Each classifier was trained using seizure and non-seizure data randomly chosen from the fourteen other patients in the dataset. Since REACT is being employed in the place of a trained clinician, data from the original, uncompressed EEG database was used in the training phase. The purpose of the study is to observe how the classifier reacts when presented with reconstructed EEG from a patient it has not encountered before. For each patient, the reconstructions of that patient's EEG recording were passed through the REACT system, producing binary seizure/non-seizure decisions for each epoch of every channel.

As the database was already annotated by clinicians, a performance benchmark of REACT on the Freiburg database could be established. It could also be used to evaluate the performance at various levels of quality degradation, in order to establish the impact on diagnostic information useful seizure detection. Figure 4.3 show a plot of the Total Percentage AUC at a given average PRD1 for compression with JPEG2000 and SPIHT, and for low CRs corresponding to approximately the same range of PRDs shown in Figure 4.1. Both algorithms produce a Total

Percentage AUC of ~96% at their lowest level of compression. This matches the results of REACT on the uncompressed data found by Faul *et al.* in [119]. As PRD1 increases, the detection rate of JPEG2000 begins to decline. At 7% PRD1, the Percentage Total AUC is just over 95%, a decline of approximately 1%. SPIHT, in contrast, does not show a decline in seizure detection performance. In fact, AUC appears to improve slightly as PRD1 increases. The improvement is slight however and it is difficult to determine it if is significant at this point. The results from both algorithms show that at 7% PRD1, there is no significant impact on the seizure information in the compressed signals.

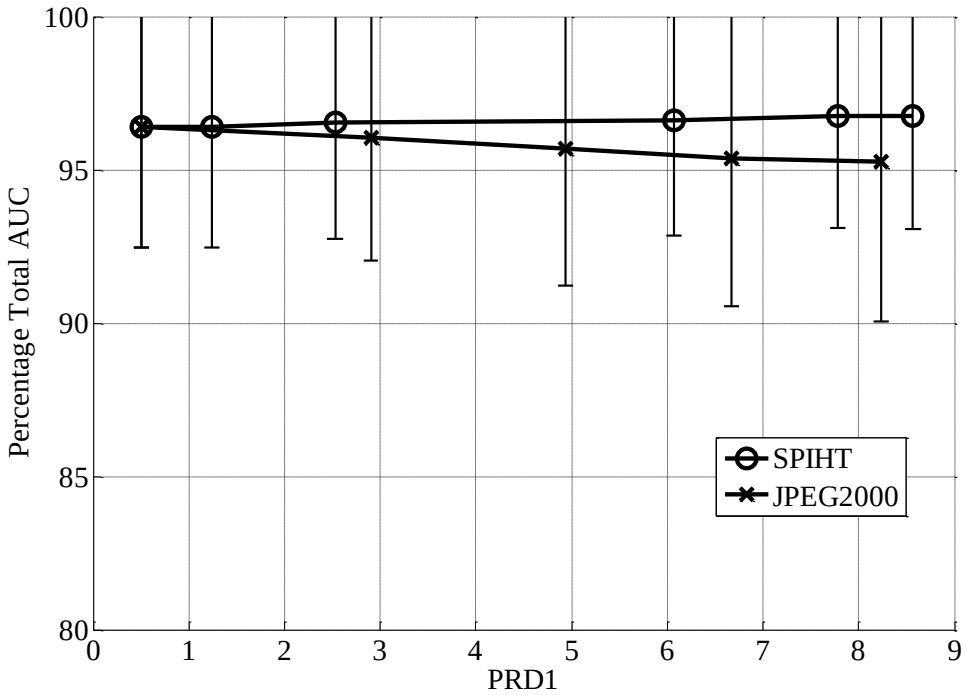

Figure 4.3: Percentage Total AUC as a factor of PRD1 for JPEG2000 and SPIHT-compressed signals for PRD1s of below 9%, showing the 95% confidence intervals.

4.4 Maximising Compression Ratio

The previous section has demonstrated that at a PRD1 of 7% or less (corresponding to reasonable visual fidelity and 99.5% energy retention of the signal according to [55]), there is negligible impact on the seizure information in EEG data compressed with JPEG2000 and SPIHT. Figure 4.3 shows that seizure detection performance is

still being maintained at PRD1 levels of close to 9%. To determine the effects of higher levels of loss on seizure detection performance, the Freiburg dataset was again compressed with JPEG2000 and SPIHT at much higher compression levels. This resulted in CRs of just over 100 for JPEG2000 and 150 for SPIHT. The corresponding PRD1s were again calculated. Figure 4.4 shows the results of this test. As compression levels increase, the compression gains of SPIHT begin to quickly outperform those of JPEG2000. At CRs higher than 11, JPEG2000s PRD1 value at a given level of compression begin to rapidly increase. After SPIHT's initially poorer performance, the rate of fidelity loss slows and at higher levels of compression, it retains a lower average PRD1 than JPEG2000.

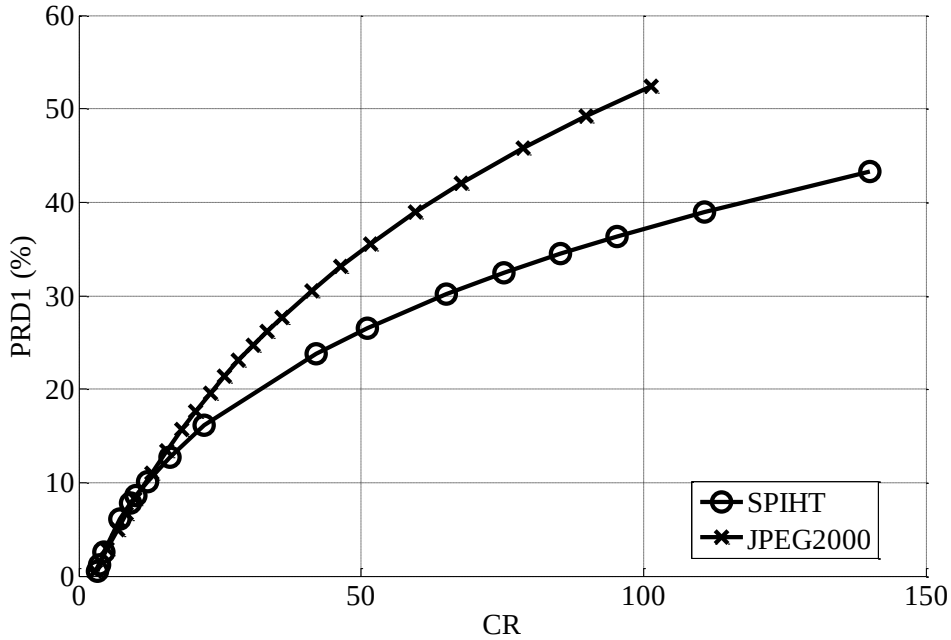

Figure 4.4: CR vs. PRD1 for JPEG2000 and SPIHT.

This can be explained by SPIHT's embedded encoding property where the bit stream is ordered from MSB to LSB. High Frequency (HF) components are generally seen as of lower importance by SPIHT and, as such, are lost when the CR is increased. JPEG2000 increases CR by zeroing coefficients below successively higher thresholds. At low levels of compression, relatively few coefficients are zeroed and the remaining ones are efficiently encoded by the AC. Thus, at low levels of compression, the PRD1 metric records greater differences between the SPIHT-compressed signals than the JPEG2000 compressed ones.

The reconstructed signals were again passed through the REACT software to determine the impact of higher levels of compression on the signals diagnostic information. Figure 4.5 gives the results of this test, showing the Percentage Total AUC at a given PRD1 for each algorithm. It can be seen that this graph follows the same general trend as Figure 4.3, with SPIHT maintaining a higher seizure detection performance that JPEG2000 for greater PRD1s. The initial decline in JPEG2000s performance can be seen to level-off until PRD1 passes 16%. Above 16% it begins to decline slowly. A Percentage Total AUC of above 90% can be said to be *'very good'* for seizure detection performance [119]. For this reason, 90% was chosen as the cut-off level for performance of automated diagnosis. JPEG2000 passes this point at approximately 30% PRD1.

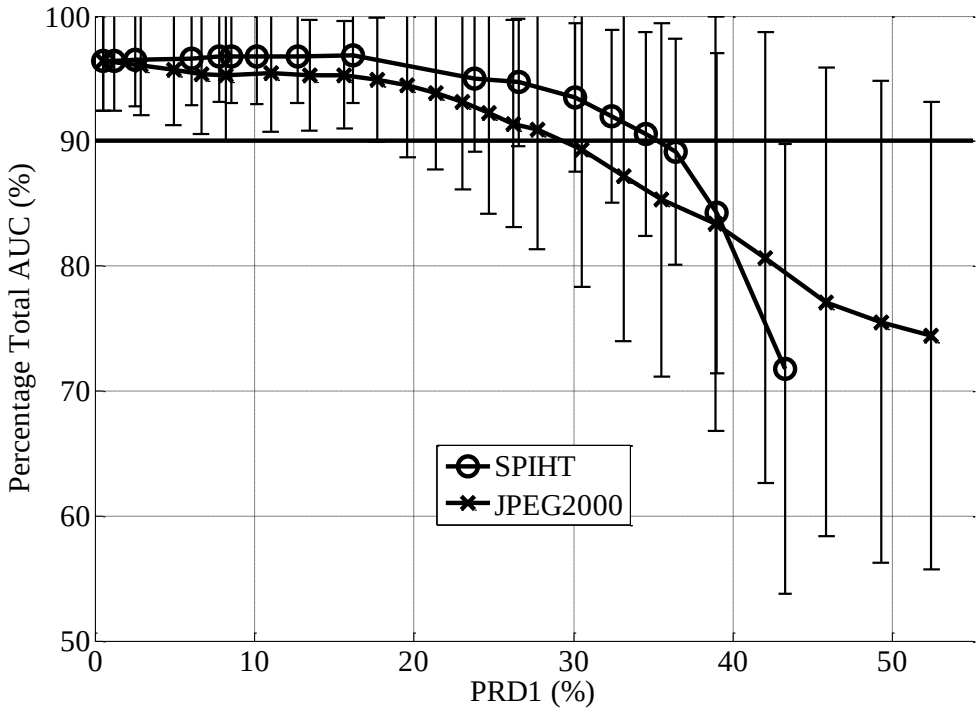

Figure 4.5: Percentage Total AUC as a factor of PRD1 for JPEG2000 and SPIHT-compressed signals for higher levels of loss, showing the 95% confidence intervals.

For SPIHT, Percentage Total AUC does not decline until PRD1 passes 18%. Performance actually increases from the lowest PRD1 until this point. While this improvement is near negligible, it can be explained by SPIHTs bit-truncation property acting as a filter, "cleaning-up" the signal prior to being processed by

REACT. The HF components of the signal are deemed as being of low importance by SPIHT and thus are the first to be discarded when the CR increases. These components generally correspond to noise in the signal and do not contain diagnostically relevant information. Above PRD1s of 18%, Percentage Total AUC begins to decline. It declines steadily until it drops below 90% AUC at a PRD1 of 36%. These results suggest that at 30% PRD1, the majority of seizure information is still maintained by both algorithms.

Finally, in order to evaluate the maximum achievable level of compression for given diagnostic performance, the Percentage Total AUC is plotted against CR in Figure 4.6. Here SPIHT's advantage in retaining better data fidelity at higher CRs can be clearly seen. Percentage Total AUC for JPEG2000 remains above 90% until the CR exceeds 30. SPIHT achieves far greater levels of compression before seizure detection performance is significantly impacted. At a CR of 90, Percentage Total AUC drops below the acceptable threshold of 90%.

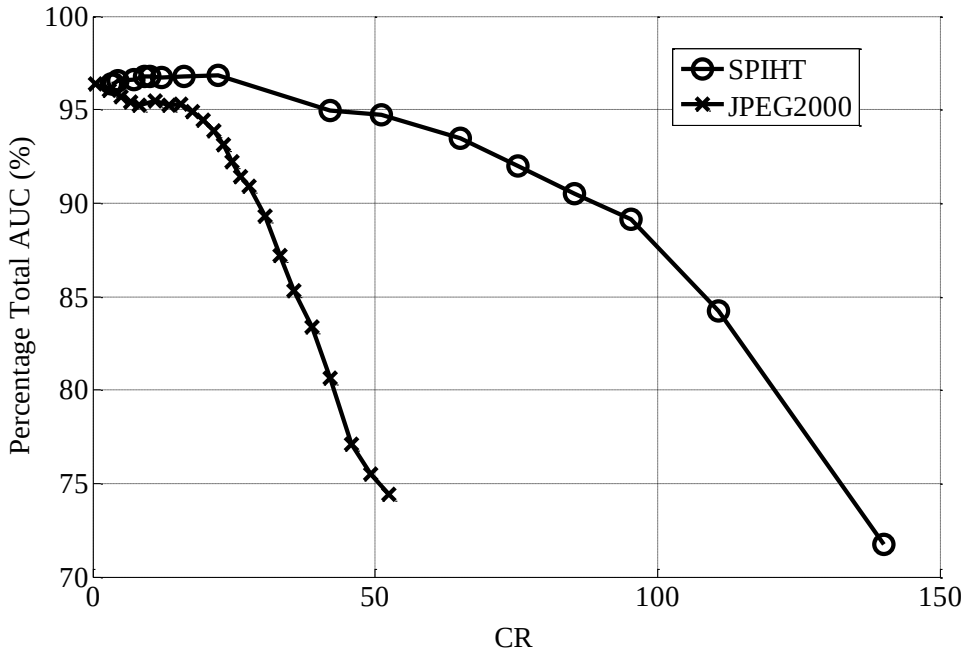

Figure 4.6: Percentage Total AUC as a factor CR for JPEG2000 and SPIHT-compressed signals for high levels of compression.

4.5 Energy Cost of Implementation

As the background of this research is the use of algorithms for ambulatory devices, an evaluation of the computation required for implementation on a portable device was carried out, with a view to estimating energy requirements and the benefits of compression. In [10] Yates and Rodriguez-Villegas determine that data compression in wireless EEG monitoring devices is of benefit if the computational cost of compression does not exceed the power saved due to the reduced time the transmission antenna is active. This implies there are two different factors to examine: 1) the computational complexity of compression on a DSP device, 2) the energy savings provided by compression prior to wireless transmission of the EEG data. To examine 1), the Analog Devices Blackfin BF537 DSP processor was chosen as a potential target for implementation [127]. As SPIHT was seen to provide better compression performance and maintain diagnostic information more effectively than JPEG2000, analysis focussed on SPIHT.

From Chapter 3, it can be seen that the SPIHT algorithm comprises of two arithmetic and two list operations. The arithmetic operations consist of compares and subtracts. Lists are used to keep track of insignificant sets and significant and insignificant coefficients. These lists dynamically vary in size. A linked list is an efficient dynamic data structure implementation which, for SPIHT, requires two core operations: 1) a push operation and 2) a list erase operation. It can therefore be seen that SPIHT compression is comprised of five unique instructions on the Blackfin BF537. The number of machine cycles for each of these operations was obtained empirically for this processor using the ADI Visual DSP++ profiling tool. These results of this analysis for each instruction operation are given in Table 4.1. Further details on estimating the power usage on the Blackfin BF537 can be found in [128].

Table 4.1: Average Numbers of Machine Cycles per operation on Analog Devices Blackfin BF537 DSP Processor.

Instruction	Number of Clock Cycles per operation
Integer compare	2
Sign compare	2
Integer subtract	2
Linked-list insert	67
Linked-list erase	62

To evaluate the energy cost of compression, the average number of operations required to compress one frame of EEG data was calculated. The Freiburg database was compressed with SPIHT at CRs ranging from 2 to 90, with the number of instruction operations tracked so that the average value could be determined. These values, and the total number of clock cycles required, can be found in Table 4.2.

Due to SPIHT's embedded coding property, the higher the CR required, the lower the complexity of the encoding operation. Assuming a clock speed of 50 MHz for the Blackfin DSP, the corresponding processor load factor can be estimated and is shown in the rightmost column of Table 4.2. Even allowing for an additional scaling factor to take any processor overhead into account, it can be seen that the algorithm does not significantly load the processor. These results indicate that the SPIHT compression would cause less than 0.1% load on the Blackfin processor at CR = 4 (<2% PRD1) and a 0.03% load at CR = 30 (~20% PRD1).

Table 4.2: Average number of operations per frame, number of machine cycles/frame, cycles/second and Processor Load for SPIHT Compression on Blackfin BF537 Processor, as a function of CR.

CR	Compare	Subtract	List Push	List Erase	Total Cycles	MIPS	50MHz Load (%)
2	54532	3437	131887	62733	252589	63148	0.01
4	51065	1729	119568	52122	224484	56122	0.01
8	45488	738	69904	26058	142188	35548	0.006
15	40397	340	41861	12743	95341	23836	0.004
20	38005	247	32234	9518	80005	20002	0.004
30	34621	158	22037	6579	63394	15849	0.003
40	32184	113	16692	5062	54051	13513	0.003
60	28859	69	11389	3456	43773	10944	0.002
70	27587	57	9800	2974	40418	10105	0.002
90	25581	41	7722	2308	35651	8913	0.002

Once the computational cost of compressing EEG signals using SPIHT was found to not significantly load the Blackfin processor, it was necessary to evaluate 2). For wireless transmission of compressed or uncompressed EEG data, Bluetooth Low Energy (LE) is a recently-introduced, low-powered transmission protocol that can be considered. Here, the expected power consumption for a typical commercial implementation of this protocol was considered. From [129] it can be estimated that the Nordic nRF8001 Bluetooth LE transmitter has a power-per-bit expenditure of ~33nJ/b. Table 4.3 gives the energy required to transmit a single four second frame of EEG data at CRs from 2 to 90.

Table 4.3: Energy Required to Transmit a Frame of EEG Data with Bluetooth LE.

Compression Ratio	2	7	9	50	60	90
nRF8001	0.54 mJ	0.07 mJ	60 µJ	10.8 µJ	9 µJ	6µJ

From Table 4.3, it can be seen that reducing the size of the data greatly reduces the cost of transmitting the data. From Table 4.2 and [127], [130] and [128] it can be estimated that SPIHT consumes ~15.9µJ of energy to compress 1 frame on the BF537 processor at a CR of 50:1. Combining the total energy to compress and transmit the data at this CR gives approximately 26.7µJ for compression and transmission. This corresponds to approximately 5% of the energy required to transmit the frame uncompressed. Even at a relatively low CR of 7:1, the energy to compress the data rises to ~64µJ, resulting in total energy for compression and transmission of 134µJ, equating to ~25% of the energy required to transmit the frame uncompressed. These results show that SPIHT satisfies the requirements set out in [10]. Both compression and transmission of the data results in a net decrease in the energy expenditure required if used on an ambulatory device.

4.6 Summary

This chapter presented two approaches to compressing EEG data using a modified JPEG2000 algorithm and SPIHT. These compression algorithms were implemented to examine their potential to compress EEG data on an ambulatory device, while maintaining diagnostically relevant information. The monitoring of seizure events, particularly in cases of epilepsy or potential epilepsy, was identified as a likely use for an AEEG device. A publicly-available database of EEG from patients with medically intractable focal epilepsy was used for testing. Initial research focused on compressing the database with low levels of PRD1. It was found that at low levels of fidelity loss, SPIHT provides a slightly better CR to PRD1 result. At 7% PRD1 JPEG2000 has an average CR of 9, while SPIHT has a CR of 8.3.

To ensure that PRD1s of 7% and lower did not unduly impact on the diagnostic integrity of the data, a proven automated seizure detection algorithm was employed.

It was found that low levels of fidelity loss had no impact on the seizure information contained within the signals. On the original dataset, REACT gave a Percentage Total AUC of 96%. At 7% PRD1, the Percentage Total AUC for JPEG2000 and for SPIHT did not drop below 95%.

A primary goal of this research was to examine the maximum potential compression gains that can be achieved with these algorithms, while maintaining seizure detection performance. The dataset was again compressed with higher levels of compression/loss. The previous tests were repeated at these higher levels, with the reconstructed signals again examined by the REACT system to monitor the impact on seizure data. SPIHT was seen to outperform JPEG2000 in terms of maintaining seizure detection performance at higher PRD1s. SPIHT maintains seizure detection performance for PRD1s up to 36%, while JPEG2000 drops below this point at 30%. By examining the CRs achieved by both algorithms at these levels of loss, it can be seen that SPIHT achieves a maximum CR of 90, while JPEG2000 achieves a maximum CR of 30.

Finally, an analysis was performed on the computational complexity of compressing and wirelessly transmitting EEG data. SPIHT was used for this analysis as it was found to provide better compression performance than JPEG2000. It was determined that SPIHT performs compression without significantly loading an Analog Devices Blackfin BF537 DSP processor. Because of the embedded nature of SPIHT, higher CRs correspond to even lower processor loading. The reduction in energy required to transmit a frame of EEG data for a range of CRs was also calculated. The analysis was performed using the data available for the Nordic nRF8001 Bluetooth LE transmitter. At the maximum level of compression, the amount of energy required to transmit is reduced by a factor of 10^3. This suggests that SPIHT could be implemented on a portable device and improve device performance by lowering the overall energy expenditure of the device. The next chapter builds upon the results presented here by examining an alternative approach to employing SPIHT to compress EEG data.

Chapter 5 The Effects of Wavelet Coefficient Quantisation in EEG Compression

5.1 Introduction

During the EEG compression research described previously, the quantisation bit-level was selected to ensure the DWT coefficients could be adequately represented after quantisation. Reducing the bits per coefficient through additional quantisation can offer a means of lossy compression that increase compression gains without adding to algorithm complexity. Quantisation is used as part of the overall compression algorithm in the majority of EEG compression research, yet the choice of quantisation level selected often appears to be arbitrary. Quantisation is a relatively simple operation where a large sequence of numbers is mapped onto a smaller scale, therefore requiring fewer bits to represent any given coefficient. However, this is a non-invertible, lossy operation, where the original value cannot be completely recovered after the mapping takes place. For this reason, bit-rates are often only selected to ensure all coefficients are adequately represented after the quantisation operation, ensuring it has minimal impact on the compressed signals quality. It was noted during early stages of research that decreasing the bit-level may

greatly improve compression levels, without undue impact on signal quality. It was therefore decided to investigate the possibility of varying the quantisation bit-rate as part of the compression process. As before, the quantisation operation was performed after the DWT operation

5.2 Research Methodology

Compression was performed on the Freiburg database as outlined in Chapter 3. Two variations on SPIHT based compression approaches were examined. This was done in order to isolate and compare the effects of varying quantisation levels of DWT coefficients. Both approaches involved the DWT, quantisation and SPIHT components. The first approach employs the traditional SPIHT approach (as used in Chapter 4) where the desired CR was selected prior to compression and was achieved by terminating encoding at the desired bit-length. For this approach, the quantisation level of the DWT coefficients was set at 16 bits. This higher bit-level was selected to isolate the compressive effects to that of SPIHT's bit-ordering/discarding. This approach was dubbed "Standard SPIHT" for this chapter to differentiate it from the second approach and the SPIHT compression done in the previous chapter. In the second approach, the number of bits available to the quantiser was varied and the resulting coefficients encoded using Non-Truncated SPIHT. In this approach, SPIHT was used as an entropy coder to gain maximum compressive gains from the lower bit-rates. This approach was taken to isolate the effects of varying the quantisation level in order to examine its specific effects. This approach was dubbed "Quantised SPIHT" or "QSPIHT".

In addition to CR and PRD1, for this study, two metrics were chosen to further evaluate the validity of the compressed results:

- The **Power Spectral Density (PSD)** is a method of analysing the contribution of each frequency to the overall signal power. It describes how the power of a time series is distributed with frequency. The PSD of the signals after compression were plotted against the PSD of the original signals to evaluate the impact of the lossy compression on the energy of the signal. The Welch method of PSD estimation was applied to the signals being analysed [131]. A segment length of 64 with a 50% overlap using the Hamming windowing method and 64 length window was used.

- Secondly, the **Cumulative Density Function (CDF)** is a measure of probability distribution of a random variable. Given a continuous random variable X, the CDF is denoted as a function $F(x)$, and is defined for a number x by:

$$F(x) = P(X \leq x) = \int_{-\infty}^{x} f(s)ds \tag{10}$$

That is, for a given value x, $F(x)$ gives the probability that the observed value of X will be less than or equal to x. The CDF was used to examine the likelihood of a compressed frame having a PRD1 at or below a specific value when the given compression parameters are applied.

5.3 Results

5.3.1 Standard SPIHT Compression

For this approach, the quantisation level was fixed at 16 bits. The signals were compressed with SPIHT at a range of lossy compression settings, ranging from CRs of 2 to 200, and then decompressed. The PRD1 of each frame was calculated and then the mean and standard deviation over the whole database was determined. Table 5.1 presents the results of this work.

As previously stated, two PRD1 limits are proposed for use in this research. The 7% and 30% limits were used as lower and higher cut-off points for seizure detection applications [55], [130], [132]. While the previous chapter found that a higher compression level could be acceptable with SPIHT compression, the lower level of 30% PRD1 found acceptable for JPEG2000 was selected here to ensure no loss in seizure information. These limits were therefore used as operating points for comparative reasons. It can be seen from Table 5.1 that a CR setting of 5 (dubbed 'CR5' to aid discussion of the results) gives a PRD1 of 5.99%, which lies within the 7% cut-off limit. Looking at the 30% limit, it can be seen that a CR setting of 35 (CR35) gives a PRD1 of 29.26%.

Table 5.1: Results for Standard SPIHT Compression.

CR	Average PRD1 (%)	Standard Deviation (%)
200	63.49	20.67
160	58.63	20.29
110	50.78	19.73
55	36.97	19.08
40	31.40	18.92
35	29.26	18.85
30	26.90	18.50
10	12.29	11.02
7	8.94	8.97
6	7.67	7.95
5	5.99	6.18
2	0.52	0.34

The final column gives the standard deviation of the PRD1 results. At the proposed settings, the standard deviation is ±6.18% and ±18.85% respectively. This suggests that while the average PRD1 results fall within the limits, it is obvious that some frames can be well above the desired limits. Further analysis of these results is provided later in this chapter.

5.3.2 QSPIHT Compression

For this section, the database was compressed by quantising the data in the range of 1 to 15 bits, and compressed using Non-Truncated SPIHT. Table 5.2 gives the CRs for the database after SPIHT compression has been applied. The PRD1 values were recorded for each frame and then averaged over the whole database at each quantisation level. Table 5.2 gives the average PRD1 and standard deviation at each quantisation level.

Table 5.2: Results for QSPIHT Compression.

Quantisation Level	QSPIHT CR	Average PRD1 (%)	Standard Deviation(%)
1	613.20	68.15	13.18
2	260.13	50.09	15.43
3	128.78	35.04	15.23
4	70.88	23.66	13.88
5	40.14	15.58	12.11
6	22.39	9.89	9.56
7	13.05	6.09	7.00
8	8.14	3.67	5.09
9	5.51	2.18	3.66
10	4.11	1.32	2.89
11	3.27	0.83	2.49
12	2.74	0.56	2.34
13	2.36	0.42	2.29
14	2.09	0.34	2.28
15	1.88	0.31	2.27

Looking at the results, it can be seen that while the PRD1 initially increases slowly, the rate of increase gets larger as the quantisation level approaches 1 bit. Taking the initial 7% PRD1 limit, it can be seen that at 7 bit quantisation (Q7) the PRD1 is 6.09%. For the 30% PRD1 limit, far lower quantisation levels can be tolerated. In this case, 4 bit quantisation (Q4) is required to bring the results below the 30% cut-off point, giving an average PRD1 of 23.66%. Again the standard deviation is given in the last column of the table. For the suggested limits of 7% and 30% the standard deviation of PRD1 is ±7.00% and ±13.88% respectively. Further analysis of the distribution of the results is therefore required and provided later in this chapter.

5.3.3 Comparison and Analysis

In order to evaluate the performance of each approach, it is necessary to look at the PRD1 achieved by each at any given CR. Figure 5.1 gives a plot of the CR vs. PRD1 for both methods.

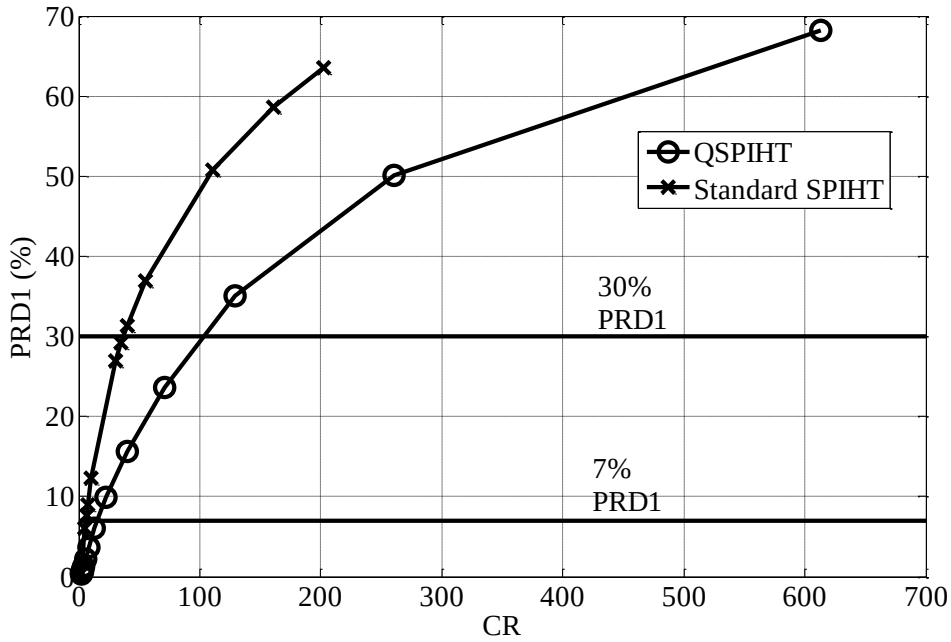

Figure 5.1: Plot of PRD1 vs. CR for Standard SPIHT and QSPIHT approaches.

While the CRs for the Standard SPIHT approach are known prior to compression, the exact CRs for the QSPIHT approach can only be determined after compression has taken place. This is due to the variable compression parameter for QSPIHT being provided by the quantisation block, with SPIHT being employed as an entropy encoder, i.e. in Non-Truncated mode. Figure 5.2 gives a magnified view of Figure 5.1 from 0% to 10% PRD1. Looking at Figure 5.2 it can be seen that both approaches initially have very similar PRD1 and CR values. This is to be expected as at this point both approaches have little loss in signal fidelity, keeping CRs low.

As the compression rate increases, the curves diverge. It is clear from the graph that QSPIHT out-performs Standard SPIHT compression in terms of PRD1 at a given CR. While the largest gains are at the higher CRs, these results fall outside the upper limits of loss assumed to be acceptable in this research. Below the 30% limit, the QSPIHT approach still provides an advantage. At 30% PRD1, the QSPIHT approach gives a CR of just over 100, while the Standard SPIHT approach gives a CR of approximately 40.

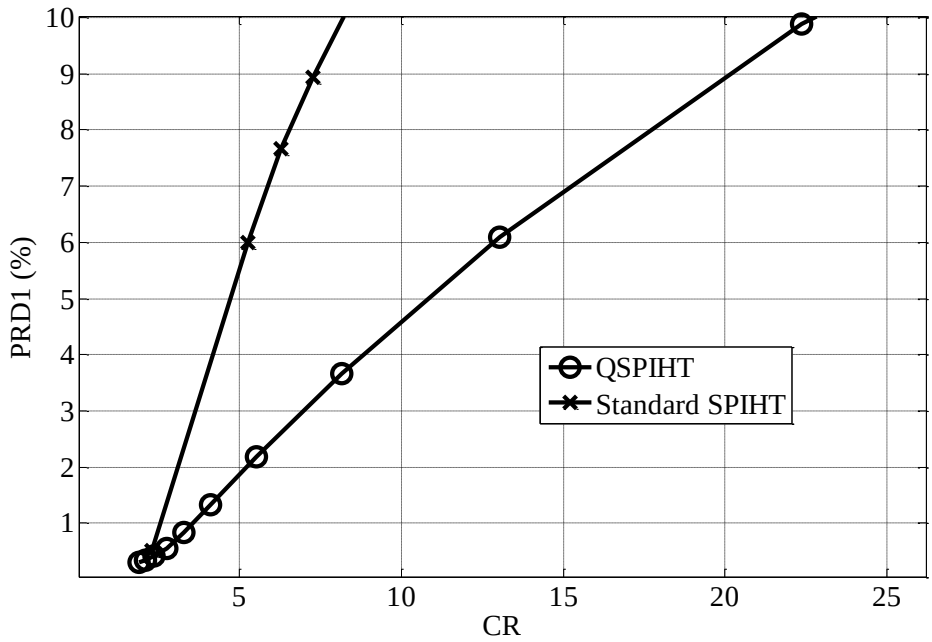

Figure 5.2: Plot of PRD vs. CR for PRD1s up to 10%.

Within the 7% PRD1 limit, the advantage of the quantisation approach is still substantial. At Q7, the average PRD1 falls below this 7% limit and gives a CR of 13.05. At 7% PRD1, Standard SPIHT gives a CR of approximately 6.

In order to analyse the distribution of the PRD1 results at the proposed compression settings, the Cumulative Density Function (CDF) for the resulting frames was calculated and plotted. Figure 5.3 shows the CDF of the QSPIHT and Standard SPIHT approaches at Q7 and CR5 respectively for the 7% PRD1 limit. Looking at Figure 5.3 it can be seen that the CDF of both approaches are very similar. Both rise rapidly until the probability goes above 0.9, where a shallower increase can be observed. This is to be expected as the (relatively) low compression settings maintain most of the signal fidelity. Examining the 7% PRD1 (x = 7), it can be seen that the probability of a given frame having a PRD1 of 7% or less for both approaches is 0.8 or 80%.

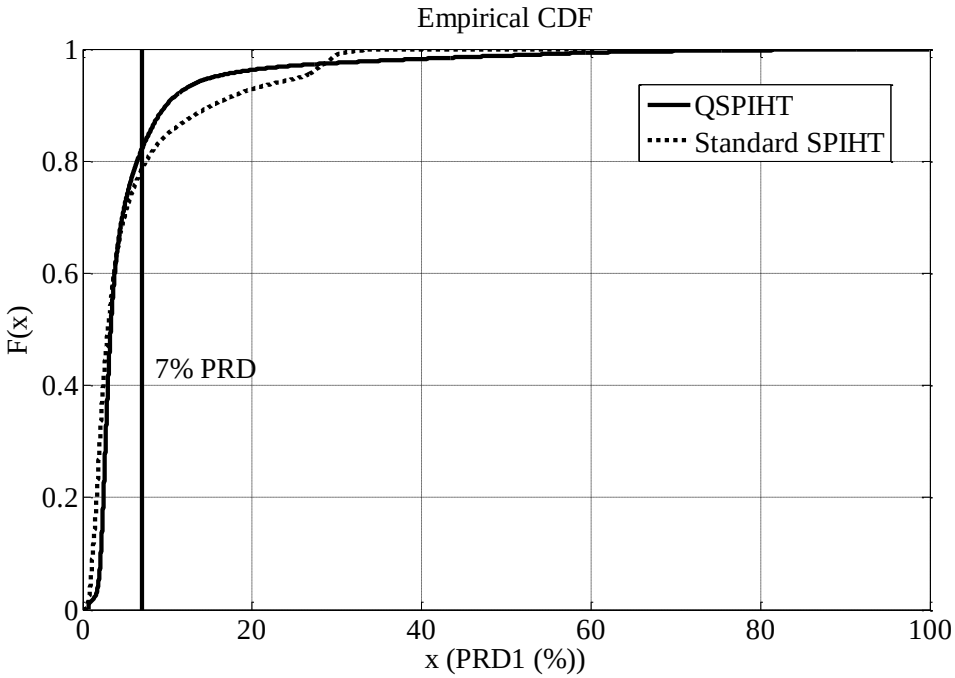

Figure 5.3: Cumulative Distribution Function of PRD1 results per frame at proposed 7% PRD settings.

Figure 5.4 shows the CDF of both algorithms at the proposed 30% PRD1 settings (Q4 and CR35). Again both CDFs follow a similar distribution. Standard SPIHT starts higher than QSPIHT, implying a higher proportion of frames with PRD1s below 10%. Above this however, QSPIHT rises faster than Standard SPIHT, implying the QSPIHT approach gives lower PRD1s than Standard SPIHT in this range. At 30% PRD1 (x = 30) there is a 0.8 or 80% chance for QSPIHT and approximately 0.75 or 75% chance for Standard SPIHT that a given frame will have a PRD1 equal to or lower than the cut-off.

Since PRD1 is a measure of the level of difference between two signals and not, by definition, an objective evaluation of the impact of the loss of diagnostically relevant information in the signal, it should not be used as the sole metric to evaluate the performance of the algorithms. To do this, a visual inspection and PSD analysis was performed on a selection of reconstructed files whose PRD1s were close to the above limits. Figure 5.5 and Figure 5.6 give the PSDs of the original signal and those of the QSPIHT and Standard SPIHT approaches at the 30% and 7% cut-off PRD1s, given in Plots (i-ii) in each Figure. Figure 5.5 is a randomly chosen EEG signals containing no seizure information, while Figure 5.6 was chosen to contain periods of seizure data. The parameters found to give optimum results in the section above were used

to select the signals for comparison. Specifically, these were CR35 and Q4 at 30% PRD1 and CR5 and Q7 at 7% PRD1 for Standard SPIHT and QSPIHT respectively. Performance was judged on how closely the PSD of the reconstructed signals visually matched that of the original signal, i.e. how well the energy is maintained in the signal after lossy compression.

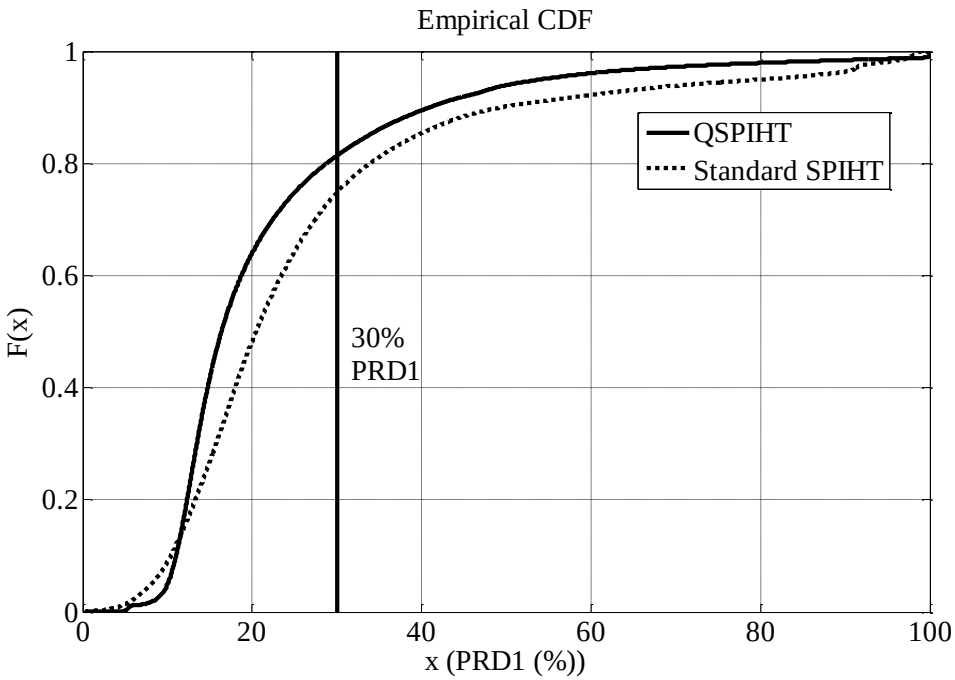

Figure 5.4: Cumulative Distribution Function of PRD1 results per frame at proposed 30% PRD settings.

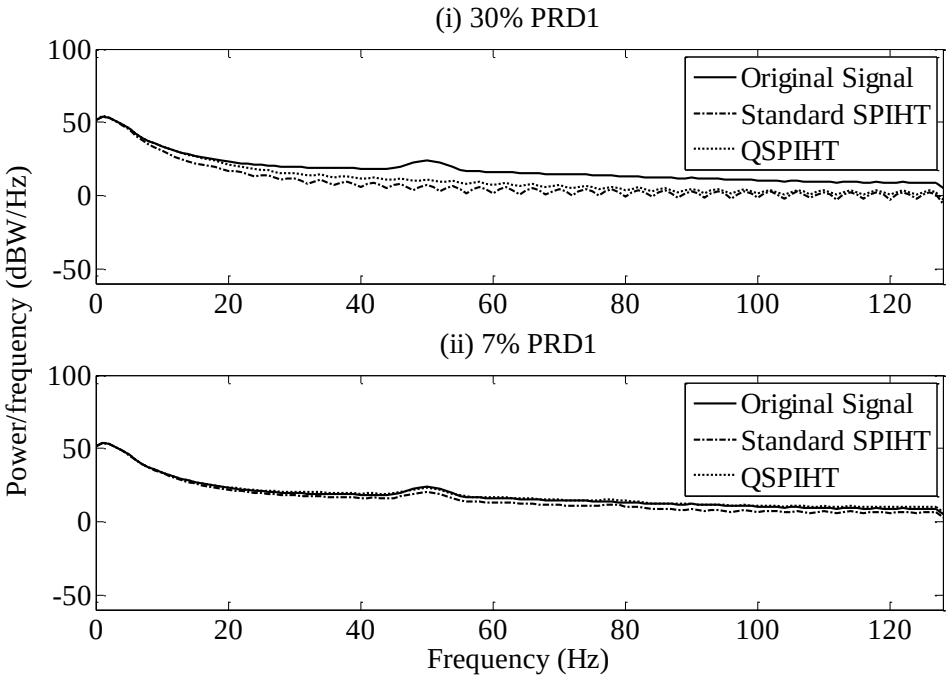

Figure 5.5: Welch Power Spectral Density (PSD) of non-seizure EEG sample.

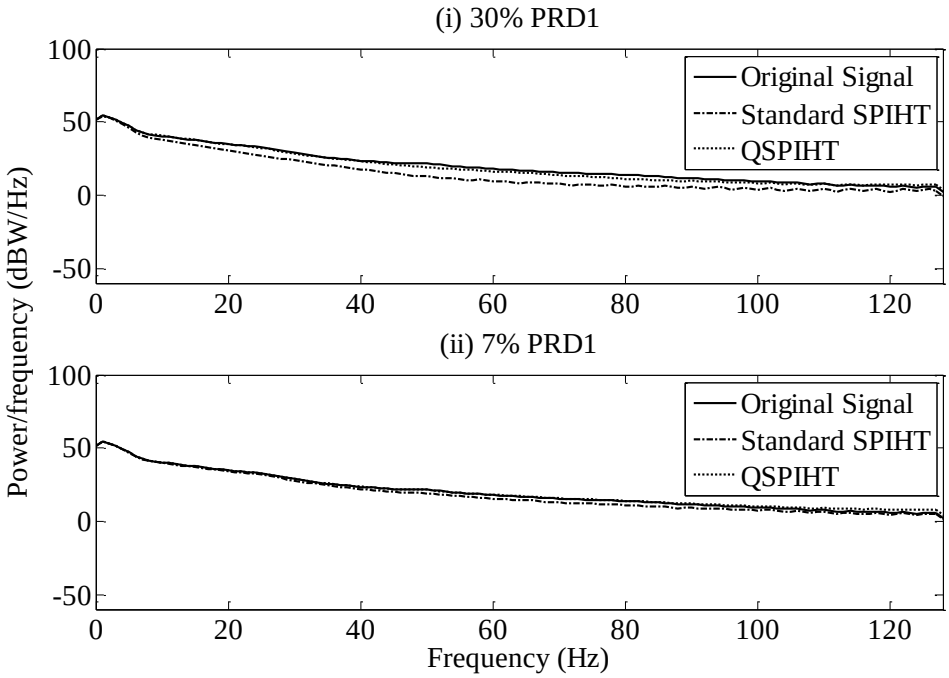

Figure 5.6: Welch Power Spectral Density (PSD) of EEG sample containing seizure.

Generally all four reconstructed signals maintain a PSD close to that of the original signal, particularly in the case of the low PRD signals. Figure 5.5 shows the greatest amount of variation in the signals PSDs with all PSDs being very similar in Figure

5.6. Plot (i) shows Standard SPIHT at CR35. The greatest variation in original and reconstructed signals PSDs can be seen here, with the reconstructed signals power being generally slightly lower than the original. Plot (i) also shows QSPIHT at Q4. Here the PSD is closer to that of the original signal, although some variation is still visible. Plot (ii) shows Standard SPIHT at CR5. Again an improvement can be seen in the reconstructed signals PSD but some loss in fidelity is still evident. Finally, Plot (ii) also displays QSPIHT at Q7. Here almost no variation in PSD between the original and reconstructed signals is visible, suggesting almost no loss in signal information during compression.

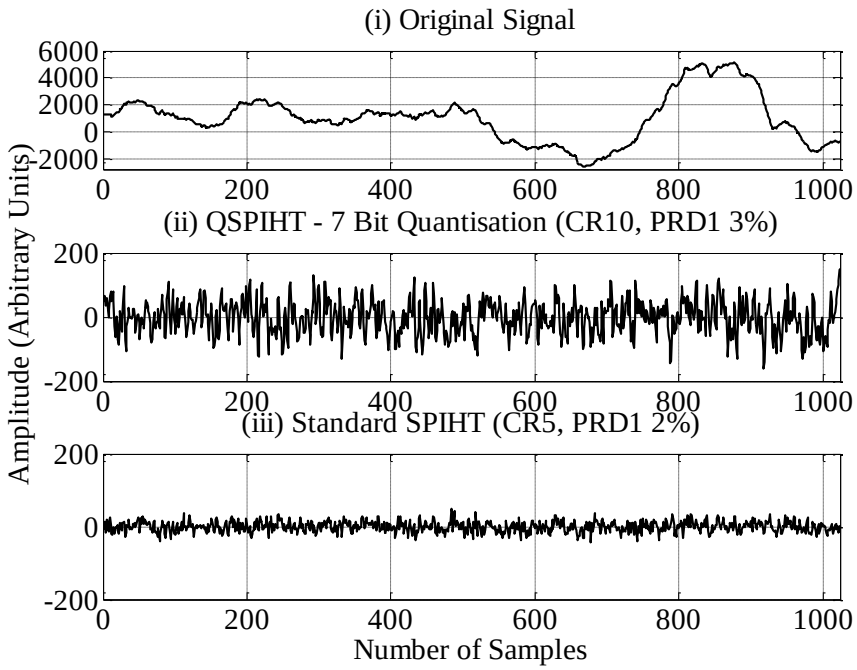

Figure 5.7: Plot of sample EEG signal. (i) Original EEG Signal and error signals after compression with (ii) QSPIHT at Q7, and (iii) Standard SPIHT at CR5.

A visual inspection was also performed on the signals. Figure 5.7 shows a sample of the database with (i) the original EEG signal, and the signal compressed with (ii) QSPIHT at Q4 and (iii) Standard SPIHT at CR5. This signal was chosen at random and give CRs of 10 and 5 and PRD1s of 3% and 2% respectively. Visually, these three signals are near identical. No differences between the three can be discerned, suggesting very high retention of signal integrity. Figure 5.8 shows a plot of (i) the same original EEG signal, and the corresponding sample compressed with (ii)

QSPIHT at Q4 and (iii) Standard SPIHT at CR35. At these settings, it gives a CR of 42 and 35 and PRD of 14% and 17% respectively. At this higher level of loss, some visual discrepancies can be seen. These higher levels of compression cause a smoothing effect on the signals due to the loss of finer detail coefficients. While some of the finer details are lost in the compression, the general shape of the signal is very well maintained. This again suggests the majority of the signal information is maintained at this compression level.

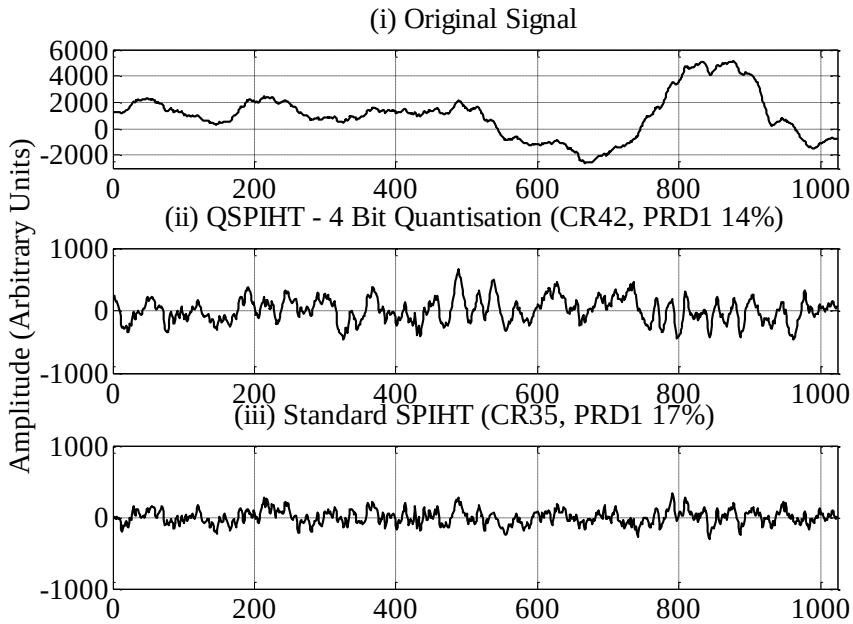

Figure 5.8: Plots of sample EEG signal: (i) Original EEG Signal and resulting errors after compression with (ii) QSPIHT at Q4, and (iii) Standard SPIHT at CR35.

The similarities, visually and in the PSDs, of the original and reconstructed signals after compression lends credence to the choice of the 7% and 30% PRDs as operating points, as most of the signals power is preserved at each compression level. When QSPIHTs superior PSD results are combined with the compression results from Sections 5.3.1 and 5.3.2 above, a clear advantage in increasing quantisation level (reducing bit-rate) to improve CR performance can be seen. These observations are backed-up by the conclusions reached in Chapter 4 which found Standard SPIHT could maintain diagnostic integrity up to PRD1s of 36% at a bit-level of 10.

5.4 Comparison with Other Work

Additional testing was done on two publically available EEG databases to directly compare the benefits of this compression approach with similar EEG research. It should be noted that the alternative definition of PRD1 (i.e. PRD) , employed by [55], does not remove the signal mean prior to calculation. In the case of [54] and [55], QSPIHT was applied to the same databases to aid comparison. The databases used were the MIT-BIH Polysomnographic database and the CHB-MIT Scalp EEG database [133]. Table 5.3 gives the results of QSPIHT run on these databases for bit-levels 4 to 9.

For transform based compression, Cárdenas-Barrera reported an average PRD of 9.54% and CR of 7.79; while at 7 bit quantisation the average CR is 5.68 with an average PRD of 6.02% in [55]. Table 5.3 gives the corresponding results for QSPIHT. At Q7, a CR of 9.5 at a PRD1 of 6.93% is achieved. It is interesting to note the advantage of using SPIHT as an entropy encoder, increasing the CRs from 7.79 to 13.021 and 5.68 to 9.5024 for 6 and 7 bit quantisation respectively.

Table 5.3: CR and PRD1 results for QSPIHT run on MIT-BIH Polysomnographic and CHB-MIT Scalp EEG databases.

	MIT-BIH Polysomnographic		**CHB-MIT Scalp EEG**	
Bit Level	**CR**	**PRD1(%)**	**CR**	**PRD1(%)**
4	34.47	29.89	24.33	16.60
5	20.04	19.24	13.42	10.03
6	13.02	11.81	8.02	5.71
7	9.50	6.93	5.33	3.08
8	7.34	4.08	3.93	1.61
9	3.73	2.54	3.14	0.84

An alternative approach to compression is presented in [54]. Bazán-Prieto *et al.* report achieving a CR of 5.97 at 4.61% PRD1 and 11.23 CR at 10.45% PRD1 for the CHB-MIT Scalp EEG database. On the same database, QSPIHT gave a CR of 5.33 at 3.08% PRD1 and 13.42 CR at 10% PRD1. This was achieved at Q7 and Q5 respectively. For the MIT-BIH Polysomnographic database, a CR of 4.11 is reported at 3.79% PRD1 and 8.21 CR at 10.26% PRD1. QSPIHT achieved a CR of 3.73 at a

2.54% PRD1 and 13.02 CR at 11.81% PRD1. This was achieved at Q9 and Q6 respectively.

5.5 Summary

This chapter examined two methods of EEG compression based on reducing data length by: (i) ordering the coefficients into hierarchical trees and then discarding those that fall below the threshold value and (ii) rounding coefficients to integer values using varying levels of quantisation and losslessly compressing them. This was done by applying the SPIHT algorithm at a variety of compression levels in the first approach and varying the quantisation level for the second. Two limits of signal loss were used to evaluate the compression algorithms performance against each other in relation to real-world applications. It was found that (ii) achieved higher CRs at a given PRD1 than (i). At a 7% PRD1, (ii) achieved a CR of 13.05 while (i) achieved 6. At 30% PRD1, (ii) achieved a CR of 100 compared to 40 with (i). The validity of these results was evaluated by comparing the information contained in the signals after they had been decompressed, with that of the original signal. It was found that the reconstructed signals maintain the energy spectrum of the original signal well, particularly at low PRD1s. Furthermore, it was found that the PSD of data compressed using (ii) was closer to that of the original signals than (i). This suggests that (ii) achieves higher CRs than (i) while maintaining better data fidelity. Thus, it appears to be more beneficial to the integrity of the EEG data to use a compression method that represents all signal coefficients, even in a reduced form, rather than one that simply discards coefficients.

This work may be extended by applying the results found here to the design of an EEG compression algorithm that makes use of higher quantisation levels as the basis of compression. Combining higher quantisation levels with other methods of data compression may offer a means of further increasing CRs without undue impact on the EEG signals. While SPIHT was used here in Non-Truncating mode, the results may be improved by combining higher quantisation levels, with a measure of lossy compression.

Chapter 6 examines the impact of bit errors on compressed bioelectric signals and investigates methodologies to protect against these effects, without undue data overheads.

Chapter 6 ECG Compression with SPIHT in the Presence of Bit Errors

6.1 Introduction

A general feature of signal compression is that as the compression level increases, the importance of an individual bit to the reconstructed signal also increases; this is particularly true in the case of an embedded encoder such as SPIHT where the encoded bits are arranged in order of importance. In the case of ambulatory capture of signals, a bit error may cause irreplaceably corrupted data. In the worst-case scenario, the corruption may go undetected and result in misdiagnosis. The final stage of this research examines the effects of bit errors on SPIHT-compressed biomedical signals and looks at how these bit streams can be protected to preserve diagnostic integrity. This chapter focuses on the effects of bit errors on compressed bit streams and the impact the location of these errors has on diagnostically relevant signal information.

For this research it was decided to look at ECG data, given that ECG is typically envisioned as being part of an ambulatory-care system. ECG signals are more widely researched than EEG, with established, standardised metrics to measure the diagnostic information relating to a wide variety of conditions [17], [25], [26]. SPIHT compression of ECG data has already been examined by a number of researchers (e.g. [75], [134]–[137]]) and found to give good compression gains to

fidelity loss results. It was decided to further existing research in this area by looking at the effects of bit errors on these signals, and how to protect against them. The ECG data was initially compressed with the SPIHT algorithm, using the same approach as outlined in Chapter 4 for the compression of EEG data using SPIHT. Based on an understanding of the effects of transmission bit errors on compressed signals, a further goal of this research is to design error-protection schemes which do not overly inflate the size of the compressed data, as this would negate the benefits of signal compression to begin with.

The initial part of this chapter focuses on classifying the importance of location of a bit error in regards to the resulting signal integrity. Next, it examines the impact of randomly distributed bit errors, at a range of Bit Error Ratios (BERs), on the signal fidelity. Finally this chapter examines the impact of increasing compression on these signals, specifically in relation to the same BERs at lossless compression.

6.2 MIT-BIH ECG Database

The database used for this study was the MIT-BIH Arrhythmia database, which is a collection of ECG signals widely used for evaluation of arrhythmia detectors [133], [138]. It contains 48 half-hour excerpts of two-channel ambulatory ECG recordings, at 360 samples per second per channel with 11-bit resolution. The database consists of 23 of the records, chosen at random from a set of 24-hour ambulatory recordings, while the remaining 25 were selected to include less common arrhythmias that are clinically significant and deemed necessary to include for a complete arrhythmia database. Although this database was originally created for testing of arrhythmia detectors, it has since become the most widely used database for other ECG processing procedures, including compression (e.g. [81], [134], [137], [139]).

6.3 ECG-specific Performance Evaluation

6.3.1 Heart Rate Variability (HRV)

Heart Rate Variability (HRV) is a term used to describe variations in instantaneous heart rate and RR intervals [25]. It encompasses a wide range of time-domain, statistical and frequency-domain measurements that are used to look for abnormalities in cardiac operation. The number of metrics available has led to

confusion in the most appropriate metric to monitor for desired applications, with several metrics recording the same information in different ways. A number of guidelines have been published to aid in selection of the appropriate metrics. A joint task force consisting of the European Society of Cardiology and the North American Society of Pacing and Electrophysiology published guidelines on HRV measurements, their physiological interpretation and clinical usage to guard against incorrect conclusions and excessive or unfounded extrapolation of observations [25]. In these guidelines they give the most commonly found HRV measurements in the time and frequency domains, defining what they are and outlining the information they provide. The guidelines also provide a table of the approximate correspondence between time domain and frequency domain measurements for 24hr ECG recordings. Although this guideline was published in 1996, the outline of HRV metrics, their physiological correlates and the correspondence between time and frequency domain measurements has not changed significantly.

The American College of Cardiology/American Heart Association/American College of Physicians-American Society of Internal Medicine (ACC/AHA/ACP-ASIM) Task Force on Clinical Competence was formed in 1998 specifically to improve the skills necessary to competently perform cardiovascular care. In 1999 they published practice guidelines for ambulatory ECG (AECG) [26]. The stated purpose of this guideline is to provide information to a clinician on the use of AECG to assist them in clinical decision making. It outlines the advantages of AECG usage as well as some of its limitations, dividing clinical situations into three classifications:

Class I: Conditions for which there is evidence and/or general agreement that a given procedure or treatment is useful and effective.

Class II: Conditions for which there is conflicting evidence and/or a divergence of opinion about the usefulness/efficacy of a procedure or treatment

Class IIa: Weight of evidence/opinion is in favour of usefulness/efficacy

Class IIb: Usefulness/efficacy is less well established by evidence/opinion

Class III: Conditions for which there is evidence and/or general agreement that the procedure/treatment is not useful/effective, and in some cases may be harmful.

These classifications make it easy to establish the usefulness of using an AECG device to monitor specific cardiac conditions. Furthermore [26] provides information on the relevant parts of the QRS complex for specific diagnoses (see Figure 2.1). Similar to [25], it provides information on the diagnostic information contained in various HRV metrics as well as a table of correlates between time and frequency domain measurements.

6.3.2 Selected Metrics

A sub-set of HRV metrics was chosen to aid in the monitoring of loss of clinically relevant signal information. The BioSig Toolbox [140] provides a range of tools for automated analysis of HRV metrics in ECG signals. By comparing the results of these metrics on the original signal and those performed on the signals after compression and other processing, it is possible to observe the impact of compression on the diagnostic information in the signal. From the available literature ([25], [26]), several metrics were chosen. The purpose of these metrics and the reason for their inclusion are as follows:

- meanNN: this is the average value of the Normal-to-Normal (NN) intervals. NN intervals are the normalised intervals between adjacent QRS complexes, measured between the R components of the complex (Figure 2.1). Variations in meanNN indicate changes in the cardiac rhythm, e.g. increased or decreased heart rate.
- SDNN standard deviation between all NN intervals. Standard deviation can be calculated as the square root of the overall signal variance. SDNN reflects the cyclical components responsible for variability in the period of recording. This is often referred to as an estimate of overall HRV. In [25] it is explained that SDNN approximately corresponds to Total Power in the frequency domain .
- HF Power is the power in the high frequency range of 0.15-0.4 Hz. It reflects the parasympathetic tone, i.e. the autonomous system that reduces heat-rate [26]. As HF components are generally given lower priority by encoders such as SPIHT, it was included in analysis due to its potentially greater susceptibility to bit errors.

- LF/HF Ratio is the ratio between Low Frequency (LF) components and High Frequency (HF) components. LF is given as the power in low frequency range of 0.04-0.15 Hz. It reflects sympathovagal modulations, i.e. the modulations between the sympathetic nervous systems and the vagus nerve [26]. As it is a measure of the ratio between LF and HF components, variations in both are simultaneously reflected.

Two further metrics were used to measure the accuracy of the beat reconstruction. Beat detection is important for arrhythmia detection [141], [142]. It relies on accurately detecting the "beat", or R wave fiducial point, in successive QRS complexes. In [143], Afonso *et al.* outline a filter bank based beat detection algorithm with a very high detection accuracy on the MIT/BIH database. This accuracy is measured by the beat detection algorithm detecting the fiducial point of the waveform, within a window of error, in comparison to the actual fiducial point as identified by clinicians, and as provided with the MIT/BIH database. Accuracy is determined by means of two benchmark parameters: Sensitivity (Se) and Positive Predictability (PP). Se determines the percentage of true beats correctly detected by the algorithm, while PP gives the percentage of beat detections which were really true beats. These are given by the formulae:

$$Se = \frac{TP}{TP + FN} \times 100 \tag{11}$$

$$PP = \frac{TP}{TP + FP} \times 100 \tag{12}$$

In this case TPs are beats correctly detected, FNs are missed beats and FPs are beats detected by the algorithm but do not exist in the original signal.

It is clear from the descriptions of the above metrics that the results will be expressed in a range of units and scales. This creates a difficulty in presenting the results in an easy-to-read format. For this reason, all ECG specific metrics performance was measured as a Percentage Similarity (*PSim*) between the metric as measured on the original signal, and the same metric as measured on the reconstructed signal. This can be expressed as

$$PSim = 100 - \left(\frac{|y - \bar{y}|}{y} \times 100 \right) \quad (13)$$

where y is the value of the metric from the original signal and $\bar{y}$ is the corresponding value of the same metric from the processed signal. This has the advantage that all results are expressed in the same units and on the same scale, allowing for easier comparison. In conjunction with these ECG specific metrics, PRD1 and CR were also used. An explanation of PRD1 and CR can be found in Chapter 3. Examination of acceptable levels of fidelity loss have been presented in other research e.g. Zigel *et al.* [117]. In this paper, the authors proposed quality groups for compressed ECG signals, and examined the utility of various signal measures as predictors of these quality groups. These quality groups range from *'very good'* to *'bad'*, based on how closely they match the original signal and maintain the diagnostic information contained within them. For example, classification based on PRD1 is given in Table 6.1.

Table 6.1: PRD Quality groups proposed by Zigel *et al*. **[117]** based on PRD1.

Quality Groups	PRD Ranges (%)	Corresponding Percentage Similarity Ranges for PRD1 (%)
'very good'	0-2	100-98
'good'	2-9	98-91
'not good'	9-19	91-81
'bad'	19-60	81-40

6.4 Experimental Procedure

6.4.1 ECG Compression with SPIHT

SPIHT's embedded nature means the encoder can stop encoding when the desired CR is reached and that the encoded bit stream will be ordered from Most-Significant

Bit (MSB) to Least-Significant Bit (LSB). Initially the MIT-BIH database was compressed using Non-Truncated SPIHT. Each ECG signal was split into windows of size 1024 and encoded using SPIHT. As noted previously in Chapter 3, SPIHT possesses inherent signal compression behaviour (even without truncation of the encoded bit stream). This creates a natural variation in the size of the compressed frames due to some frames compressing more efficiently than others because of the bit-ordering operation carried out by SPIHT. Table 6.2 shows the statistical analysis of the length of the frames after SPIHT (before truncation of the encoded bit stream), giving the maximum, minimum, average and standard deviation of the encoded frame lengths (note that the input frame is 11264 bits long – 1024 ECG samples at 11 bits/sample).The variation in compressed bit-length can be explained by the variation in complexity of the signal being represented. SPIHT represents frames with small variations in coefficients more efficiently, resulting in short bit streams. Similarly, large variations in coefficients result in SPIHT requiring longer bit streams to represent all coefficients.

Table 6.2: Statistical analysis of Non-Truncated SPIHT encoded MIT-BIH database**.**

	Bit Length	CR
Mean	4296.5	2.6
Max	7523	20.4
Min	551	1.5
Standard Deviation	±968.5	±0.7860

6.4.2 Effect of Error Location

As SPIHT orders the compressed bit stream from MSB to LSB, the location of an erroneous bit will affect the impact it has on the reconstructed signal. The length of the compressed frames was then analysed and a fixed length for each frame of 5098 bits was selected as it gave a 90% chance of the frame having a PRD1 of just over 1% or lower and 100% chance of it being lower than 3% PRD1. This corresponds to a result of *'very good'* or *'good'* for the quality of the reconstructed ECG signal

(Table 6.1). Figure 6.1 shows the Cumulative Distribution Frequency (CDF) of the PRD1 for all MIT-BIH database entries reconstructed from a bit-length of 5098, showing that there is a 100% chance that any given frame will have a PRD1 of 3% or lower. In order to classify this effect, each frame was divided into 16 segments of equal length and a single bit error was introduced at random into each section. The signals were then decompressed and the aforementioned performance metrics evaluated. Figure 6.2 shows a plot of the performance metrics in relation to where the error occurs in the signal. The x-axis shows the region the bit error occurred in ascending order from Least-Significant Section (LSS) to Most-Significant Section (MSS). The MSS corresponds to the section at the beginning of the compressed bit stream; i.e. the section including the bits deemed most important by the SPIHT encoder. The LSS corresponds to the section containing the final bits of the compressed stream; i.e. those deemed least important by SPIHT.

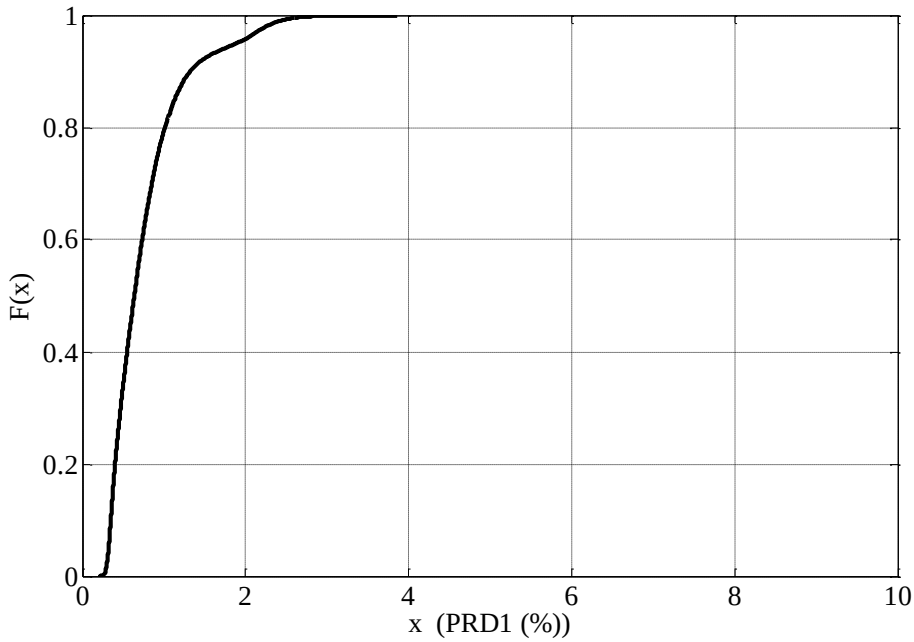

Figure 6.1: CDF of PRD1 for frames of length 5098.

As can be expected, the results deteriorate the closer the bit error gets to the MSS. A bit error in the latter part of the signal has little to no impact on the signal. Only PRD1 is affected by bit errors outside the first portion of the signal. Psim for PRD1 declines slowly from 100% as the location of the bit error moves closer to the MSB.

A sharp decline in performance can be seen when the bit error occurs in the MSS. It can be seen that the PSim for PRD1 falls to 7%, suggesting the resulting signal bears little resemblance to the original. This is also suggested by the Psim for SDNN, LF/HF Ratio and HF Power, all having 0% similarities to their original values. PP, Sensitivity and meanNN perform better but are still far below what would be acceptable for clinical applications.

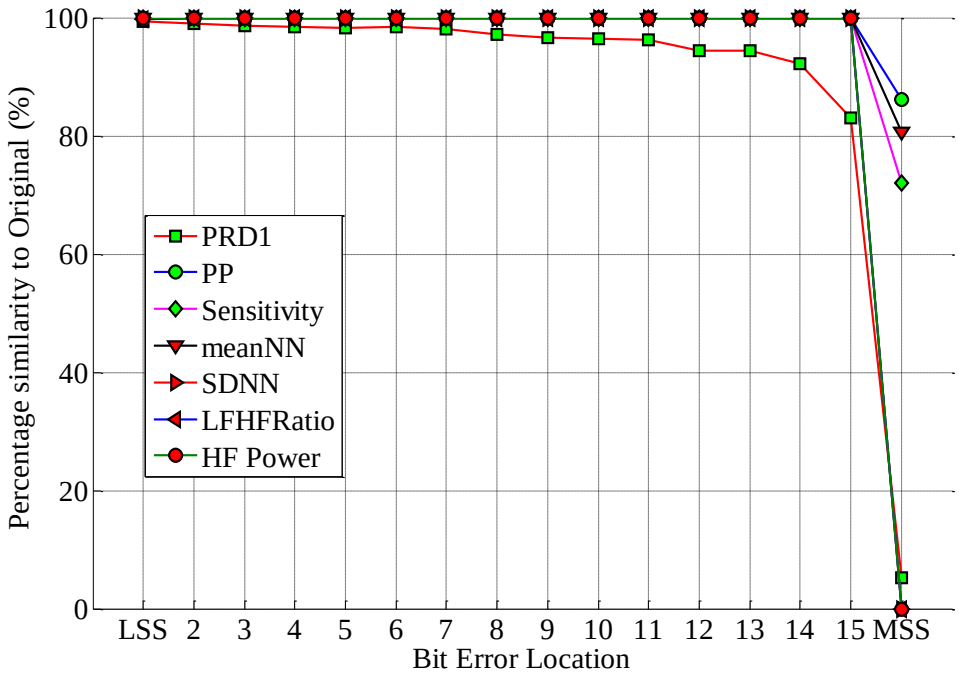

Figure 6.2: Plot of Performance Metrics as a function of Bit Error Location.

The most interesting result from this is that single bit errors have relatively little effect on the reconstructed signal until they are very close to the MSB. This is consistent with the work of Twomey *et. al* [137] who found that ECG signals could be compressed up to 30:1 with SPIHT, while maintaining diagnostic quality.

6.4.3 Effect of BER on Compression Performance

To evaluate the effects of noise on ECG signals, BERs from the range {0, 10^{-6}, 10^{-5}, 10^{-4}, 10^{-3}, 10^{-2}} were applied to the signals compressed with Non-Truncated SPIHT for each ECG record before decompression and reconstruction. For this test, no fixed bit-length was used. The entire ECG record was compressed in individual frames and then concatenated to form a single compressed bit stream. Bits errors were

introduced at random to the stream; the number of errors was dependant on the current BER and the length of the concatenated stream. Finally, the concatenated bit stream was re-split into its original frames and reconstructed into a single signal to match the original ECG record. Metric results were then calculated on these reconstructed signals.

Noise was modelled as random, normally-distributed bit errors. This simple approach was chosen as the research objective was to analyse SPIHT's robustness to random bit errors. However, it is noted that this error distribution may not always be completely valid; for example, in [144], the authors analysed the distribution of bit errors in the IEEE 802.11 wireless communication standard with a variety of hardware. They observed that the likelihood of a bit being received in error increases the later the error occurs in the bit stream. The implications of this in respect to this research are discussed later in this chapter.

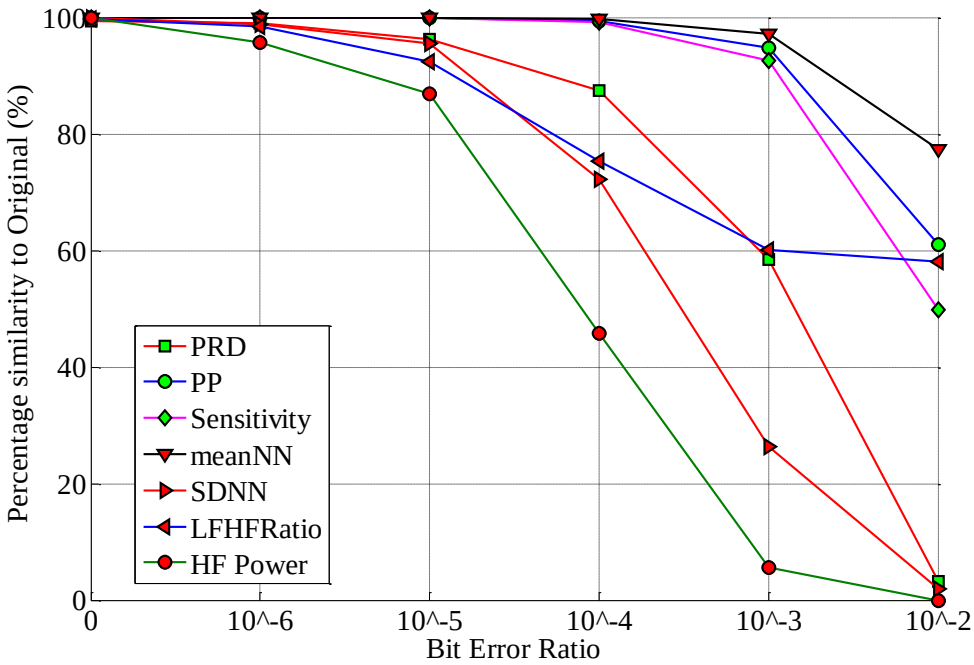

Figure 6.3: Range of BERs for Non-Truncated SPIHT-Compressed Signals.

Figure 6.3 shows a plot of each metric over this range of BERs. It can be seen that a BER of 10^{-6} has little-to-no impact on the metrics. This is not surprising as the results from the section above demonstrate that only errors in the MSS have a strong effect on the signal. As the signal in this case is losslessly compressed, the

probability of a significant bit being in error is low. It is clear from the graph that HF Power is the most susceptible to error. This can be explained by HF components being given lower priority by the SPIHT encoder and therefore encoded later in the compressed bit stream. This increases the chances of bit errors occurring in a location that either directly or indirectly affects these coefficients. The effect of error can be seen from a BER of 10^{-5} where PSim for HF Power falls to just under 90% similarity with its original value. At BERs of 10^{-4} and higher, the similarity drops significantly. The other metrics are more tolerant to errors. As before, meanNN, PP and Se are the most robust with PSim values above 90% until the BER reaches 10^{-2}. This can be expected as these 3 metrics rely mainly on the location of the peak of the R complex remaining intact and are not affected by other changes in the signal. The coefficients representing the R complex are given high priority by the SPIHT encoder and encoded early in the compressed bit stream. Therefore bit errors that occur outside the early portion of the signal do not impact on the location of the R complex. PRD1 results suggest the signal structure is well maintained as high as BERs of 10^{-4}, whereby it falls just outside the limit of *'good'* proposed in [117]. Above this level it shows a rapid decline. SDNN and meanNN are more sensitive to higher BERs with results above 10^{-5} suggesting poor data fidelity. Table 6.3 and Table 6.4 give further statistical details of the results found. Table 6.3 gives the total number of TPs, FPs and FNs over the entire database, as given by the employed beat-detection algorithm. As previously mentioned, the location of the "beat" or R complex is the primary factor influencing the PP, Se, and meanNN. As observed in Figure 6.3, the number of TPs stays high until the BER exceeds 10^{-3}. At this level the number of TPs is greatly reduced, while the number of FN increases greatly. This shows that the resulting signal no longer maintains the correct placement of the R complex, as detected by the beat detection algorithm.

Table 6.3: Total number of TP, FP and FNs for entire database at a sample of CRs.

BER	Non Truncated			4:1 CR			30:1 CR		
	TP	FP	FN	TP	FP	FN	TP	FP	FN
0	106367	2265	6278	106360	2222	6285	105144	2699	7501
10^{-6}	106357	2263	6288	106341	2233	6304	105115	2717	7530
10^{-5}	106280	2317	6365	106281	2280	6364	105077	2762	7568
10^{-4}	105631	2769	7014	105519	2875	7126	104359	3219	8286
10^{-3}	98459	7554	14186	98505	7443	14141	97464	7335	15181
10^{-2}	52385	36182	60260	52240	36071	60406	51642	33468	61003

Table 6.4 extends the results presented in Figure 6.3 by giving the maximum, minimum and standard deviation of the PSim values for SDNN, LF/HF Ratio, PRD1 and HF Power. The primary results of interest in this table are the minimum results for the "diagnostic" metrics, i.e. all those listed, excluding PRD1. With HF power for example, it has a minimum PSim value of 0, at BERs as low as 10^{-6}. In a clinical situation, consistent result retention would be required. These results show that it would be necessary to implement some form of error protection, even at relatively low-levels of BER and compression. Chapter 7 seeks to address this by proposing a methodology to protect compressed ECG streams against bit errors.

Table 6.4: Max, Min and Standard Deviation of PSim SDNN, LF/HF Ratio, PRD1 and HF Power Values for Non-Truncated SPIHT compression.

	SDNN			LF/HF Ratio			PRD1			HF Power		
BER	Max	Min	Std Dev	Max	Min	Std Dev	Max	Min	Std Dev	Max	Min	Std Dev
0	100	98.85	0.23	100	96.40	0.75	99.65	98.20	0.34	100.00	96.16	0.57
10^{-6}	100	47.80	7.57	100	77.22	3.88	99.63	93.17	1.39	100.00	0.00	14.77
10^{-5}	100	64.68	6.74	100	74.00	5.78	99.40	91.86	2.27	100.00	0.00	22.77
10^{-4}	99.40	0.00	31.83	99.72	0.00	30.19	95.88	71.30	4.35	97.07	0.00	39.56
10^{-3}	98.99	0.00	33.08	99.60	0.00	32.05	72.90	35.83	8.62	94.98	0.00	18.62
10^{-2}	53.30	0.00	9.98	98.48	0.00	32.10	20.45	0.00	5.14	0.00	0.00	0.00

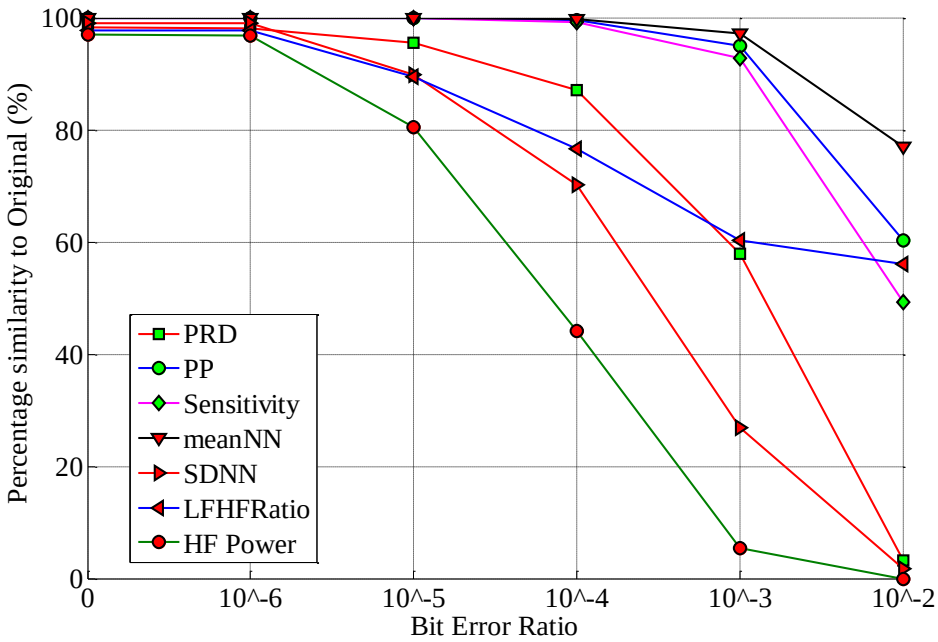

Figure 6.4: Range of BERs for signals compressed at 4:1.

Figure 6.4 shows the database compressed at 4:1 over the same range of BERs. The general trend in behaviour of the metrics is very similar to that displayed in Figure 6.3 with slightly lower starting values for some metrics and some slightly more pronounced effects of higher BERs. Figure 6.5 and Figure 6.6 shows the results of the same tests at CRs of 16 and 30 respectively. The three graphs appear very similar. The degradation curve of the metric results at higher BERs remains consistent across CRs. Upon further inspection however, a number of differences can be seen. Primarily, these differences can be seen when no bit errors occur (BER = 0). Again the PP, Se and meanNN metrics are the most robust to both noise and compression levels. At higher CRs, the initial average metric values of PSim for PRD1, SDNN, LF/HF Ratio and HF Power become successively lower. The reason for this can be explained by the fact that increased CRs result in a shorter bit stream and thus a proportionally lower numbers of bit errors. Thus, there is less data to be transmitted and, as such, will not encounter as many bit errors. The impact of BERs on average metric values can be anticipated if the metric value is known for the compressed signal with no errors. This property is returned to in Chapter 7 when a methodology to protect against bit errors is presented, while seeking to minimise the size of the data being transmitted. Table 6.3 also lists the number of TPs, FPs, and

FNs for CRs of 4 and 30. The values for each confirm the observations made based on Figure 6.4, Figure 6.5 and Figure 6.6 for PP, Se, and meanNN.

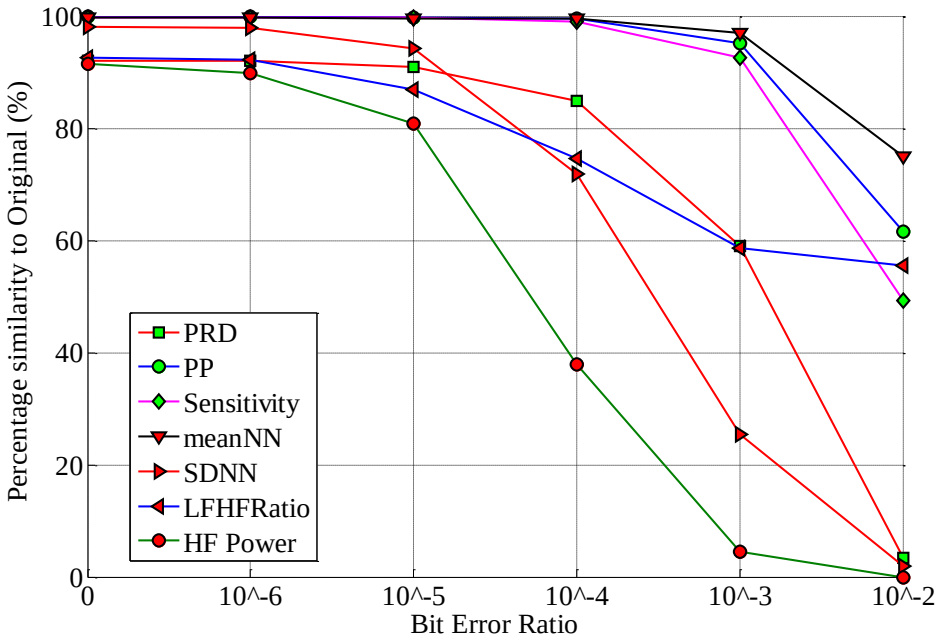

Figure 6.5: Range of BERs for signals compressed at 16:1.

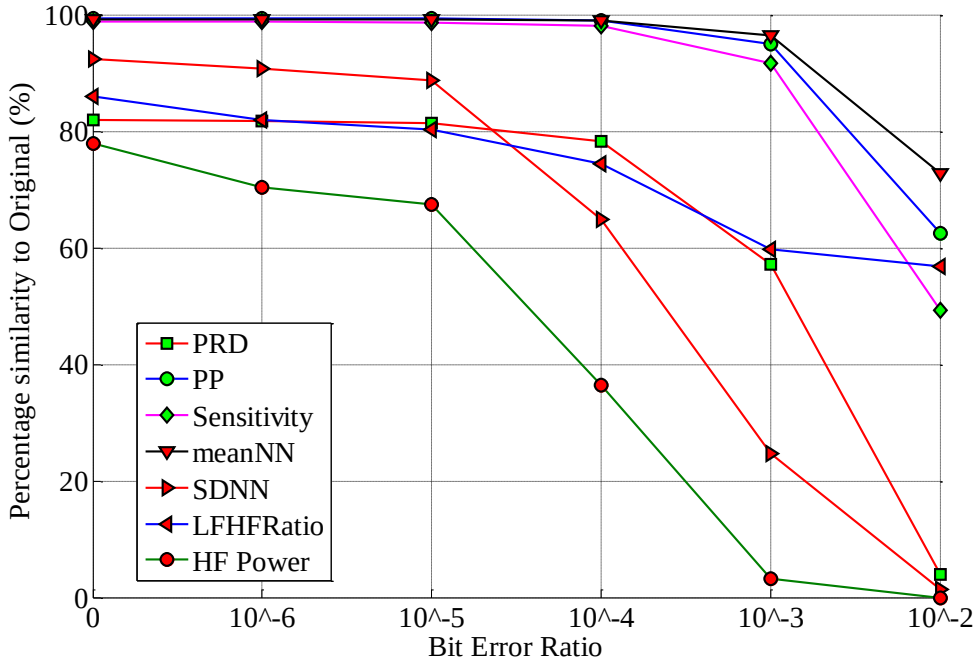

Figure 6.6: Range of BERs for signals compressed at 30:1.

6.5 Summary

This chapter investigated the effects of errors on ECG signals compressed with SPIHT; firstly to quantify the effects of error location on signal reconstruction, and secondly as a function of BER and CR to examine the impact of random errors at a desired compression level. The aim of this research was to assess the robustness of SPIHT-compressed ECG data if it were to be transmitted in a noisy environment. SPIHT compression creates a bit stream where the bits are ordered in decreasing importance. It was found that bit errors that occurred in the early part of the compressed bit stream could greatly impact on the diagnostic information in the resulting signal, while bit errors that occurred later in the bit stream did not significantly impact on it.

Previous research on the distribution of bit errors in the IEEE 802.11 standard has shown that the latter portion of the bit stream is more likely to encounter error bits. This would suggest that it would have a reduced impact on SPIHT-compressed ECG signals as the errors would be more likely to occur outside the important sections of the signal. A normal distribution of errors was assumed in this research.

When bit errors appear at random in the compressed signal, it was found that BERs below 10^{-4} had only a marginal impact on the signals diagnostic information, as reflected in the metrics used. The exception to this is HF Power which is extremely sensitive to both increased CR and BER. This is not surprising due to high frequency components being given lower priority in SPIHT and thus recorded later in the bit stream. Higher CRs impact the more sensitive metrics but they still follow the same degradation curve as at lower CRs.

Once the impact of bit errors on SPIHT-compressed ECG signals is established, it is possible to look at potential methods to protect against these effects. Chapter 7 investigates possible ways to protect the compressed signals, while minimising the overheads needed to provide this protection. Practical implementations are tested using protection schemes based on RS codes and the results of these tests.

Chapter 7 Preservation of Quality in SPIHT-Compressed ECG Signals in the Presence of Bit Errors

7.1 Introduction

This chapter builds on the outcome of the work described in Chapter 6, which investigated the effects of bit errors on SPIHT-compressed ECG signals. In particular, this chapter proposes a protection scheme to ensure signal integrity, while maintaining a low system overhead. Signal integrity is judged through the overall signal quality, as well as through the impact on specific diagnostic measures. The previous chapter found that bit errors outside the early part of the bit stream had little effect on the signal fidelity. Here, the percentage of the signal that needs to be protected from bit errors to ensure signal quality is investigated. A "hypothetical" error-protection scheme, with no bit-overheads and capable of protection from an infinite number of errors, is first used to examine the proportion of the bit stream that needs protecting in noisy transmission conditions. A statistical analysis of the location of the bit errors is performed to identify the number of errors that would

typically need to be handled by an error-protection scheme. Using this information, a "real-world" error protection scheme is proposed using Reed-Solomon (RS) codes. The RS codes are examined by testing the proposed scheme against a range of high BERs. Finally, the prospect of maximising compression while maintaining signal protection (in the presence of the additional overhead because of the addition of error protection), is examined by using the previously designed RS code with increased compression levels. The scheme proposed here is designed to protect SPIHT-compressed ECG signals that may encounter BERs as high as 10^{-2}.

7.2 Reed-Solomon Codes

For practical implementations of an error protection scheme, Reed-Solomon (RS) codes were chosen. RS codes are a form of cyclical error correction codes based on finite field arithmetic. An RS code is designated a $[n, k]$ code where n is the total length of the block (in symbols) and k is the length (in symbols) of the message being encoded. Each symbol in n could be represented as an m-bit value. RS codes are implemented over a finite field F with 2^m elements. This gives:

$$n = 2^m - 1 \tag{14}$$

The number of errors any given code can correct (t) is given as:

$$t = \frac{n - k}{2} \tag{15}$$

Thus it is possible to design an RS code with a desired t as:

$$k = n - 2t \tag{16}$$

For this research, the encoded bit stream produced by SPIHT was represented as a stream of 8-bit symbols (i.e. $m = 8$).

Due to the nature of the data being transmitted, the length of the message (number of 8-bit symbols) being encoded can vary. This can result in k being far shorter than the

desired value obtained from (15) above. When this occurs, an RS property known as shortening is employed to minimise the amount of data to be transmitted. For example, let the message size to be encoded be l. This causes k to be reduced by $(k - l) = p$ symbols. The encoder then reduces $[n, k]$ by an equal amount (p) and padding the unused portion with zero-valued symbols that are not transmitted. A new, shortened RS code of $[n - p, k - p]$ is produced. As n and k are reduced by the same amount, t remains the same as for the full length RS code. When the encoded message is received, an equal number of zeros is added by the decoder.

7.3 Testing and Results

In order to examine the impact of bit errors on the compressed signals, a simulated noisy environment was created. This involved applying a number of bit errors to an encoded signal, the quantity of which was based on the length of the encoded recording and the specified BER. Similarly to Chapter 6, BERs were applied from the range $\{10^{-6}, 10^{-5}, 10^{-4}, 10^{-3}, 10^{-2}\}$. The compressed signals were concatenated into a single bit stream, with bit errors applied at random. The final bit stream was then split back into their original form and then reconstructed into a single ECG record.

To evaluate the impact of a given BER and CR on a signal, a range of performance measurement metrics were recorded. The same metrics as outlined in Chapter 6 were used, where full details on these metrics and the reason for their selection can be found. The metric results were again evaluated in terms of Percentage Similarity (PSim) as given in Eq (11) of the previous chapter.

7.3.1 Ideal Error Correction in a Error-Prone Channel

Chapter 6 examined the impact of a range of bit errors on ECG data compressed using Non-Truncated SPIHT. The initial objective of this research was to determine the percentage of the compressed signal that contains the information necessary to accurately reconstruct the signal. SPIHTs bit-ordering property results in the early part of the compressed bit stream containing the most important bits for accurate reconstruction. This is confirmed by the results found in Chapter 6. By extension,

these results show that it is possible to accurately reconstruct a signal even if the latter part of the signal is corrupted. By focusing protection on the early part of the signal it should be possible to largely preserve diagnostic information without undue data overhead. To determine how many bits need to be protected for accurate reconstruction, a "hypothetical" data protection scheme was simulated that protected against an infinite number of errors within a given payload segment, and assumed no data overhead. This protection scheme was then implemented on a range of percentages of the overall bit stream length (i.e. a range of different "protected regions") prior to transmission through the noisy channels. The performance metrics were again calculated on the resulting signals.

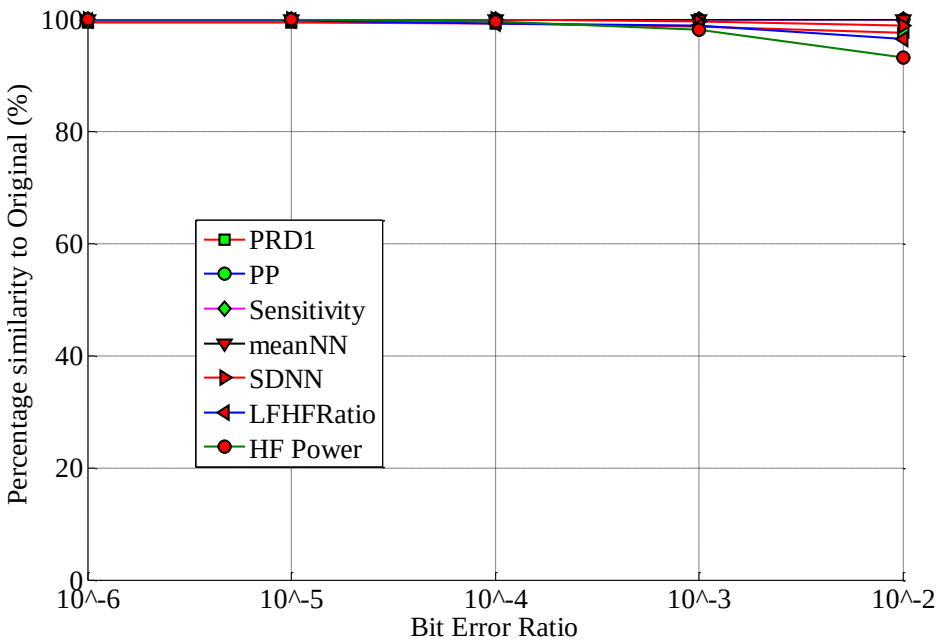

Figure 7.1: Plot of BER vs. Percentage Similarity for signals with 50% encoded bits protected (*'very good'* protection).

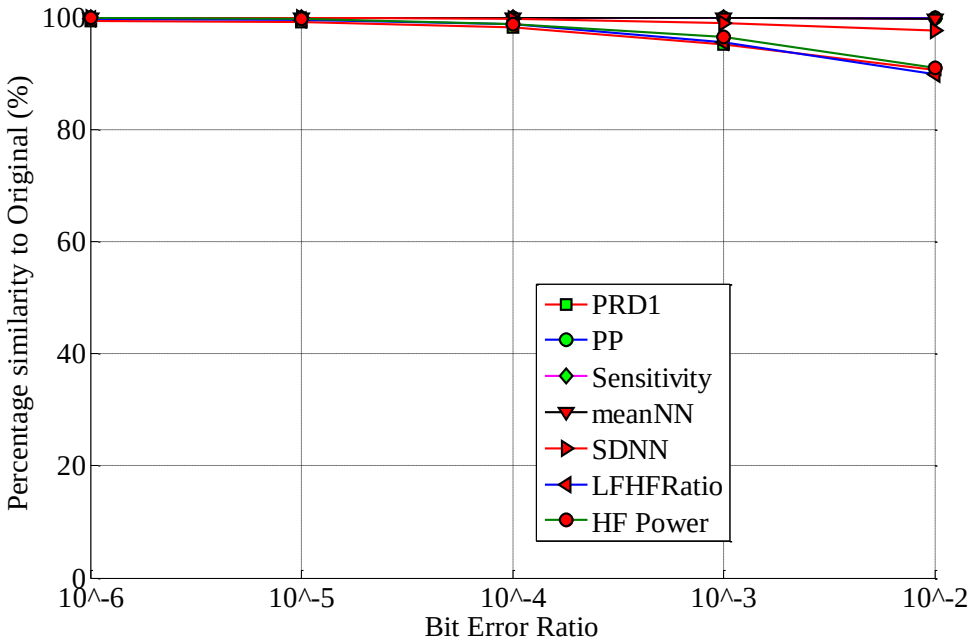

Figure 7.2: Plot of BER vs. Percentage Similarity for signals with 12.5% encoded bits protected (*'good'* protection).

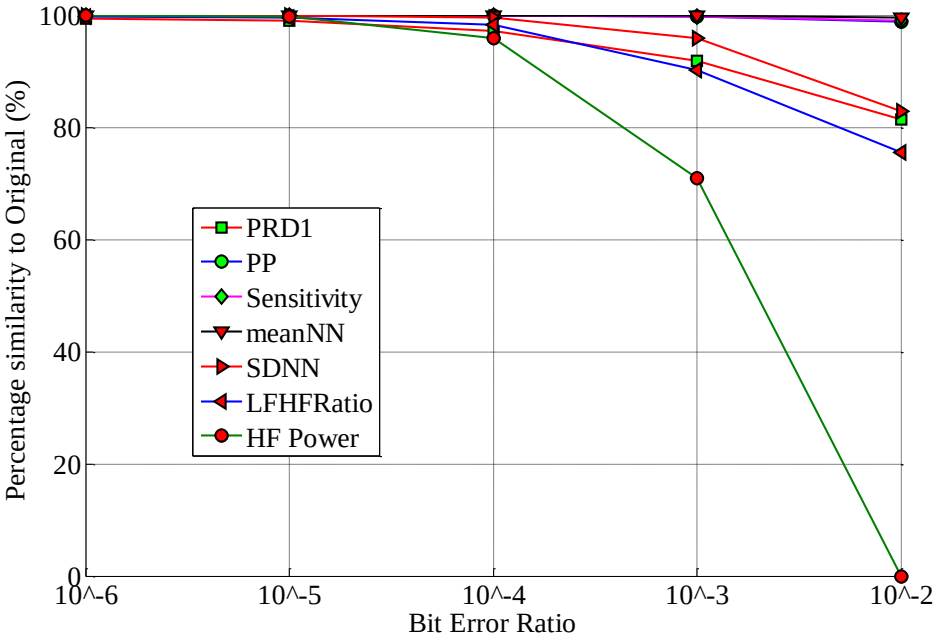

Figure 7.3: Plot of BER vs. Percentage Similarity for signals with 6.7% encoded bits protected.

Figure 7.1, Figure 7.2 and Figure 7.3 show a selection of these results for protection of 50% ($1/2$), 12.5% ($1/8$) and 6.7% ($\sim 1/16$) of the encoded signal length. Examining the figures, it is clear that the smaller the percentage protected the more sensitive the signal is to errors (as would be expected). This is reflected in the degradation in the percentage similarity measures used. For example, focusing on PRD1 as one simple measure of signal fidelity (while acknowledging its limitations when used by itself), it can be seen from Figure 7.1 that with 50% of the bits protected, all the PRD1 value stays inside the *'very good'* range (based on [117], given already in Table 6.1) with a PSim of 98%. Decreasing the amount protected to 12.5% (Figure 7.2) the length of the bit stream, it can be seen that the PRD1 values remain inside the *'good'* range with a minimum PSim of 91%, occurring at the highest BER of 10^{-2}. At 8% protection, the PRD1 goes from *'very good'* to *'good'* when the BER reaches 10^{-3} before dropping to *'not good'* when the BER reaches 10^{-2}. The choice of these ranges for evaluation of quality control can be further supported by the results of the other, ECG specific performance metrics. It can be seen in Figure 7.1 and Figure 7.2 that these metrics results stay close to the PSim for PRD1 results. Only in Figure 7.3 can a large deviation between the PSim for PRD1 and the other PSim metrics be seen; with PSim for HF Power having 0% similarity with the original value when the BER reaches 10^{-2}. When 50% or 12.5% of the bit stream is protected, the metrics have a minimum of 90% similarity with the corresponding result on the uncompressed data (i.e. PSim for HF Power for 12.5% protection is >90%).

Lower levels of protections show similar results with greater sensitivity to noise. They were excluded here for the sake of brevity.

Table 7.1: Average number of errors in Protected Region (per frame).

Length of Protected Region	BER 10^{-6}	BER 10^{-5}	BER 10^{-4}	BER 10^{-3}	BER 10^{-2}
50	0.00	0.02	0.22	2.14	21.49
25	0.00	0.01	0.10	1.09	10.77
12.5	0.00	0.01	0.05	0.53	5.37
8.3	0.00	0.00	0.04	0.36	3.61
6.7	0.00	0.00	0.03	0.28	2.87
5	0.00	0.00	0.02	0.22	2.16

To design a real-world implementation of this error protection scheme, an analysis of the number of errors that may be encountered in a typical data block was undertaken. During the previous simulations, the number of error occurrences in each protected region was recorded. Table 7.1 lists the average number of errors to occur in a protected zone on a per-frame basis. However, this study takes a more conservative approach (given that the payload is a biomedical signal) and examines the maximum expected number of errors encountered in any given frame.

Table 7.2: Maximum number of errors to occur in Protected Region (per frame).

Length of Protected Region (%)	BER 10^{-6}	BER 10^{-5}	BER 10^{-4}	BER 10^{-3}	BER 10^{-2}
50	1	2	4	12	53
25	1	2	3	9	31
12.5	1	2	3	5	19
8.3	1	1	2	4	16
6.7	1	1	3	4	12
5	1	1	2	4	11

Table 7.2 gives the maximum number of errors encountered in the protected region of any single frame during the simulation. To properly protect the bit stream during

transmission, it is necessary to implement a protection scheme that can correct up to the corresponding number of errors for a given BER.

7.3.2 Designing a Practical Error Protection Scheme

While the previous scenario involved a protection scheme and assumed no overheads, RS codes must make a trade-off between the number of errors that can be corrected (t) and the data overhead of the protection bits ($n-k$). Using Table 7.2 and the results in Figure 7.1, Figure 7.2, and Figure 7.3, t can be determined for a desired signal quality at an expected BER. Substituting this value into Eq. (14), it is possible to determine the size of the encoded message contained in each RS packet (k). However, due to the addition of the RS parity symbols, the size of the protected portion of the signal is also enlarged, marginally increasing the likelihood that it will encounter a bit error and reducing the compression ratio. For this reason it may be necessary to increase t above the values recorded in Table 7.2.

At low BERs, this can be achieved by doubling the number of expected errors, with little impact on the system overhead. At higher BERs (and larger amounts of data being protected), this becomes more difficult. To investigate further, two cases were investigated where a high BER of up to 10^{-2} may occur. This BER was deliberately selected to be higher than would generally be expected in order to examine cases where extremely high numbers of erroneous bits may be encountered. The desired quality in the received signal was either

1) *'good'* or better
2) *'very good'*

From the previous section, it was discovered that protecting 12.5% of the encoded bit stream satisfied *1)*, while protecting 50% of the encoded bit stream was necessary to satisfy *2)*. These operating points shall be referred to as *'good'* and *'very good'* protection for the remainder of this chapter.

To address the issue of the added bits due to the RS coding for *'good'* protection the estimated maximum number of errors is calculated as the maximum encountered error from Table 7.2, and increased by a fifth, based on empirical testing. In this case t is calculated as 23. As previously mentioned, $m = 8$ has been selected for this research. This results in a value of n equal to 255. From this, k can be calculated as

(255-(2x23)) = 209. Figure 7.4 shows the plot of the performance metrics after being transmitted through a noisy channel with an RS code of [255,209]. It can be seen that the results are as expected, with the results being nearly identical to those of Figure 7.2, where the "perfect" error-protection scheme was employed. It should be noted that from Table 6.2, it can be determined that the average bit-length of 12.5% (i.e. *'good'* protection) of the compressed signal is 538 bits. For $m = 8$, this results in an average p size of 68 symbols. Thus on average, a shortened RS code of [114,68] will be transmitted. Performance varies slightly for some metrics but PRD1 is maintained in the range of *'good'* or better across all BERs. PSim for HF Power can be seen to be lower than that of Figure 7.2, suggesting that if HF Power is essential to diagnostic purposes, a larger percentage of the bit stream would need to be protected to ensure its preservation. Analysis of the simulations shows that the number of errors encountered by each frame did not exceed t at any time.

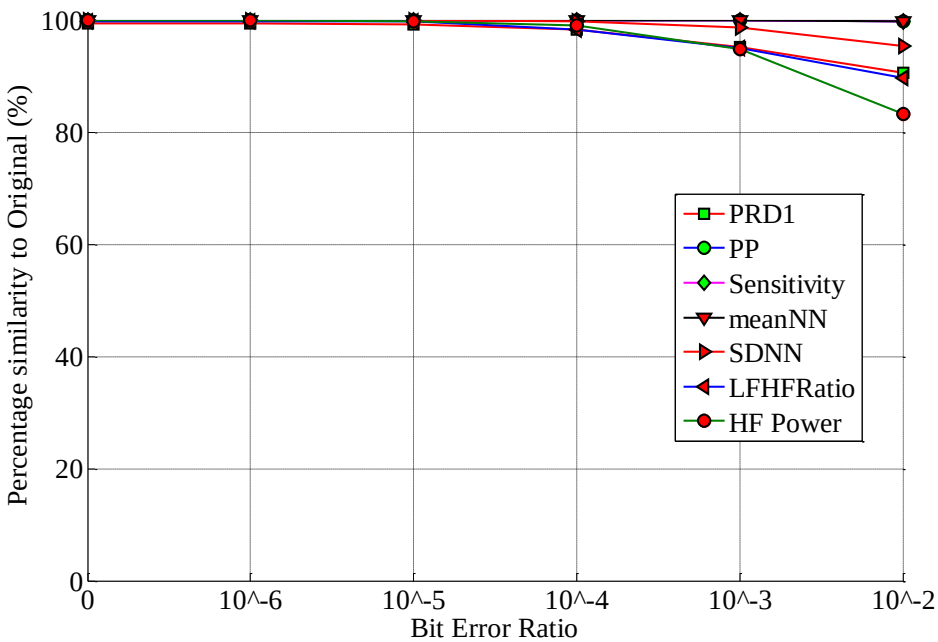

Figure 7.4: Plot of BER vs. Percentage Similarity for Signals with *'good'* protection from RS Code [255,209].

In the case of *'very good'* protection the design is complicated slightly by the fact that more than one RS-encoded packet will be needed to ensure adequate protection. From Table 6.2 (Chapter 6) it can be seen that the average length of bits to be

protected will be 2149 bits with 50% protection. At $n = 255$, each RS packet will be (255x8) = 2040 bits; smaller than the number of bits to be protected. In practical implementations, a proportion of this will also be set-aside for error protection bits. The bit stream will therefore have to be split among multiple RS-encoded packets. In this case, the error rate must be calculated by dividing the number of bits to be protected (2149) by the maximum number of errors (53). From this it can be seen that 1 bit in 41 will be in error. The new expected number of errors per frame will therefore be ((255x8)/41) = 50 errors. Figure 7.5 shows the metric results of the simulation using RS codes of [255,155] for half the SPIHT encoded bit stream. These results are identical to the previous results of Figure 7.1, with PRD1 staying within the *'very good'* range throughout all BERs. Again *t* was not found to be exceeded at any time. Testing of values of *k* less than this was found to result in packets where the number of errors exceeded the value of *t* and thus resulted in errors that could not be corrected by the RS code.

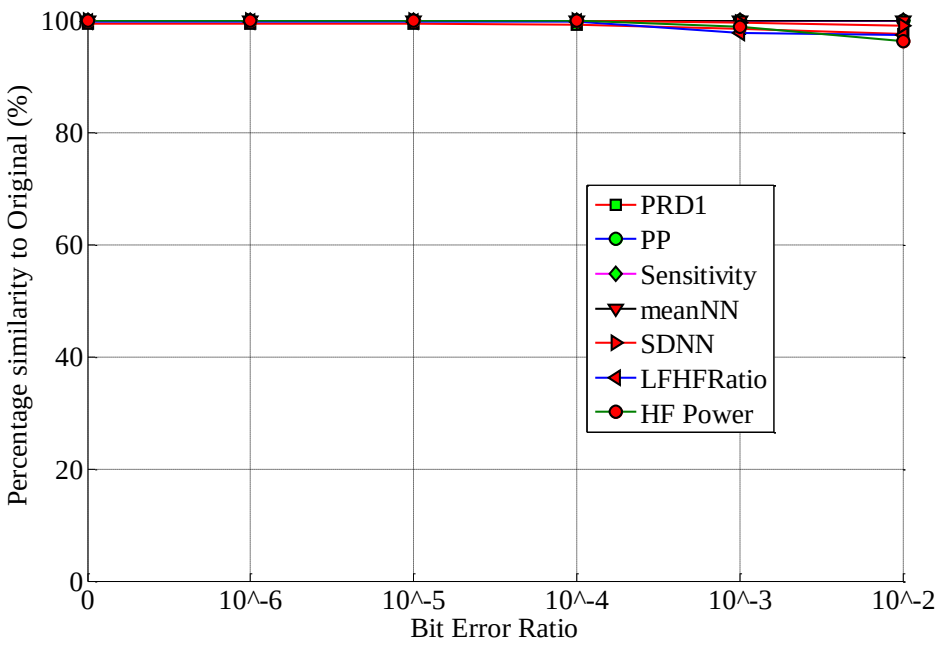

Figure 7.5: Plot of BER vs. Percentage Similarity for Signals with *'very good'* protection from RS Code [255,155].

7.3.3 The Impact of RS Coding on Compression Ratio

Note that the previous section discussed the effect of error correction without reference to truncation of the encoded bit stream produced by SPIHT. As the primary goal of this thesis is to investigate methodologies to minimise the size of biomedical signals, the effects of increased compression through truncation of the RS protected signals was also investigated. The addition of parity symbols in the transmitted message results in a reduction in the net CR of the Non-Truncated SPIHT-compressed signal. Knowledge of the impact of this is necessary to minimize the bandwidth required for factors such as transmission, storage, and power consumption. As previously mentioned, SPIHT compresses the MIT-BIH database to an average CR of 2.6, when not truncating the encoded bit stream. In the case of *'good'* protection, t is set as 23. This equates to an increase of 184 bits per transmitted frame. This was found to reduce the average CR from 2.6 to 2.4.

With *'very good'* protection, the calculations are again complicated by some of the signals requiring more than one RS packet to ensure adequate protection. Using the average bit stream length, a t value of 50 results in 800 extra bits per frame, assuming two RS packets per frame. Here the average CR without truncation of the encoded bit stream is reduced to 1.85. It should be noted however, that while the CR is reduced, the loss in CR has been offset by protection against high BERs. In situations where a lower BER is expected, a smaller t value will bring this CR closer to the original value.

Significant reductions in signal size can be made by using SPIHT in lossy mode. Research again focused on the specific quality points identified in Section 7.3.2 above. From Table 6.2 it can be seen that the average CR without error protection is 2.6. Therefore, providing *'good'* protection (protecting 12.5% of the compressed bit stream) corresponds to a CR of approximately 20 (in relation to the original frame length). As mentioned above, the inclusion of the parity symbols for the RS codes results in a decrease in overall CR. In this case, it was found to give a net CR of ~15. Figure 7.6 shows the performance metrics for a net CR of ~15 (with *'good'* protection). It can be seen that performance is not greatly impacted across the full range of BER, since all, or almost all the transmitted bits are protected. For the case of a CR without error protection of 12, addition of parity symbols was found to give

a net CR of 10 (for *'good'* protection). Figure 7.7 shows the performance metrics for this level of compression. A degradation in performance metrics occurs as BER increases. It can be seen that for low BER, performance is better than for the higher compression level in Figure 7.6. When the BER reaches 10^{-2}, performance is equal to that seen in Figure 7.6.

A similar situation can be observed where *'very good'* protection is required. Protecting 50% of the encoded bit stream gives a CR approximately equal to 5 (with respect to the original frame). As with the case of *'good'* protection, this CR was reduced by the addition of the parity symbols and was found to give an average net CR of 3.7. Figure 7.8 shows a plot of these results. It can be seen that there is little change in performance metrics as the BER increases. Figure 7.9 shows *'very good'* protection with a CR of 3 (which gives a net CR of 2.47). Again it can be seen that metric performance at BERs of 10^{-3} and lower exceeds that shown in Figure 7.8. From a system design point of view it is useful to select the minimum acceptable performance by looking at the maximum acceptable CR to maintain diagnostic information. This value can then be used to set the amount of each frame that will need protection. The overall CR can be decided by examining the remaining bandwidth available, and tailoring the compressed signal size to suit it.

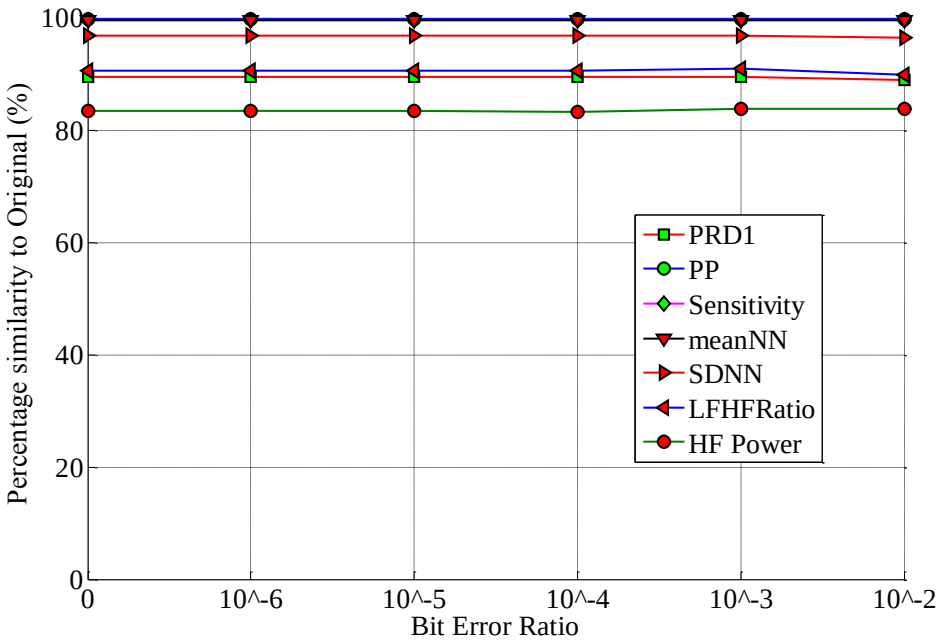

Figure 7.6: Plot of performance metrics with *'good'* protection and a net CR of 15.

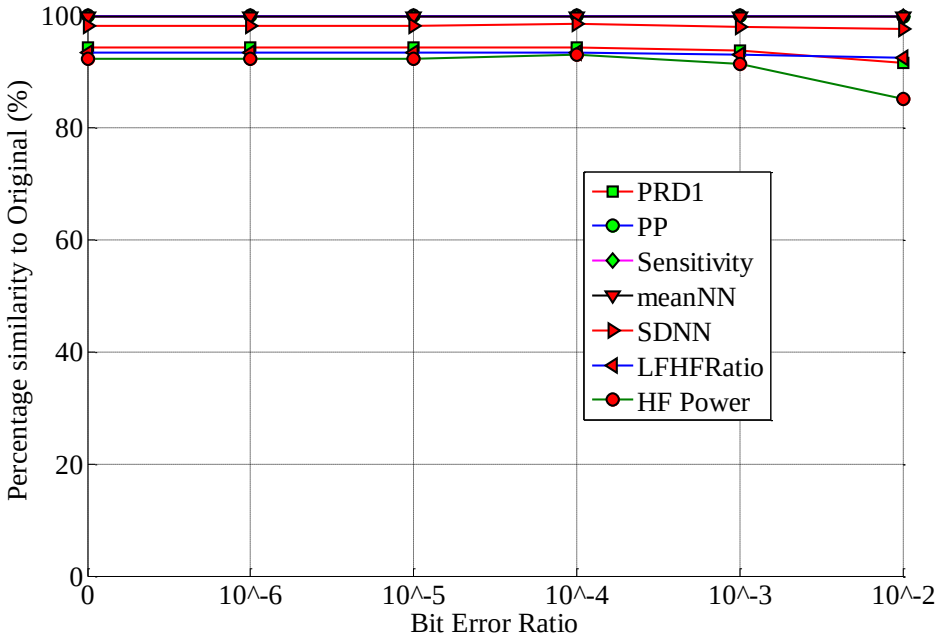

Figure 7.7: Plot of performance metrics with *'good'* protection and a net CR of 10.

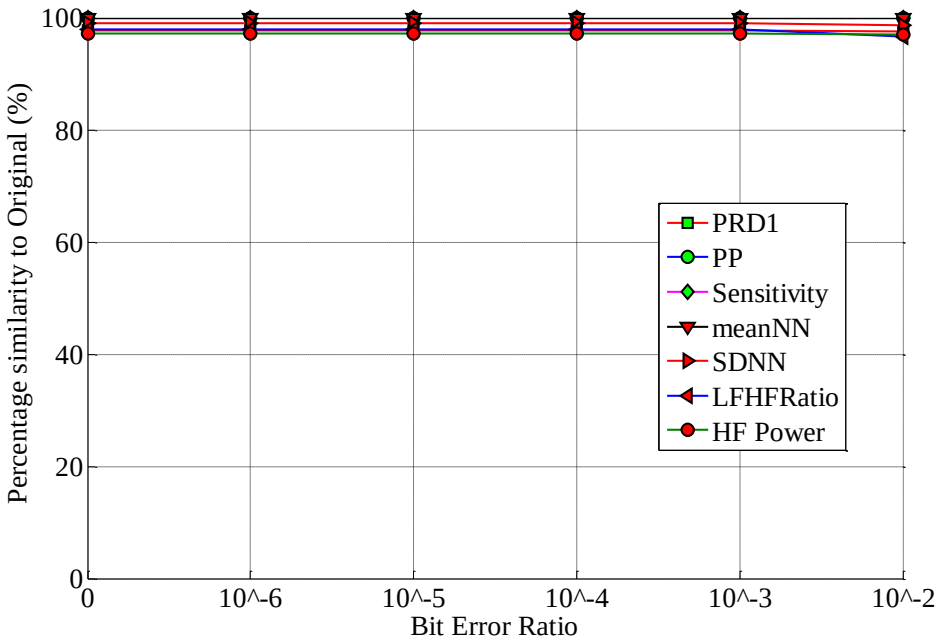

Figure 7.8: Plot of performance metrics with *'very good'* protection and a net CR of 3.7.

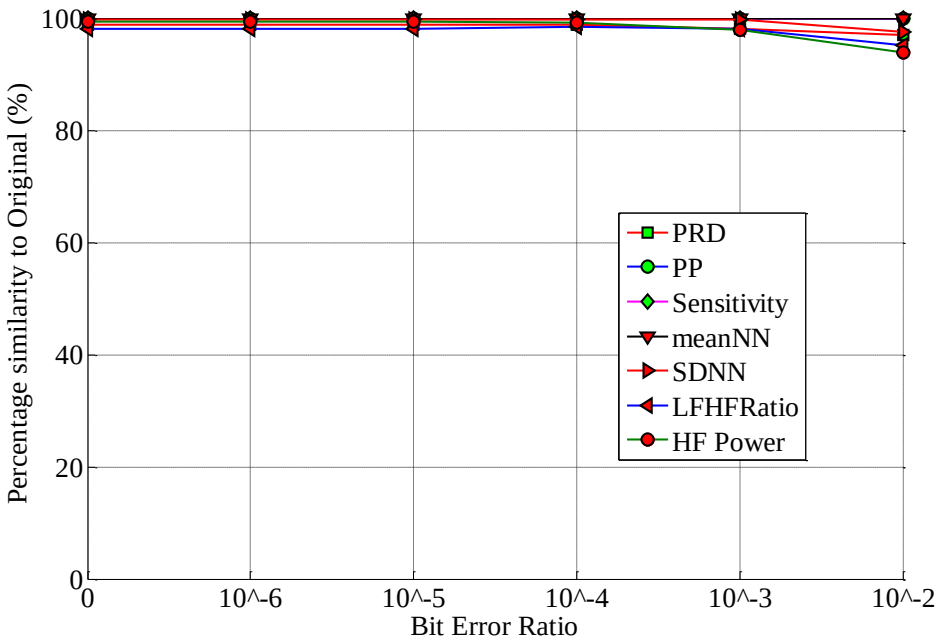

Figure 7.9: Plot of performance metrics with *'very good'* protection and a net CR of 2.47.

7.4 Summary

This chapter extended the work done in Chapter 6 and examined methodologies to protect SPIHT-compressed ECG signals from the effects of bit errors. Initially, a hypothetical bit error protection scheme was employed that offered perfect protection with no overhead. This was used to exploit the bit-ordering property of SPIHT and examine what percentage of the encoded signal would need to be protected to preserve diagnostic integrity. It was found that 50% of the Non-Truncated SPIHT encoded bits need to be protected to ensure high signal fidelity, while protecting 12.5% of the encoded bits would result in some distortion but maintain diagnostic integrity. These results were used to design an RS implementation to give the same level of protection where BERs as high as 10^{-2} can be expected.

Finally, the use of lossy SPIHT compression with these schemes was investigated. Compression by bit stream truncation (i.e. lossy SPIHT compression) is analogous to exposing these same signal portions to high levels of noise. For this reason it is possible to design a protection system by finding the highest acceptable level of lossy compression and encompassing this amount of data in an error protection scheme. If system bandwidth allows, any further bits transmitted outside this level would improve signal fidelity for BERs lower than 10^{-2}. The research outlined in this chapter may be of particular interest to designers of wireless healthcare systems, wherein limitations on bandwidth or storage space must be adhered to.

Chapter 8 Conclusions

8.1 Introduction

This final chapter recaps on the contents of the thesis and summarises the work done, the observations made and the results found. It will begin by summarising the main topics presented in this thesis and the main results and observations on each of these topics. Finally, a list of the primary contributions arising from these results and some possible avenues of future work that would build upon these contributions are given.

8.2 Overview of the Thesis

This thesis has investigated methods of compressing and protecting biomedical signals for use on a portable device. The key goal of this research was to investigate methodologies of minimising the biomedical data size while preserving diagnostic integrity. The research began by comparing the compression ability of two transform-based compression algorithms on EEG data. JPEG2000 and SPIHT were used to compress EEG data, first at low levels of loss where little-to-no fidelity is sacrificed, and then at higher levels of compression. A computer aided diagnosis (CAD) system was used to verify that the diagnostic integrity of the EEG data is

maintained and to determine the maximum acceptable level of lossy compression for the two algorithms. An analysis of the feasibility of implementing the SPIHT algorithm on a mobile platform was performed, firstly by examining the processor load required to perform the compression and secondly by determining the benefit of compression prior to transmission in terms of power savings due to a reduction in the duration of time the antenna is active.

The next body of research focussed on an alternative approach to transform-based compression, whereby the level of loss was controlled by the quantisation operation. The SPIHT algorithm was employed in two manners. First it was employed in its traditional way, with fixed quantisation and DWT levels and compression/loss controlled by specifying a desired CR for the SPIHT encoder. Secondly, the algorithm was used with variable quantisation levels, fixed DWT levels and the SPIHT encoder used as an entropy encoder in Non-Truncated SPIHT mode. The compression results of both approaches were examined in terms of CR and PRD1 and analysis of the EEG data after compression to ensure sufficient information is retained.

The final portion of the thesis examined the impact of bit errors on compressed biomedical signals. ECG data was compressed with the SPIHT algorithms at a range of compression levels. The importance of the error location was investigated by introducing bit errors in different portions of the compressed bit stream and examining the impact on the reconstructed signal. Random bit errors were then introduced at BERs ranging from 10^{-6} to 10^{-2} on the compressed data at a range of CRs. The impact these had on the reconstructed signals were again examined. Based on these findings, the final section of this thesis looked at how to protect the compressed data from these effects. SPIHTs embedded encoding property was exploited to minimise the amount of data necessary to protect, thus keeping the overheads associated with data protection to a minimum. A practical implementation was proposed and tested using RS codes as error-correcting codes. These were tested on signals compressed with SPIHT in Non-Truncating mode and with signals compressed at higher CRs.

8.3 Main Conclusions

A summary of the main conclusions reached can be given as follows:

1. Chapter 4 - Compression of EEG Signals with JPEG2000 and SPIHT

   EEG data were compressed with two different compression algorithms. The Freiburg EEG database was first compressed using JPEG2000 and SPIHT at levels of loss approximately equal to 7% PRD1. The integrity of the reconstructed data was verified by use of a CAD system. It was found that there was little-to-no deterioration in seizure detection performance at this level of loss. At low levels of loss, JPEG2000 was seen to provide a slight compression advantage over SPIHT, achieving average CRs of approximately 9 and 8.3 respectively (at 7% PRD1). As there was little impact on seizure information at this level of loss, higher levels of compression were investigated. To determine the maximum levels of loss acceptable, higher CRs were tested for decline in seizure detection performance. At higher levels of fidelity loss, SPIHT was found to offer significant compression gains over JPEG2000. It was found that PRD1s as high as 30% for JPEG2000 compression and 36% for SPIHT could be tolerated before detection performance was significantly impaired. This gave CRs of 30 and 90 respectively. An analysis of the practical possibilities of implementing the SPIHT algorithm on a portable device was performed. The computational load required to perform compression on an Analog Devices Blackfin BF537 was analysed. It was found that SPIHT compression did not significantly load the processor and, due to SPIHTs embedded encoding property, the higher the level of compression, the lower the processor load. At the maximum acceptable level of compression previously found (a CR of 90) SPIHT would only cause a 0.002% load on the processor. The potential energy savings in transmitting compressed data over Bluetooth LE were also investigated. It was found that SPIHT compression prior to transmission would result in a net decrease in energy expenditure. Even a modest CR of 7 results in a reduction of the energy required to transmit a frame of data by 75%.

2. Chapter 5 - The Effects of Wavelet Coefficient Quantisation in EEG Compression

   An alternative approach to maximising gains in transform-based compression was investigated. The effects of reducing the bit-level of the quantised coefficients were tested using SPIHT as an entropy encoder, with uniform quantisation. Compression using this approach was compared to the standard SPIHT compression approach of bit stream truncation. It was found that lower bit-levels could still potentially maintain more signal information than the traditional bit stream truncation approach. Higher compression levels at a given level of loss were recorded in comparison to the standard SPIHT methodology. At levels of loss of less that 7% PRD1, the standard SPIHT approach achieved a CR of 5. At the same average level of loss, QSPIHT achieved an average CR of 13.05. Using 30% PRD1 as a cut-off level, an average CR of 40 was recorded for standard SPIHT, compared to just over 100 for QSPIHT. Signal fidelity was verified by analysing the energy envelope of the signal before and after compression and by visual analysis.

3. Chapter 6 - ECG Compression with SPIHT in the Presence of Bit Errors

   The impact of bit errors on SPIHT-compressed ECG data was investigated. A number of performance metrics were chosen to monitor the impact on diagnostic quality. SPIHT was used to compress the ECG signals. SPIHTs bit-ordering property organises the compressed bit stream from MSB to LSB, with respect to importance of bits for signal reconstruction. An analysis was first performed to classify the affect of bit error location on the reconstructed signal after being compressing with Non-Truncated SPIHT. It was determined that bit errors outside the initial section of the bit stream did not have a significant impact on the signal. This led to an investigation into the effects of BERs ranging from 10^{-6} to 10^{-2} on signal quality. It was found that BERs below 10^{-4} had marginal impact on the average signal diagnostic information.

4. Chapter 7 - Preservation of Quality in SPIHT-Compressed ECG Signals in the Presence of Bit Errors

   Practical signal protection schemes were tested using RS codes. It was found that it was possible to protect against BERs as high as 10^{-2} without impacting on the performance of the diagnostic metrics by protecting 50% of the compressed bit stream. If the diagnostic purpose does not require complete integrity, lower proportions of the bit stream can be protected. Protecting 12.5% of the bit stream was found to maintain the majority of the signal information. Finally, these protection tests were extended to test the effects of higher CRs on the signals. These were performed to allow for system designers to design a protection scheme based on the intended diagnostic purposes and the bandwidth or storage space available to them.

8.4 Summary of Contributions

The primary contributions of this thesis are:

1. Analysis and comparison of two compression algorithms suitable for an ambulatory EEG device.
2. Determining the maximum level of signal fidelity loss for EEG compression using JPEG2000 and SPIHT in order to maintain diagnostic information for seizure events.
3. Analysis of computational and energy requirements for embedded implementation of compression, and quantification of potential energy savings in an ambulatory device.
4. Examining the benefits of lowering the quantisation level in transform based compression of EEG signals.
5. Classifying the impact of bit errors in relation to their location in the bit stream of SPIHT-compressed ECG signals, and determining the proportions of the bit stream that needs to be protected from errors to preserve a range of diagnostic measurements for SPIHT-compressed ECG.
6. Proposal of a methodology to design RS codes to achieve these levels of protection and testing their functionality with selected performance targets.

8.5 Suggestions for future work

There are several potential areas that could be focused upon for future work:

1. Real-time implementation of the compression algorithms on a portable device to fully analyse power usage.
2. Expanding on the results of the quantisation level reduction research (Chapter 5) by combining higher quantisation levels with SPIHTs truncated bit stream compression. This could potentially give far better compression gains in relation to fidelity loss.
3. An in-depth comparison between the compression algorithms researched here and other non-transform based compression methods in terms of compression gains in relation to fidelity loss and complexity. It is possible that another approach may provide better compression results, but it is likely that any gains would be offset by added computational complexity.
4. The ECG bit error protection research could be expanded to include EEG bit error protection. Measuring the impact on diagnostic information may again prove problematic, but this could be in part addressed by adoption of some of the methods outlined in this thesis.
5. Finally, this research would ideally be implemented on a hardware system as part of a larger EEG and ECG monitoring, ambulatory device.

References

[1] S. Schappert and C. Nelson, 'National Ambulatory Medical Care Survey: 1995-96 summary.', *Vital and health statistics. Series 13, Data from the National Health Survey*, no. 142, pp. i–vi, 1–122, Nov. 1999.

[2] K. Motoi, S. Taniguchi, T. Yuji, M. Ogawa, N. Tanaka, K. Hata, M. Baek, H. Ueno, M. Wakugawa, T. Sonoda, S. Fukunaga, Y. Higashi, K. Matsumura, T. Yamakoshi, S. Tanaka, T. Fujimoto, H. Asanoi, and K. Yamakoshi, 'Development of a ubiquitous healthcare monitoring system combined with non-conscious and ambulatory physiological measurements and its application to medical care', in *Annual International Conference of the IEEE Engineering in Medicine and Biology Society (EMBC)*, 2011, pp. 8211 –8214.

[3] M. Plescia, S. Koontz, and S. Laurent, 'Community assessment in a vertically integrated health care system.', *American Journal of Public Health*, vol. 91, no. 5, pp. 811–814, May 2001.

[4] 'Avoiding hospital admissions'. [Online]. Available: http://www.kingsfund.org.uk/publications/avoiding-hospital-admissions. [Accessed: 05-Feb-2013].

[5] 'Data briefing: Emergency hospital admissions for ambulatory care-sensitive conditions | The King's Fund'. [Online]. Available: http://www.kingsfund.org.uk/publications/data-briefing-emergency-hospital-admissions-ambulatory-care-sensitive-conditions. [Accessed: 05-Feb-2013].

[6] G. Paré, M. Jaana, and C. Sicotte, 'Systematic Review of Home Telemonitoring for Chronic Diseases: The Evidence Base', *Journal of the American Medical Informatics Association*, vol. 14, no. 3, pp. 269–277, May 2007.

[7] F. A. McAlister, S. Stewart, S. Ferrua, and J. McMurray, 'Multidisciplinary strategies for the management of heart failure patients at high risk for admission', *Journal of the American College of Cardiology*, vol. 44, no. 4, pp. 810–819, Aug. 2004.

[8] N. Memon, Xuan Kong, and J. Cinkler, 'Context-based lossless and near-lossless compression of EEG signals', *IEEE Transactions on Information Technology in Biomedicine*, vol. 3, no. 3, pp. 231–238, Sep. 1999.

[9] T. Martin, E. Jovanov, and D. Raskovic, 'Issues in wearable computing for medical monitoring applications: a case study of a wearable ECG monitoring device', in *The Fourth International Symposium on Wearable Computers*, 2000, pp. 43 –49.

[10] D. C. Yates and E. Rodriguez-Villegas, 'A key power trade-off in wireless EEG headset design', in *3rd International IEEE/EMBS Conference on Neural Engineering*, 2007, pp. 453–456.

[11] 'Disk Drive Storage Price Decreasing with Time'. [Online]. Available: http://www.jcmit.com/disk2012.htm. [Accessed: 05-Feb-2013].

[12] ISO - International Organization for Standardization, 'ISO/IEC 15444-1:2000 - Information technology -- JPEG 2000 image coding system -- Part 1: Core coding system'. [Online]. Available: http://www.iso.org/iso/iso_catalogue/catalogue_ics/catalogue_detail_ics.htm?csnumber=27687. [Accessed: 30-Sep-2009].

[13] A. Said and W. A. Pearlman, 'A new fast and efficient image codec based on set partitioning in hierarchical trees', *IEEE Transactions On Circuits And Systems For Video Technology*, vol. 6, pp. 243–250, Jun. 1996.

[14] Yong Sun, Hui Zhang, and Guangshu Hu, 'Real-time implementation of a new low-memory SPIHT image coding algorithm using DSP chip', *IEEE Transactions on Image Processing*, vol. 11, no. 9, pp. 1112– 1116, Sep. 2002.

[15] Qin Lu, L. Du, and Bing Hu, 'Low-Power JPEG2000 Implementation on DSP-Based Camera Node in Wireless Multimedia Sensor Networks', in *International Conference on Networks Security, Wireless Communications and Trusted Computing*, 2009, vol. 1, pp. 300–303.

[16] A. J. Casson, S. Smith, J. S. Duncan, and E. Rodriguez-Villegas, 'Wearable EEG: what is it, why is it needed and what does it entail?', *Annual International Conference of the IEEE Engineering in Medicine and Biology Society (EMBC)*, pp. 5867–5870, Aug. 2008.

[17] L. Sornmo and P. Laguna, *Bioelectrical Signal Processing in Cardiac and Neurological Applications*. Academic Press Inc, 2005.

[18] D. Hill, 'Value of the EEG in Diagnosis of Epilepsy', *British Medical Journal*, vol. 1, p. 663, Mar. 1958.

[19] E. Waterhouse, 'New horizons in ambulatory electroencephalography.', *IEEE Engineering in Medicine and Biology Magazine*, vol. 22, no. 3, pp. 74–80, Jun. 2003.

[20] A. Neligan and L. Sander, 'The incidence and prevalence of epilepsy [Online] Available: http://www.epilepsysociety.org.uk/Forprofessionals/Articles-1/Introduction [Accessed: 10-July-2013]', 2005.

[21] A. J. Fowle and C. D. Binnie, 'Uses and Abuses of the EEG in Epilepsy', *Epilepsia*, vol. 41, pp. S10–S18, Mar. 2000.

[22] J. Gawłowska and J. Wranicz, 'Norman J. "Jeff" Holter (1914–1983)', *Cardiology Journal*, vol. 16, no. 4, pp. 386–387, May 2009.

[23] S. S. Barold, 'Norman J. "Jeff" Holter–"Father" of Ambulatory ECG Monitoring', *Journal of Interventional Cardiac Electrophysiology*, vol. 14, no. 2, pp. 117–118, Nov. 2005.

[24] P. K. Stein, M. S. Bosner, R. E. Kleiger, and B. M. Conger, 'Heart rate variability: A measure of cardiac autonomic tone', *American Heart Journal*, vol. 127, no. 5, pp. 1376–1381, May 1994.

[25] Task Force of the European Society of Cardiology and The North American Society of Pacing and Electrophysiology, 'Heart Rate Variability Standards of Measurement, Physiological Interpretation, and Clinical Use', *Circulation*, vol. 93, no. 5, pp. 1043–1065, Mar. 1996.

[26] M. H. Crawford, S. J. Bernstein, P. C. Deedwania, J. P. DiMarco, K. J. Ferrick, A. Garson Jr, L. A. Green, H. L. Greene, M. J. Silka, P. H. Stone, C. M. Tracy, R. J. Gibbons, J. S. Alpert, K. A. Eagle, T. J. Gardner, A. Garson Jr, G. Gregoratos, R. O. Russell, T. J. Ryan, and S. C. Smith Jr, 'ACC/AHA guidelines for ambulatory electrocardiography: A report of the American College of Cardiology/American Heart Association Task Force on Practice Guidelines (Committee to Revise the Guidelines for Ambulatory Electrocardiography) developed in collaboration with the North American Society for Pacing and Electrophysiology', *Journal of the American College of Cardiology*, vol. 34, no. 3, pp. 912–948, Sep. 1999.

[27] J.R Ives and J.F Woods, '4-Channel 24 hour cassette recorder for long-term EEG monitoring of ambulatory patients', *Electroencephalography and Clinical Neurophysiology*, vol. 39, no. 1, pp. 88–92, Jul. 1975.

[28] J. Gotman, 'Automatic detection of seizures and spikes', *Journal of Clinical Neurophysiology: Official Publication of the American Electroencephalographic Society*, vol. 16, no. 2, pp. 130–140, Mar. 1999.

[29] G. L. Morris, J. Galezowska, R. Leroy, and R. North, 'The results of computer-assisted ambulatory 16-channel EEG', *Electroencephalography and Clinical Neurophysiology*, vol. 91, no. 3, pp. 229–231, Sep. 1994.

[30] D. E. Blum, J. Eskola, J. J. Bortz, and R. S. Fisher, 'Patient awareness of seizures', *Neurology*, vol. 47, no. 1, pp. 260–264, Jul. 1996.

[31] K. Doi, 'Computer-aided diagnosis in medical imaging: Historical review, current status and future potential', *Computerized Medical Imaging and Graphics*, vol. 31, no. 4–5, pp. 198–211, Jun. 2007.

[32] J. Liporace, W. Tatum IV, G. Lee Morris III, and J. French, 'Clinical utility of sleep-deprived versus computer-assisted ambulatory 16-channel EEG in epilepsy patients: a multi-center study', *Epilepsy Research*, vol. 32, no. 3, pp. 357–362, Nov. 1998.

[33] U. Seneviratne, A. Mohamed, M. Cook, and W. D'Souza, 'The utility of ambulatory electroencephalography in routine clinical practice: A critical review', *Epilepsy Research*, vol. 105, no. 1–2, pp. 1–12, Jul. 2013.

[34] C. M. Foley, A. Legido, D. K. Miles, D. A. Chandler, and W. D. Grover, 'Long-Term Computer-Assisted Outpatient Electroencephalogram Monitoring in Children and Adolescents', *Journal of Child Neurology*, vol. 15, no. 1, pp. 49–55, Jan. 2000.

[35] U. R. Acharya, S. Vinitha Sree, G. Swapna, R. J. Martis, and J. S. Suri, 'Automated EEG analysis of epilepsy: A review', *Knowledge-Based Systems*, vol. 45, pp. 147–165, Jun. 2013.

[36] C. A. Marsan and L. Zivin, 'Factors related to the occurrence of typical paroxysmal abnormalities in the EEG records of epileptic patients', *Epilepsia*, vol. 11, no. 4, pp. 361–381, Dec. 1970.

[37] S. J. M. Smith, ‘EEG in the diagnosis, classification, and management of patients with epilepsy’, *Journal of Neurology, Neurosurgery & Psychiatry*, vol. 76, no. suppl_2, pp. ii2–ii7, Jun. 2005.

[38] C. D. Binnie and H. Stefan, ‘Modern electroencephalography: its role in epilepsy management’, *Clinical Neurophysiology*, vol. 110, no. 10, pp. 1671–1697, Oct. 1999.

[39] A. J. Casson and E. Rodriguez-Villegas, ‘On data reduction in EEG monitoring: Comparison between ambulatory and non-ambulatory recordings’, in *Annual International Conference of the IEEE Engineering in Medicine and Biology Society (EMBC)*, 2008, pp. 5885–5888.

[40] A. J. Casson, D. C. Yates, S. Patel, and E. Rodriguez-Villegas, ‘Algorithm for AEEG data selection leading to wireless and long term epilepsy monitoring.’, in *Annual International Conference of the IEEE Engineering in Medicine and Biology Society (EMBC)*, 2007, pp. 2456–2459.

[41] A. J. Casson and E. Rodriguez-Villegas, ‘Data reduction techniques to facilitate wireless and long term AEEG epilepsy monitoring’, in *3rd International IEEE/EMBS Conference on Neural Engineering*, 2007, pp. 298–301.

[42] A. J. Casson and E. Rodriguez-Villegas, ‘Toward Online Data Reduction for Portable Electroencephalography Systems in Epilepsy’, *IEEE Transactions on Biomedical Engineering*, vol. 56, no. 12, pp. 2816–2825, Jul. 2009.

[43] A. Avila, R. Santoyo, and S. O. Martinez, ‘Hardware/software implementation of the EEG signal compression module for an ambulatory monitoring subsystem’, in *Proceedings of the 6th International Caribbean Conference on Devices, Circuits and Systems*, 2006, pp. 125–129.

[44] D. Prilutskiy, S. Selishchev, and A. Ustinov, ‘A Device for Wireless Transmission of Electrocardiographic and Electroencephalographic Data’, *Biomedical Engineering*, vol. 45, no. 6, pp. 214–217, Mar. 2012.

[45] K. Kang, K.-J. Park, J.-J. Song, C.-H. Yoon, and L. Sha, ‘A Medical-Grade Wireless Architecture for Remote Electrocardiography’, *IEEE Transactions on Information Technology in Biomedicine*, vol. 15, no. 2, pp. 260 –267, Mar. 2011.

[46] C.-Y. Huang and S.-G. Miaou, ‘Transmitting SPIHT compressed ECG data over a next-generation mobile telecardiology testbed’, in *Annual International Conference of the IEEE Engineering in Medicine and Biology Society (EMBC)*, 2001, vol. 4, pp. 3525–3528.

[47] K. Sayood, *Introduction to Data Compression, Third Edition*, 3rd ed. Morgan Kaufmann, 2005.

[48] N. Sriraam and C. Eswaran, ‘Performance Evaluation of Neural Network and Linear Predictors for Near-Lossless Compression of EEG Signals’, *IEEE Transactions on Information Technology in Biomedicine*, vol. 12, no. 1, pp. 87–93, Jan. 2008.

[49] N. Sriraam, ‘Neural network based near- lossless compression of EEG signals with non uniform quantization’, *Annual International Conference of the IEEE Engineering in Medicine and Biology Society (EMBC)*, pp. 3236–3240, Jan. 2007.

[50] D. Gopikrishna, A. Makur, and I. Bangalore, ‘A High Performance Scheme for EEG Compression Using a Multichannel Model’, *Lecture Notes In Computer Science*, pp. 443–451, 2002.

[51] A. E. Cetin and H. Köymen, ‘Compression of digital biomedical signals’, *The Biomedical Engineering Handbook: Second Edition*, 2000.

[52] M. Blanco-Velasco, F. Cruz-Roldán, F. López-Ferreras, Á. Bravo-Santos, and D. Martínez-Muñoz, ‘A low computational complexity algorithm for ECG signal compression’, *Medical Engineering & Physics*, vol. 26, no. 7, pp. 553–568, Sep. 2004.

[53] N. Sriraam, ‘Quality-on-Demand Compression of EEG Signals for Telemedicine Applications Using Neural Network Predictors’, *International Journal of Telemedicine and Applications*, vol. Jan. 2011, pp. 8:1–8:13, Jan2011.

[54] C. Bazán-Prieto, M. Blanco-Velasco, J. Cárdenas-Barrera, and F. Cruz-Roldán, ‘Retained energy-based coding for EEG signals’, *Medical Engineering & Physics*, vol. 34, no. 7, pp. 892–899, Sep. 2012.

[55] J. L. Cárdenas-Barrera, J. V. Lorenzo-Ginori, and E. Rodríguez-Valdivia, ‘A wavelet-packets based algorithm for EEG signal compression’, *Medical Informatics & The Internet in Medicine*, vol. 29, no. 1, pp. 15–27, Mar. 2004.

[56] G. Higgins, B. McGinley, S. Faul, R. P. McEvoy, M. Glavin, W. Marnane, and E. Jones, ‘The Effects of Lossy Compression on Diagnostically Relevant Seizure Information in EEG Signals’, *IEEE Journal of Biomedical and Health Informatics*, vol. 17, no. 1, pp. 121–127, Jan. 2013.

[57] A. Cohen, I. Daubechies, and J.-C. Feauveau, ‘Biorthogonal bases of compactly supported wavelets’, *Communications on Pure and Applied Mathematics*, vol. 45, no. 5, pp. 485–560, Oct. 1992.

[58] M. L. Hilton, B. D. Jawerth, and A. Sengupta, ‘Compressing Still and Moving Images with Wavelets’, *Multimedia Systems*, vol. 2, no. 5, pp. 218–227, Dec. 1994.

[59] M. L. Hilton, ‘Wavelet and wavelet packet compression of electrocardiograms’, *IEEE Transactions on Biomedical Engineering*, vol. 44, no. 5, pp. 394–402, May 1997.

[60] V. Raissi Dehkordi, H. Daou, and F. Labeau, ‘A Channel Differential EZW Coding Scheme for EEG Data Compression’, *IEEE Transactions on Information Technology in Biomedicine*, vol. 15, pp. 831–838, Nov. 2011.

[61] M. S. Manikandan and S. Dandapat, ‘Wavelet threshold based ECG compression using USZZQ and Huffman coding of DSM’, *Biomedical Signal Processing and Control*, vol. 1, no. 4, pp. 261–270, Oct. 2006.

[62] M. D. Adams, ‘The JPEG-2000 still image compression standard’, *Standards Contribution, ISO/IEC JTC 1/SC 29/WG 1 N 2412*, 2001.

[63] P. G. Howard and J. S. Vitter, ‘Analysis of Arithmetic Coding for Data Compression’, *Information Processing and Management*, vol. 28, no. 6, pp. 749–763, Dec. 1992.

[64] E. Bodden, M. Clasen, and J. Kneis, ‘Arithmetic Coding revealed - A guided tour from theory to praxis’, Sable Research Group, School of Computer Science, McGill University, Montréal, Québec, Canada, SABLE-TR-2007-5, May 2007.

[65] R. Gallager, ‘Variations on a theme by Huffman’, *IEEE Transactions on Information Theory*, vol. 24, no. 6, pp. 668–674, Nov. 1978.

[66] I. H. Witten, R. M. Neal, and J. G. Cleary, ‘Arithmetic coding for data compression’, *Communications of the ACM*, vol. 30, no. 6, pp. 520–540, Jun. 1987.

[67] A. Moffat and A. Turpin, *Compression and Coding Algorithms*. Springer, 2002.
[68] N. Abramson, *Information Theory and Coding*, vol. 61. McGraw-Hill New York, 1963.
[69] R. Pasco, 'Source coding algorithms for fast data compression (Ph.D. Thesis abstr.)', *IEEE Transactions on Information Theory*, vol. 23, no. 4, p. 548, Jul. 1977.
[70] J. J. Rissanen, 'Arithmetic codings as number representations', *Acta Polytechnica Scandinavica*, vol. 31, pp. 44–51, 1979.
[71] G. G. Langdon, 'Arithmetic coding', *IBM Journal of Research and Development*, vol. 23, no. 2, pp. 149–162, Mar. 1979.
[72] A. Moffat, R. M. Neal, and I. H. Witten, 'Arithmetic coding revisited', *ACM Transactions on Information Systems*, vol. 16, no. 3, pp. 256–294, Jul. 1998.
[73] A. Bilgin, M. W. Marcellin, and M. I. Altbach, 'Compression of electrocardiogram signals using JPEG2000', *IEEE Transactions on Consumer Electronics*, vol. 49, no. 4, pp. 833–840, Nov. 2003.
[74] K. Srinivasan, J. Dauwels, and M. R. Reddy, 'A two-dimensional approach for lossless EEG compression', *Biomedical Signal Processing and Control*, vol. 6, no. 4, pp. 387–394, Oct. 2011.
[75] Zhitao Lu, Dong Youn Kim, and W. A. Pearlman, 'Wavelet compression of ECG signals by the set partitioning in hierarchical trees algorithm', *IEEE Transactions on Biomedical Engineering*, vol. 47, no. 7, pp. 849–856, Jul. 2000.
[76] M. Pooyan, A. Taheri, M. Moazami-Goudarzi, and I. Saboori, 'Wavelet compression of ECG signals using SPIHT algorithm', *World Academy of Science, Engineering and Technology*, no. 2, pp. 212–215, Feb. 2005.
[77] M. Raad and A. Mertins, 'From lossy to lossless audio coding using SPIHT', in *Proceedings of the 5th International Conference on Digital Audio Effects*, 2002, pp. 245–250.
[78] J. M. Shapiro, 'Embedded Image Coding Using Zerotrees of Wavelet Coefficients', *IEEE Transactions On Signal Processing*, vol. 41, p. 12, Dec. 1993.
[79] W. A. Pearlman and A. Said, 'Set Partition Coding: Part I of Set Partition Coding and Image Wavelet Coding Systems', *Now Publishers Inc.*, vol. 1, 2008.
[80] S. Ktata, K. Ouni, and N. Ellouze, 'A Novel Compression Algorithm for Electrocardiogram Signals based on Wavelet Transform and SPIHT', *International Journal of Information and Communication Engineering*, vol. 5, no. 3, Autumn 2009.
[81] A. Alesanco and J. Garcia, 'Automatic Real-Time ECG Coding Methodology Guaranteeing Signal Interpretation Quality', *IEEE Transactions on Biomedical Engineering*, vol. 55, no. 11, pp. 2519 –2527, Nov. 2008.
[82] S. Nayebi, M. H. Miranbeigi, and A. M. Nasrabadi, 'An improved method for 2-D ECG compression based on SPIHT algorithm', in *Annual International Conference of the IEEE Engineering in Medicine and Biology Society (EMBC)*, 2008, pp. 2952 –2955.
[83] I. Mohammad Rezazadeh, M. Hassan Moradi, and A. Motie Nasrabadi, 'Implementing of SPIHT and Sub-band Energy Compression (SEC) Method on Two-Dimensional ECG Compression: A Novel Approach', in *Annual*

International Conference of the IEEE Engineering in Medicine and Biology Society (EMBC), 2005, pp. 3763 –3766.

[84] S.-C. Tai, C. Sun, and W.-C. Yan, 'A 2-D ECG compression method based on wavelet transform and modified SPIHT', *IEEE Transactions on Biomedical Engineering*, vol. 52, no. 6, pp. 999 –1008, Jun. 2005.

[85] K. Srinivasan and M. R. Reddy, 'Efficient preprocessing technique for real-time lossless EEG compression', *Electronics Letters*, vol. 46, no. 1, pp. 26–27, Jan. 2010.

[86] H. Daou and F. Labeau, 'Pre-Processing of multi-channel EEG for improved compression performance using SPIHT', in *Annual International Conference of the IEEE Engineering in Medicine and Biology Society (EMBC)*, 2012, pp. 2232 –2235.

[87] I. S. Reed and G. Solomon, 'Polynomial Codes Over Certain Finite Fields', *Journal of the Society for Industrial and Applied Mathematics*, vol. 8, no. 2, pp. 300–304, Jun. 1960.

[88] 'ISO/IEC 10149:1995 - Information technology -- Data interchange on read-only 120 mm optical data disks (CD-ROM)'. [Online]. Available: http://www.iso.org/iso/catalogue_detail.htm?csnumber=25869. [Accessed: 31-Jan-2013].

[89] 'ISO/IEC 29341-8-16:2008 - Information technology -- UPnP Device Architecture -- Part 8-16: Internet Gateway Device Control Protocol - Wide Area Network Digital Subscriber Line Configuration Service'. [Online]. Available: http://www.iso.org/iso/home/store/catalogue_tc/catalogue_detail.htm?csnumber=52734. [Accessed: 31-Jan-2013].

[90] 'White Paper Blu-ray Disc Format–General', *Internet Citation,[Available Online: http://www.blu-raydisc.com/en/Technical/TechnicalWhitePapers/General.aspx] [Accessed: 04-Apr-2013]*. [Online]. Available: http://www.blu-raydisc.com/en/Technical/TechnicalWhitePapers/General.aspx. [Accessed: 17-Jul-2013].

[91] J. Nayak, P. S. Bhat, M. S. Kumar, and U. R. Acharya, 'Reliable transmission and storage of medical images with patient information using error control codes', in *Proceedings of the IEEE India Annual Conference*, 2004, pp. 147 –150.

[92] R. McSweeney, C. Spagnol, E. Popovici, and L. Giancardi, 'Implementation of Source and Channel Coding for Power Reduction in Medical Application Wireless Sensor Network', in *Third International Conference on Sensor Technologies and Applications*, 2009, pp. 271 –276.

[93] R. McSweeney, C. Spagnol, and E. Popovici, 'Comparative study of software vs. hardware implementations of shortened Reed-Solomon code for Wireless Body Area Networks', in *27th International Conference on Microelectronics Proceedings*, 2010, pp. 223 –226.

[94] R. McSweeney and E. Popovici, 'Lossless EEG data source coding for seizure prone activity', in *IEEE International Conference on Information Technology and Applications in Biomedicine*, 2010, pp. 1 –4.

[95] T. Ma, M. Hempel, D. Peng, and H. Sharif, 'Rate-switching unequal error protection for wireless electrocardiogram (ECG) transmission', in *Military Communications Conference (MILCOM)*, 2010, pp. 1181–1186.

[96] S.-G. Miaou and Z.-H. Lin, ‘An integrated ECG compression and error protection scheme for Bluetooth transmission in home tele-care applications’, *Biomedical Engineering: Applications, Basis and Communications*, vol. 16, no. 04, pp. 213–223, 2004.
[97] A. Graps, ‘An introduction to wavelets’, *IEEE Computational Science Engineering*, vol. 2, no. 2, pp. 50 –61, Summer 1995.
[98] C. K. Chui, *An introduction to wavelets*, vol. 1. Academic Pr, 1992.
[99] A. Haar, ‘Zur theorie der orthogonalen funktionensysteme’, *Mathematische Annalen*, vol. 69, no. 3, pp. 331–371, Mar. 1910.
[100] I. Daubechies, ‘Orthonormal bases of compactly supported wavelets’, *Communications on Pure and Applied Mathematics*, vol. 41, no. 7, pp. 909–996, Oct. 1988.
[101] W. Sweldens, ‘The lifting scheme: A construction of second generation wavelets’, *SIAM Journal on Mathematical Analysis*, vol. 29, no. 2, pp. 511–546, 1998.
[102] I. Daubechies, *Ten Lectures on Wavelets*, 1st ed. SIAM: Society for Industrial and Applied Mathematics, 1992.
[103] I. Daubechies and W. Sweldens, ‘Factoring wavelet transforms into lifting steps’, *Journal of Fourier Analysis and Applications*, vol. 4, no. 3, pp. 247–269, May 1998.
[104] W. Sweldens, ‘Wavelets and the lifting scheme: A 5 minute tour’, *ZAMM-Zeitschrift fur Angewandte Mathematik und Mechanik*, vol. 76, no. 2, pp. 41–44, Jul. 1996.
[105] M. Unser and T. Blu, ‘Mathematical properties of the JPEG2000 wavelet filters’, *IEEE Transactions on Image Processing*, vol. 12, no. 9, pp. 1080–1090, Sep. 2003.
[106] ‘EEG Database — Seizure Prediction in Freiburg, Germany’. [Online]. Available: https://epilepsy.uni-freiburg.de/freiburg-seizure-prediction-project/eeg-database. [Accessed: 16-Nov-2011].
[107] B. Schelter, M. Winterhalder, T. Maiwald, A. Brandt, A. Schad, A. Schulze-Bonhage, and J. Timmer, ‘Testing statistical significance of multivariate time series analysis techniques for epileptic seizure prediction’, *Chaos*, vol. 16, p. 013108, Mar. 2006.
[108] F. Gilliam, R. Kuzniecky, and E. Faught, ‘Ambulatory EEG monitoring’, *Journal of Clinical Neurophysiology*, vol. 16, no. 2, pp. 111–115, Mar. 1999.
[109] S. O’Regan, S. Faul, and W. Marnane, ‘Automatic detection of EEG artefacts arising from head movements’, in *Annual International Conference of the IEEE Engineering in Medicine and Biology Society (EMBC)*, 2010, pp. 6353–6356.
[110] L. Vigon, M. R. Saatchi, J. E. Mayhew, and R. Fernandes, ‘Quantitative evaluation of techniques for ocular artefact filtering of EEG waveforms’, *IEE Proceedings on Science, Measurement and Technology*, vol. 147, no. 5, pp. 219–228, Sep. 2000.
[111] M. Divjak, D. Zazula, and A. Holobar, ‘Assessment of artefact suppression by ICA and spatial filtering on reduced sets of EEG signals’, in *Annual International Conference of the IEEE Engineering in Medicine and Biology Society (EMBC)*, 2011, pp. 4422–4425.
[112] M. Blanco-Velasco, F. Cruz-Roldán, J. I. Godino-Llorente, J. Blanco-Velasco, C. Armiens-Aparicio, and F. López-Ferreras, ‘On the use of PRD and CR

parameters for ECG compression', *Medical Engineering and Physics*, vol. 27, no. 9, pp. 798–802, Nov. 2005.

[113] Ke Chu Yi, Mingui Sun, Ching Chung Li, and R. J. Sclabassi, 'A lossless compression algorithm for multichannel EEG', in *Proceedings of the First Joint BMES/EMBS Conference*, 1999, vol. 1, p. 429.

[114] J. Ylöstalo, 'Data compression methods for EEG', *Technology and Health Care*, vol. 7, no. 4, pp. 285–300, Jan. 1999.

[115] Y. Wongsawat, S. Oraintara, and K. R. Rao, 'Integer Sub-Optimal Karhunen-Loeve Transform For Multi-Channel Lossless EEG Compression', in *European Signal Processing Conference*, 2006.

[116] G. Higgins, B. McGinley, M. Glavin, and E. Jones, 'Low power compression of EEG signals using JPEG2000', in *4th International ICST Conference on Pervasive Computing Technologies for Healthcare*, 2010, pp. 1 –4.

[117] Y. Zigel, A. Cohen, and A. Katz, 'The weighted diagnostic distortion (WDD) measure for ECG signal compression', *IEEE Transactions on Biomedical Engineering*, vol. 47, no. 11, pp. 1422–1430, Nov. 2000.

[118] J. J. Bailey, A. S. Berson, A. Garson Jr, L. G. Horan, P. W. Macfarlane, D. W. Mortara, and C. Zywietz, 'Recommendations for standardization and specifications in automated electrocardiography: bandwidth and digital signal processing. A report for health professionals by an ad hoc writing group of the Committee on Electrocardiography and Cardiac Electrophysiology of the Council on Clinical Cardiology, American Heart Association', *Circulation*, vol. 81, no. 2, pp. 730–739, Feb. 1990.

[119] S. Faul, A. Temko, and W. Marnane, 'Age-independent Seizure Detection', *Annual International Conference of the IEEE Engineering in Medicine and Biology Society (EMBC)*, pp. 6612 – 6615, 2009.

[120] R. P. McEvoy, S. Faul, and W. P. Marnane, 'Ambulatory REACT: Real-time seizure detection with a DSP microprocessor', in *Annual International Conference of the IEEE Engineering in Medicine and Biology Society (EMBC)*, 2010, pp. 2443–2446.

[121] S. Faul, A. Temko, G. Lightbody, and G. Boylan, 'A method of analysing an electroencephalogram (EEG) signal, Patent Application: 0906029.4', 2009.

[122] A. Temko, E. M. Thomas, W. P. Marnane, G. Lightbody, and G. Boylan, 'EEG Based Neonatal Seizure Detection with Support Vector Machines', *Clinical Neurophysiology*, vol. 122, no. 3, pp. 464–473, Mar. 2011.

[123] D. Kelleher, A. Temko, D. Nash, B. McNamara, and W. Marnane, 'SVM detection of epileptiform activity in routine EEG', in *Annual International Conference of the IEEE Engineering in Medicine and Biology Society (EMBC)*, 2010, pp. 6369–6372.

[124] A. Temko, R. P. McEvoy, D. Dwyer, S. Faul, G. Lightbody, and W. Marnane, 'REACT: Real-time EEG analysis for event detection', in *Proceedings of the AMA-IEEE Medical Technology Conference on Individualized Healthcare*, 2010, vol. 1, pp. 21–23.

[125] A. Temko, E. Thomas, G. Boylan, W. Marnane, and G. Lightbody, 'An SVM-based system and its performance for detection of seizures in neonates', in *Annual International Conference of the IEEE Engineering in Medicine and Biology Society (EMBC)*, 2009, pp. 2643–2646.

[126] A. Temko, E. M. Thomas, W. P. Marnane, G. Lightbody, and G. Boylan, 'Performance Assessment for EEG Based Neonatal Seizure Detectors', *Clinical Neurophysiology*, vol. 122, no. 3, pp. 474–482, Mar. 2011.

[127] ‘ADSP-BF537 | Blackfin Processor with Embedded Network Connectivity | Blackfin Processors | Processors and DSP | Analog Devices’. [Online]. Available: http://www.analog.com/en/processors-dsp/blackfin/adsp-bf537/products/product.html. [Accessed: 14-Jun-2012].

[128] ‘EE-298: Estimating Power for ADSP-BF538/BF539 Blackfin Processors (Rev 2, 07/2007)’. [Online]. Available: http://www.analog.com/en/processors-dsp/blackfin/products/application-notes/resources/index.html. [Accessed: 15-Jun-2012].

[129] ‘nRF8001, μBlue, Bluetooth low energy - Nordic Semiconductor’. [Online]. Available: http://www.nordicsemi.com/eng/Products/Bluetooth-R-low-energy/nRF8001. [Accessed: 08-Jun-2012].

[130] G. Higgins, B. McGinley, N. Walsh, M. Glavin, and E. Jones, ‘Lossy compression of EEG signals using SPIHT’, *Electronics Letters*, vol. 47, no. 18, pp. 1017–1018, Sep. 2011.

[131] P. Welch, ‘The use of fast Fourier transform for the estimation of power spectra: A method based on time averaging over short, modified periodograms’, *IEEE Transactions on Audio and Electroacoustics*, vol. 15, no. 2, pp. 70– 73, Jun. 1967.

[132] G. Higgins, S. Faul, R. P. McEvoy, B. McGinley, M. Glavin, W. P. Marnane, and E. Jones, ‘EEG Compression Using JPEG2000: How Much Loss Is Too Much?’, in *Annual Conference of the IEEE Engineering in Medicine and Biology Society (EMBC)*, 2010, pp. 614–617.

[133] A. L. Goldberger, L. A. N. Amaral, L. Glass, J. M. Hausdorff, P. C. Ivanov, R. G. Mark, J. E. Mietus, G. B. Moody, C.-K. Peng, and H. E. Stanley, ‘PhysioBank, PhysioToolkit, and PhysioNet Components of a New Research Resource for Complex Physiologic Signals’, *Circulation*, vol. 101, no. 23, pp. e215–e220, Jun. 2000.

[134] H. Adel, O. Zahran, W. Al-Nauimy, S. El-Halafawy, T. El-Sayed, and F. E. A. El-Samie, ‘SPIHT compression of ECG signals using an image processing concept’, in *8th International Conference on Informatics and Systems*, 2012, pp. BIO14 –BIO19.

[135] A. Alesanco and J. Garcia, ‘Automatic Real-Time ECG Coding Methodology Guaranteeing Signal Interpretation Quality’, *IEEE Transactions on Biomedical Engineering*, vol. 55, no. 11, pp. 2519–2527, Nov. 2008.

[136] M. S. Manikandan and S. Dandapat, ‘Effective quality-controlled SPIHT-based ECG coding strategy under noise environments’, *Electronics Letters*, vol. 44, no. 20, pp. 1182 –1183, Sep. 2008.

[137] N. Twomey, N. Walsh, O. Doyle, B. McGinley, M. Glavin, E. Jones, and W. P. Marnane, ‘The effect of lossy ECG compression on QRS and HRV feature extraction’, in *Annual International Conference of the IEEE Engineering in Medicine and Biology Society (EMBC)*, 2010, pp. 634 –637.

[138] G. B. Moody and R. G. Mark, ‘The impact of the MIT-BIH arrhythmia database’, *IEEE Engineering in Medicine and Biology Magazine*, vol. 20, no. 3, pp. 45–50, Aug. 2002.

[139] M. Blanco-Velasco, F. Cruz-Roldán, E. Moreno-Martínez, J.-I. Godino-Llorente, and K. E. Barner, ‘Embedded filter bank-based algorithm for ECG compression’, *Signal Processing*, vol. 88, no. 6, pp. 1402–1412, Jun. 2008.

[140] C. Vidaurre, T. H. Sander, and A. Schlögl, ‘BioSig: The Free and Open Source Software Library for Biomedical Signal Processing’, *Computational Intelligence and Neuroscience*, pp. 1–12, Jan. 2011.

[141] J. Pan and W. J. Tompkins, ‘A Real-Time QRS Detection Algorithm’, *IEEE Transactions on Biomedical Engineering*, vol. 32, no. 3, pp. 230 –236, Mar. 1985.

[142] P. S. Hamilton and W. J. Tompkins, ‘Quantitative Investigation of QRS Detection Rules Using the MIT/BIH Arrhythmia Database’, *IEEE Transactions on Biomedical Engineering*, vol. 33, no. 12, pp. 1157 –1165, Dec. 1986.

[143] V. X. Afonso, W. J. Tompkins, T. Q. Nguyen, and S. Luo, ‘ECG beat detection using filter banks’, *IEEE Transactions on Biomedical Engineering*, vol. 46, no. 2, pp. 192 –202, Feb. 1999.

[144] B. Han, L. Ji, S. Lee, B. Bhattacharjee, and R. R. Miller, ‘Are all bits equal?: experimental study of IEEE 802.11 communication bit errors’, *IEEE/ACM Transactions on Networking*, vol. 20, no. 6, pp. 1695–1706, Dec. 2012.

Appendix A Journal Publications Arising from this Thesis

The following journal publications have arisen as a result of the work contained in this thesis. Only the papers where I am primary author and that have been accepted for publication at the time this thesis was submitted have been included.

Garry Higgins, Brian McGinley, Edward Jones, Martin Glavin, "An evaluation on the effects of wavelet coefficient quantisation in transform based EEG compression", *Computers in Biology and Medicine*, 43, pp. 661-669, July 2013.

Garry Higgins, Brian McGinley, Stephen Faul, Robert P. McEvoy, Martin Glavin, William P. Marnane, Edward Jones, "The Effects of Lossy Compression on Diagnostically Relevant Seizure Information in EEG Signals", *IEEE Journal of Biomedical and Health Informatics*, Vol. 17, Issue 1, pp. 121-127, Jan. 2013.

Garry Higgins, Brian McGinley, Noel Walsh, Martin Glavin, Edward Jones, "Lossy Compression of EEG Signals using SPIHT", *Electronics Letters*, Issue Vol. 47, Issue 18, pp 1017-1018, Sept. 2011.

Lossy compression of EEG signals using SPIHT

G. Higgins, B. McGinley, N. Walsh, M. Glavin and E. Jones

A method of compressing electroencephalographic signals using the set partitioning in hierarchical trees (SPIHT) algorithm is described. The signals were compressed at a variety of different compression ratios (CRs), with the loss of signal integrity at each CR determined using the percentage root-mean squared difference between the reconstructed signal and the original. An analysis of the computational complexity of the SPIHT algorithm is also presented, using the Blackfin processor as an example implementation target.

Introduction: The multichannel electroencephalogram (EEG) is a tool commonly used for diagnosing a variety of neurological conditions. Diagnosis of these conditions often requires long-term monitoring of the patient's EEG activity, which necessitates storage of large amounts of data [1]. This causes both storage and wireless transmission problems for potential portable ambulatory EEG systems, since wireless communication is a significant contributor to power consumption [2]. Therefore, effective data compression is important to minimise the information needed to be transmitted and stored. A coexisting goal is that it be performed in an efficient manner so as not to unduly add to the power consumption of the device.

To minimise the amount of data to be transmitted or stored in a portable device, the amount of compression, expressed as compression ratio (CR), needs to be maximised. Lossy compression can attain higher CRs than lossless, but with a loss in signal fidelity. It is desirable to use a compression algorithm that maximises CR, while also maximising signal fidelity and minimising computation. In this Letter, the SPIHT algorithm is investigated for the task of ambulatory EEG compression.

Compression method: Set partitioning in hierarchical trees (SPIHT) is an image compression method proposed by Said and Pearlman in [3]. In this application, the CDF 9/7 biorthogonal discrete wavelet transform (DWT) was used owing to its widespread use in a variety of compression applications. A seven-level DWT decomposition was performed as this was found to give the best compression performance. The DWT coefficients are quantised using a standard integer quantisation method and passed to the SPIHT encoder. As SPIHT's output bit stream is ordered by importance, the encoder can terminate encoding at any point.

Testing: For lossy compression, a standard measure of compression performance is the percentage RMS distortion (PRD) between the original and reconstructed signals, defined as:

$$PRD = \left(\frac{\|x - \hat{x}\|}{\|x\|} \right) \quad (1)$$

where x and $\hat{x}$ are the original and reconstructed signals, respectively, and $\| \ \|$ represents the Euclidean or L^2 norm. Compression ratio (CR) represents the ratio between the bit rate of the original signal and the bit rate of the compressed signal.

The EEG dataset used was provided by the University of Freiburg, Germany [4, 5]. This contains a mixture of both seizure and non-seizure data for 21 patients. The database was chosen because of its public availability, and contains six-channel EEG signals. While clinical systems typically use 64 or 128 channels, six channels are more likely to be feasible for a real-world implementation of an AEEG seizure detection device [6]. The EEG signals were compressed and reconstructed at CRs ranging from 2 to 50. The PRD of each reconstructed signal was then calculated. No prefiltering was applied to the signals prior to compression, and each channel was compressed and decompressed independently.

The complexity of the SPIHT algorithm was also analysed by determining the average number of operations required to compress one frame of the EEG for each of the CRs considered. The SPIHT algorithm is composed of two arithmetic and two list operations. The arithmetic operations are subtracts and compares. SPIHT employs lists to maintain track of insignificant sets and significant and insignificant coefficients. These lists dynamically vary in size. A linked list is an efficient dynamic data structure implementation which, for SPIHT, requires two core operations: (i) a push operation and (ii) a list erase operation. The number of machine cycles for each of these operations was obtained for the Analog Devices Blackfin BF537 DSP processor using the ADI Visual DSP + + profiling tool; these are given in Table 1.

Table 1: Average numbers of machine cycles per operation on Analog Devices Blackfin BF537 DSP processor

Instruction	Number of clock cycles
Integer compares	2
Sign compare	2
Integer subtract	2
Linked-list insert	67
Linked-list erase	62

Results: Fig. 1 plots the average PRD for the full database against CR. The authors in [7] suggested that a PRD of 7% is sufficient for clinical evaluation of reconstructed EEG signals; for this PRD, it can be seen that a CR of about 5:1 is achievable. A further application of interest for compressed EEG is automated seizure detection. Based on the results found in [8], a PRD of up to 30% was found to have no significant impact on seizure detection in EEG signals. For this level of PRD, a CR of about 30:1 was achieved. Fig. 2 illustrates a segment of EEG alongside the same signal reconstructed with PRD values of 7 and 30%.

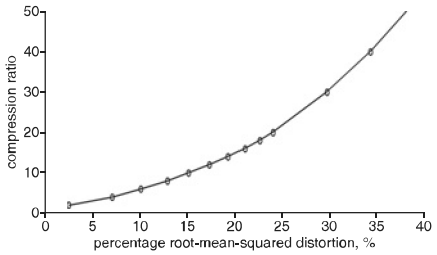

Fig. 1 *Average CR against PRD for all records in Freiburg database*

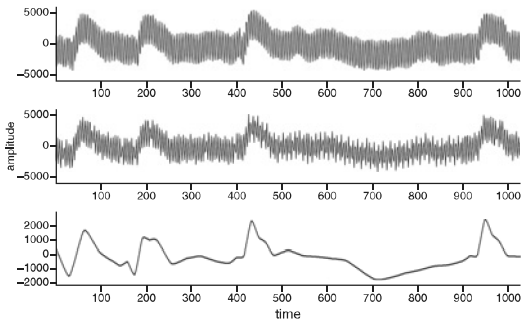

Fig. 2 *Original EEG signal (top plot), and after being reconstructed with PRD of 7% (middle plot) and PRD of 30% (lower plot)*

Table 2 details the execution count of each operation used to compress one frame of EEG signal, as well as the total number of cycles required. Assuming a clock speed of 50 MHz for the Blackfin DSP, the corresponding processor load factor can be estimated in the rightmost column of Table 2. Even allowing for an additional scaling factor to take additional processor overhead into account, it can be seen that the algorithm does not significantly load the processor.

Comparison with similar work: In [8], JPEG2000 is used to compress EEG signals at a variety of levels of fidelity loss. Using 7% PRD as the allowed loss, the results are very close to what is obtained by SPIHT. However, the paper also suggests that a PRD of 30% is allowable in order to maintain a detection rate of over 90%. For SPIHT, a PRD of 30% corresponds to approximately a 30:1 CR, which is higher than the results obtained in [8].

A wavelet packet-based method for compressing EEG signals was presented in [7]. As noted above, this paper suggested a 7% PRD as the maximum allowable loss, in order to maintain clinically relevant information in EEG signals. Generally speaking, results for PRDs above 12% have not been reported in the literature so it is not known what CRs are achievable for the higher PRD limit of 30% suggested in [8].

Table 2: Average number of operations per frame, number of machine cycles/frame, cycles/second and processor load for SPIHT compression on Blackfin BF537 Processor against CR

CR	Compare	Subtract	List	List	Total cycles	MIPS	50 MHz load (%)
2	22173	2381	2142	1148	263798	65950	0.132
4	18899	890	1802	851	213074	53269	0.107
6	17066	513	1316	541	156872	39218	0.079
8	15814	365	1017	418	126413	31604	0.064
10	14878	272	859	336	108685	27172	0.055
12	14137	218	738	272	95020	23755	0.048
14	13507	175	647	215	84043	21011	0.043
16	12947	148	574	182	75932	18983	0.038
18	12460	129	514	160	69536	17384	0.035
20	12030	114	465	145	64433	16109	0.033
30	10362	70	308	95	47390	11848	0.024
40	9144	50	223	70	37669	9418	0.019
50	8208	38	172	54	31364	7841	0.016

Srinivasan *et al.* proposed a method of EEG compression which also uses SPIHT [9]. That paper uses SPIHT as a preprocessing step for a method of real-time, lossless EEG compression. However, the compression properties of SPIHT are not investigated and CR results are not reported.

Conclusions: The results presented demonstrate that SPIHT provides an efficient and flexible approach to EEG signal compression. A CR of approximately 5:1 results in a 7% PRD, which is suitable for applications requiring clinical evaluation of the reconstructed EEG. Furthermore, for automated seizure detection applications, a CR of up to 30:1 is achievable with acceptable performance. In addition, the complexity analysis demonstrates that SPIHT performs compression without significantly loading a Blackfin BF537 processor. Because of the embedded nature of SPIHT, higher CRs correspond to even lower processor loading.

Acknowledgments: The authors acknowledge the Albert-Ludwigs-Universität, Freiburg, Germany, for allowing access to their adult EEG database. This work was supported by Science Foundation Ireland under Strategic Research Cluster SFI/07/SRC/I1169.

8 April 2011
doi: 10.1049/el.2011.1037

G. Higgins, B. McGinley, N. Walsh, M. Glavin and E. Jones (*College of Engineering and Informatics, National University of Ireland Galway, University Road, Galway, Ireland*)

E-mail: g.higgins1@nuigalway.ie

References

1 Casson, A.J., Smith, S., Duncan, J.S., and Rodriguez-Villegas, E.: 'Wearable EEG: what is it, why is it needed and what does it entail?'. Annual Int. Conf. of IEEE Engineering in Medicine and Biology Society, Vancouver, BC, USA, 2008, pp. 5867–5870

2 Otto, C., Milenkovic, A., Sanders, C., and Jovanov, E.: 'System architecture of a wireless body area sensor network for ubiquitous health monitoring', *J. Mobile Multimedia*, 2006, **1**, (4), pp. 307–326

3 Said, A., and Pearlman, W.A.: 'A new fast and efficient image codec based on set partitioning in hierarchical trees', *IEEE Trans. Circuits Syst. Video Technol.*, 1996, **6**, pp. 243–250

4 'EEG Database — Seizure Prediction Project Freiburg, Germany - https://epilepsy.uni-freiburg.de/freiburg-seizure-prediction-project/eeg-database.' [Online]. Available: https://epilepsy.uni-freiburg.de/freiburg-seizure-prediction-project/eeg-database. [Accessed: 15 July 2010]

5 Schelter, B., Winterhalder, M., Maiwald, T., Brandt, A., Schad, A., Schulze-Bonhage, A., and Timmer, J.: 'Testing statistical significance of multivariate time series analysis techniques for epileptic seizure prediction', *Chaos*, 2006, **16**, (1), pp. 013108

6 Gilliam, F., Kuzniecky, R., and Faught, E.: 'Ambulatory EEG monitoring', *J. Clin. Neurophys.: Official Publication of American Electroencephalographs Society*, 1999, **16**, (2), pp. 111—115

7 Cardenas-Barrera, J.L., Lorenzo-Ginori, J.V., and Rodriguez-Valdivia, E.: 'A wavelet-packets based algorithm for EEG signal compression', *Med. Inf. Internet Med.*, 2004, **29**, (1), pp. 15–27

8 Higgins, G., *et al.*: 'EEG compression using JPEG2000: how much loss is too much?'. Proc. IEEE Engineering in Medicine and Biology Conf. (EMBC), Buenos Aires, Argentina, 2010

9 Srinivasan, K., and Reddy, M.R.: 'Efficient preprocessing technique for real-time lossless EEG compression', *Electron. Lett.*, 2010, **46**, (1), pp. 26–27

The Effects of Lossy Compression on Diagnostically Relevant Seizure Information in EEG Signals

Garry Higgins, Brian McGinley, Stephen Faul, Robert P. McEvoy, Martin Glavin, William P. Marnane, and Edward Jones

***Abstract*—This paper examines the effects of compression on electroencephalogram (EEG) signals, in the context of automated detection of epileptic seizures. Specifically, it examines the use of lossy compression on EEG signals in order to reduce the amount of data which has to be transmitted or stored, while having as little impact as possible on the information in the signal relevant to diagnosing epileptic seizures. Two popular compression methods, JPEG2000 and SPIHT, were used. A range of compression levels was selected for both algorithms in order to compress the signals with varying degrees of loss. This compression was applied to the database of epileptiform data provided by the University of Freiburg, Germany. The real-time EEG analysis for event detection automated seizure detection system was used in place of a trained clinician for scoring the reconstructed data. Results demonstrate that compression by a factor of up to 120:1 can be achieved, with minimal loss in seizure detection performance as measured by the area under the receiver operating characteristic curve of the seizure detection system.**

***Index Terms*—Electroencephalogram (EEG) compression, lossy compression, seizure detection, seizure detection performance.**

I. Introduction

MULTICHANNEL electroencephalogram (EEG) is a tool for measuring the electrical activity of the brain, and the use of EEG to diagnose a variety of neurological conditions such as epilepsy has long been established [1]. Recent years have seen an increased interest in the use of ambulatory EEG monitoring, where at-home monitoring give advantages over in-patient monitoring in diagnosing neurological conditions [2]. A wireless and mobile ambulatory EEG device would allow the patient to remain at home in their normal environment during periods of observation. Furthermore, automated seizure detection would also reduce the workload of a trained clinician monitoring EEG recordings.

With EEG signals, even a small amount of recording can generate very large amount of data [3]. Since wireless transmission is a major contributor to power consumption in a portable device [3]–[5], minimizing the amount of data to be transmitted is desirable. Lossy compression achieves much higher compression ratios (CRs) than lossless compression, but at the expense of imperfections in the reconstructed signal. A tradeoff exists between the amount of loss in signal fidelity that can be tolerated and the CR that can be achieved. Percentage root-mean squared difference (PRD) is a common measure of the loss of signal fidelity between two signals. The smaller the PRD, the lower the distortion introduced by the compression process. Higher CRs are desirable, but result in larger PRD values. By using a high-performing automated seizure detection such as real-time EEG analysis for event detection (REACT) [6]–[8] in place of a clinician, it is possible to examine its seizure detection performance on the uncompressed and reconstructed EEG data at a variety of compression levels, in a consistent and reproducible way. Two compression algorithms are examined in this paper: JPEG2000 [9] and SPIHT [10]. Both methods employ a discrete wavelet transform (DWT) as a preprocessing step, and encode the resulting wavelet coefficients into a binary stream. A database of epileptiform EEG provided by the University of Freiburg, Germany [11], was used for testing. The data were compressed at a range of levels and passed through the REACT system. The two main results of interest are the CR and seizure detection performance of REACT. The key goal of the research is to investigate the potential to maximize CR without compromizing seizure detection performance.

Recent years have seen an increase in research involving compression of EEG signals, both for AEEG devices and for other EEG monitoring applications. Casson *et al.* put forth a variety of AEEG-related research including methods of compression prior to transmission [2], [3], [12]–[14]. The compression approach taken differs from the method proposed here in that it involves only transmitting when seizure data are encountered. Here, the approach of transmitting all data in a more compressed form is used. Having these data available gives clinicians the ability to review and evaluate the results. Even when an automated seizure detection system is used, it is often the case that a clinician wishes to review the data prior to a final diagnosis. Cárdenas-Barrera *et al.* proposed a low powered wavelet packet-based approach to EEG compression [15]. While the results achieved are good, the level of loss accepted is low. Sriraam and Eswaran proposed a number of EEG compression approaches based on neural networks [16]–[18]. In [18], Sriraam proposes the use of neural network predictors for telemedical EEG applications. While this is a similar application to what is proposed here, it does not have the requirement of being implementable on a

Manuscript received January 18, 2012; revised June 18, 2012; accepted September 23, 2012. Date of current version February 4, 2013. This work was supported in part by Science Foundation Ireland under Grant SRC/07/I1169.

G. Higgins, B. McGinley, M. Glavin, and E. Jones are with the College of Engineering and Informatics, National University of Ireland Galway, Galway, Ireland (e-mail: g.higgins1@nuigalway.ie; brian.mcginley@nuigalway.ie; martin.glavin@nuigalway.ie; edward.jones@nuigalway.ie).

S. Faul, R. P. McEvoy, and W. P. Marnane are with the Department of Electrical and Electronic Engineering, University College Cork, Cork, Ireland (e-mail: stephenf@eleceng.ucc.ie; robertmce@gmail.com; liam@eleceng.ucc.ie).

Digital Object Identifier 10.1109/TITB.2012.2222426

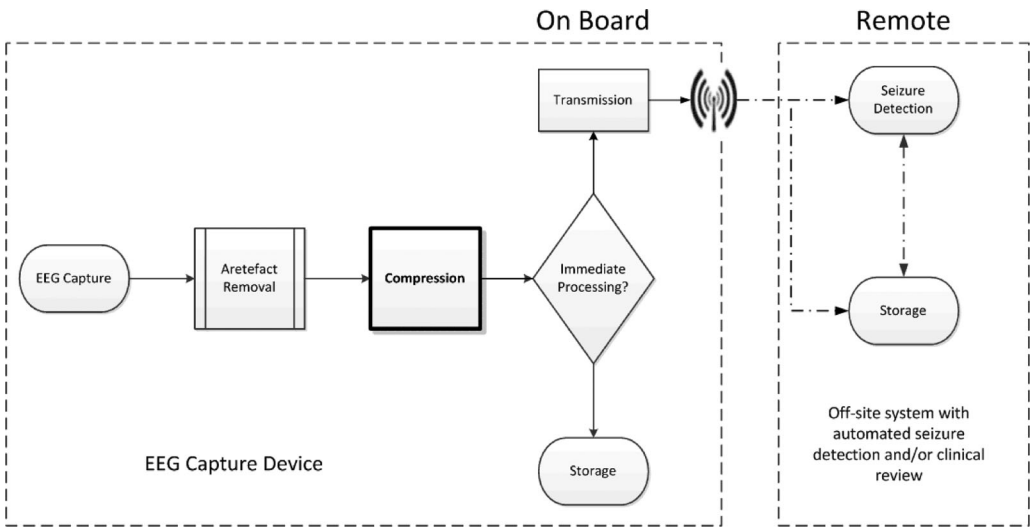

Fig. 1. Block diagram of a possible seizure detection system architecture, consisting of a low-power wearable device communicating wirelessly with a remote server.

portable device. The methodology outlined here is based on algorithms that are proven to be implementable on low-powered devices [19]–[22]. This paper extends the work of Higgins *et al.* in [23] and [24], by modifying the JPEG2000 algorithm to improve compression results and by including a comparison with the SPIHT algorithm.

II. Compression

A. Algorithm Implementation

Compression of EEG signals is useful in 1) storage and 2) transmission of the data. The two main factors for storage are reduction in the space required to store the data, and preservation of data fidelity for future review. Transmission implies that the data are to be immediately transmitted to a secondary receiver. As wireless transmission is one of the main consumers of power in a system [3]–[5], the main objective of compression prior to transmission is to minimize data size without impacting on diagnostically relevant information.

The compression research outlined here is designed to be implemented in an EEG monitoring system involving storage or transmission of data suspected to contain epileptiform data. Recording and artifact removal are done prior to compression, and transmission is done after compression.

Fig. 1 shows a possible architecture for a seizure detection system, which could be implemented in an AEEG device or similar. The system consists of a low-power wearable sensor that records, compresses, and wirelessly transmits the EEG data to a remote "server." It is also worth noting that artifact removal may be done after compression and transmission with minimal adaptation to the algorithm. It is likely, however, that lower CRs would be achieved if artifact data were also present in recordings.

B. Discrete Wavelet Transform (DWT)

This section provides an overview of the DWT, which is employed as a preprocessing step to both compression algorithms investigated in this paper. The DWT is well documented in the literature, so only a brief overview will be given here.

The DWT decomposes a signal into a set of basis functions known as wavelets [25], [26]. The initial wavelet, also known as the mother wavelet, is used to construct the other wavelets by means of dilation and shifting. The DWT coefficients are defined as the inner product of the original signal and the selected basis functions.

These coefficients provide an alternative representation of the original signal, giving good localization of the signal's energy components from both a time and frequency perspective. The CDF9/7 wavelet has already achieved wide-spread acceptance for use in compression algorithms [27], and is the wavelet function used in this paper.

C. JPEG2000

JPEG2000 is a compression algorithm designed for both lossless and lossy compression of image files. JPEG2000 Part 1 was ratified by the Joint Photographic Experts Group in 2000 [28] and contains the specifications for the core image coding system. These core components include the DWT, quantization, and an arithmetic coder (AC).

The adaptive binary AC replaces the original Huffman coder as the entropy coder for the JPEG2000 compression standard. The AC can perform near optimum entropy coding on a given dataset [29] and avoids some of the limitations of Huffman encoding [30].

Here, two changes were made to the standard JPEG2000 Part 1 system. The first was the inclusion of a thresholding stage after quantization. Thresholding allows for increased control over CR and PRD. All wavelet coefficients with magnitude below the selected threshold level are deemed to be insignificant and set to zero, allowing them to be more efficiently encoded by the AC.

The second change was made specifically to the AC. Initial tests using the standard JPEG2000 adaptive AC found that it quickly reached a maximum CR due to limitations in the

probability density function (PDF) being reset for each frame. Furthermore, it was found that the PDF of each frame had the form of a Gaussian distribution due to the effects of the DWT and quantization. By calculating the average PDF for all frames at a given threshold, a static PDF can be used for encoding and decoding. As the PDF is the same for all frames, it does not need to be either calculated dynamically or transmitted as part of the encoded message. Because it is based on the average of all the signals, it will be close to the actual distribution of the PDF minimizing the impact on the frames CR. The PDF was common across all patients at a given compression level.

D. SPIHT

Initially proposed by Said and Pearlman in [10], set partitioning in hierarchical trees (SPIHT) is a compression method originally designed for image compression. Its core principles are derived from the embedded zerotree wavelet (EZW) coder proposed by Shapiro in [31]. These coders exploit the fact that wavelet coefficients in different subbands have a temporal relationship with one another.

SPIHT provides efficient coding performance by making binary partitioning decisions, in order to determine the "significance" of each of the coefficients produced by the DWT. The partitioning decisions are performed to keep insignificant coefficients in large subsets; the larger the subsets, the more efficiently they can be represented in the coded bitstream. The threshold values used for significance checking are selected as powers of 2, which allow the wavelet coefficients to be encoded as binary numbers, through progressive bit-plane analysis. SPIHT orders the bits by significance, with the most significant bits being encoded first. This means that SPIHT allows for direct CR control of the signal being encoded as the binary bit stream can be terminated at any point.

III. Test Conditions

A. REACT

REACT is an automated seizure detection system [7], [8]. The REACT algorithm operates on EEG data by extracting a rich set of features from the time, information theory, and spectral domains. A support vector machine (SVM) classifier lies at the core of the REACT system, which uses rules that have been automatically derived using machine-learning and pattern-recognition techniques. These rules are used to classify the extracted EEG features as seizure or nonseizure. Further detail on REACT can be found in [32]–[36]. Although REACT was initially designed for use in neonatal seizure detection, subsequent research has demonstrated that it can also achieve very high seizure detection performance on adult EEG [7].

In this paper, the REACT seizure detection system is employed in place of a clinician, to rapidly analyze many hundreds of hours of EEG data and identify seizure activity. This research employs REACT to determine 1) if seizures can still be reliably detected from EEG data which have been compressed with a lossy compression algorithm and 2) the impact of increasing levels of compression and consequent signal degradation on seizure detection performance.

REACT was deemed to be a suitable alternative to a trained clinician as it has already been proven to give very accurate results for seizure detection, as previously verified by clinical review of its performance [35], [36]. The REACT system was trained on uncompressed EEG data and was tested using data that were subjected to compression and resynthesis at different compression ratios.

B. Freiburg Database

A database of EEG from patients with medically intractable focal epilepsy is maintained by the University of Freiburg [11], [37]. It contains seizure and nonseizure EEG data for 21 patients ranging in age from 13 to 50 years, sampled at 256 Hz. This dataset was chosen due to 1) its public availability; 2) the 6-channel EEG recordings provided are likely to be close to what would be recorded by an AEEG device [38]; and 3) the intracranial recordings minimize the artifacts present in the recordings. Artifact removal is something that could be carried out prior to compression in an AEEG device [39]–[41].

Of the 21 patients in the database, 15 were selected based on the quality criteria expressed in [7]. Specifically, three patients (1, 18, and 19) were discarded due to the length of seizure events being less than 10 s and three others (5, 8, and 10) were removed due to the large amount of recording artifact data present. The remaining 15 patients' EEG recordings comprise 132.7 h of data with approximately 120 min of seizure activity over 61 seizure events. For test purposes, the EEG data are processed on a frame-by-frame basis, with frames of duration 4 s. Therefore, the total number of frames is 119 430, with 1800 frames containing seizures. Prefiltering was not applied to the signals prior to compression.

While AEEG signals would normally include artifacts due to, e.g., movement, eye blinks, etc., this is not considered in this paper, since the objective here is to evaluate the effect of compression on seizure detection in EEG signals, rather than to evaluate the absolute performance of the seizure detection system. The subset of the Freiburg database used here consists of intracranial recordings which do not contain any of the artifacts that would normally occur in AEEG recordings. In a real-world implementation, artifact removal would ideally be done on the signal prior to compression, and a number of authors have proposed methods for automatic artifact removal, e.g., [42], [43]. Artifact removal in the context of the REACT system has been investigated in [6] and [39].

C. Performance Evaluation

CR quantifies the efficiency of the compression process and is calculated as

$$\mathrm{CR} = \frac{L.r}{\hat{b}} \tag{1}$$

where L is the length of the input signal in samples, r is the quantization (bit resolution) of each original sample, and $\hat{b}$ is the number of bits representing the compressed signal.

Percentage root-mean squared distortion (PRD) measures the similarity between the original and reconstructed signal and is defined as follows:

$$\text{PRD} = \left(\frac{\|x - \hat{x}\|}{\|x\|} \right) \tag{2}$$

where x and $\hat{x}$ are the original and reconstructed signals, respectively, and $\|.\|$ represents the Euclidean or l^2 norm. By comparing the PRDs and CRs of the reconstructed signals, it can be seen how increased CR relates to loss in signal quality.

Finally, a measure of seizure detection performance was required. The receiver operator characteristic (ROC) curve is a graphical plot of the relationship between sensitivity (the percentage of seizure epochs correctly classified) and specificity (the percentage of nonseizure epochs correctly classified) of the REACT classifier for a range of classification thresholds [36]. In this case, the area under the ROC curve is what is of interest. An area under curve (AUC) of 1, for example, means that the classifier detected all seizures correctly, without any false positives. An area greater than 0.9 is deemed to be a very high performing classifier [7]. Here, the results are presented as a percentage of the maximum AUC, whereby an AUC of 1 is given as 100%, 0.9 as 90%, etc.

D. Compression Parameters

In order to minimize the number of variables in operation for JPEG2000 compression, the DWT and quantization level were fixed, with only the threshold being altered to produce reconstructed signals with a range of PRD values. An 8-level DWT and 10-bit quantization of the DWT coefficients were used and the thresholds were chosen from a set that ranged from 0 to 30% of the largest coefficient. These values were chosen to introduce varying levels of loss, giving a range of PRDs from very low ($\sim$2%) to very high ($>$60%). The EEG signals were broken up into frames of size 1024 and compressed and reconstructed using the aforementioned threshold values.

Unlike with JPEG2000, it is possible with SPIHT compression to have exact bit-rate control over the compression ratio. Therefore, the signals were compressed with SPIHT at a range of defined CRs, ranging from 2:1 to 140:1. Again the EEG signals were split into frames of size 1024 and were compressed and reconstructed at these varying levels. The resulting PRDs of the reconstructed signals were calculated, relative to the original signals.

IV. Results

A. Compression Performance

All the EEG signals for the included patients were compressed and reconstructed using the aforementioned criteria. The database was processed with both algorithms using the compression parameters given ealier and the average PRD and CR values for each patient calculated. The reconstructed EEG signals were passed through the REACT system and the seizure detection performance was determined.

Fig. 2 shows a plot of the average CR versus the PRD averaged over all patients while Fig. 3 shows a magnified view of the same plot for PRD values below 10%. The compression of JPEG2000 ranges from 2:1 at its lowest to 103:1 at its highest, with PRDs of between 3% and 56%. With SPIHT, CRs range from 2:1 to 140:1, while the corresponding average PRDs were found to range from approximately 3% to 50%.

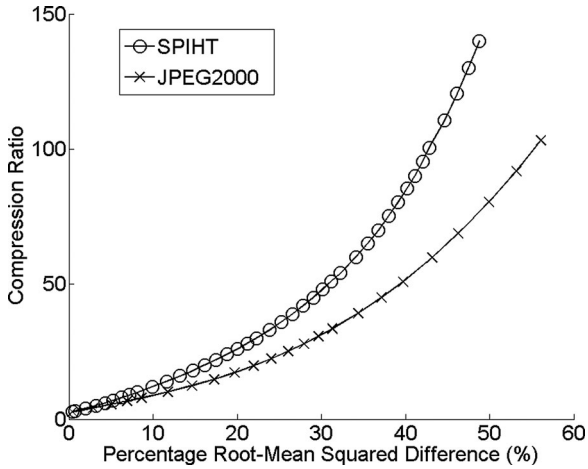

Fig. 2. Average CR versus average PRD for JPEG2000 and SPIHT.

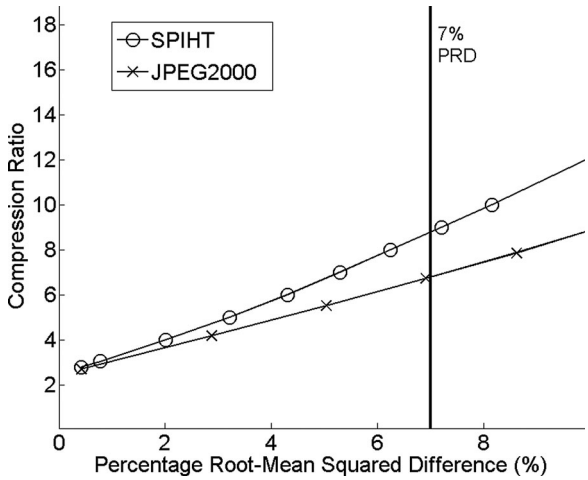

Fig. 3. Magnified view of CR versus PRD for PRD values below 10%.

Performance in this case is measured by the algorithm's ability to compress while keeping PRD low. In other words, the algorithm with the lower PRD at a given CR performs better. It can be seen that while both algorithms have approximately the same performance level at low CRs, SPIHT provides higher CRs than JPEG2000 as PRD values increase. For example, a 14:1 CR for JPEG2000 has a 17% PRD. The same CR with SPIHT, however, has a PRD of 11%.

Cárdenas-Barrera *et al. s*uggest a maximum PRD of 7% in order to maintain 99.5% of the signal energy [15]. Referring to Fig. 3, it can be seen that at 7% PRD, JPEG2000 gives an average CR of 7:1, and SPIHT achieves approximately 9:1. Looking at a plot of the original signal versus the reconstructed signals for both algorithms at these levels (see Fig. 4), both reconstructions [(b) and (c)] are practically identical to the original, indicating that practically all the detail from the original signal is preserved, particularly with SPIHT.

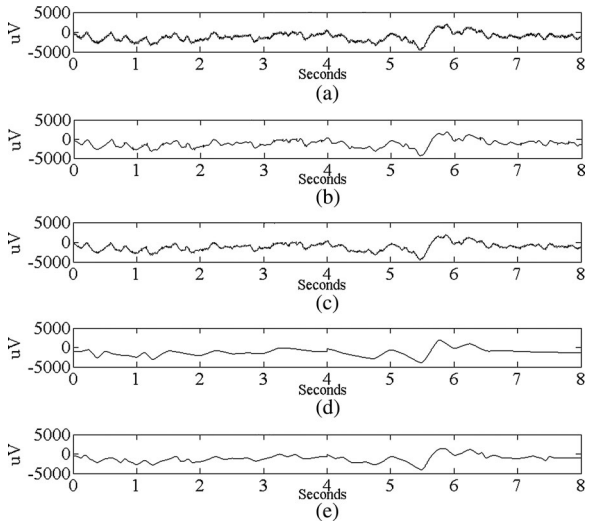

Fig. 4. EEG signal for Patient 2, Channel 1, Hour 1. (a) Original EEG and EEG reconstructed at 7% PRD using (b) JPEG2000 compression and (c) SPIHT compression and at maximum PRD using (d) JPEG2000 compression and (e) SPIHT compression.

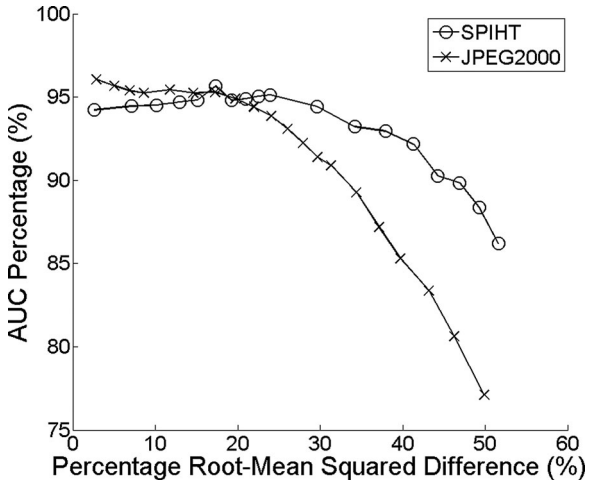

Fig. 5. Area under REACT ROC Curve (AUC) versus PRD for JPEG2000 and SPIHT.

B. Seizure Detection Performance With Increasing Compression

Fig. 5 plots the average PRD and corresponding AUC percentage for compression using both JPEG2000 and SPIHT algorithms. From [7], the average ROC area for processing the uncompressed signals is 0.9409 or 94.09% AUC percentage. At a PRD of 2.57%, SPIHT produces an average AUC percentage of 94.22%. JPEG2000 , however, gives an average ROC of 96.06%, higher than that of the uncompressed signals. The most probable explanation for this is that the wavelet coefficient thresholding described earlier may actually filter out some diagnostically irrelevant noise present in the EEG signals, as a useful by-product of the compression scheme. As the thresholding is applied to the quantized wavelet coefficients of the original signal, it can be seen that it is initially the high-pass "detail" coefficients that are discarded. Therefore, the overall shape of the signal is maintained, while the diagnostically irrelevant, finer information may be discarded. From the point of view of REACT, this appears to clean up the signal allowing for better analysis.

As the PRD increases, the AUC percentage for JPEG2000 begins to decline gradually. This is to be expected because as the PRD increases, more and more of the fidelity of the original EEG signal is being lost. Counterintuitively, SPIHT's initial 94% AUC area begins to initially increase as the PRD increases. The increase continues until it peaks at 17% PRD with a 95.65% AUC followed by a return to approximately the prepeak level. The reasons for this increase in detection rate are likely to be the same as those for JPEG2000. SPIHT's bit-ordering property means that the least "important" information is discarded first. In this case, it again acts as a filter whereby signal elements that interfere with the seizure detection, such as signal artifacts, are removed. Despite JPEG2000's initially better performance than SPIHT, it has a more rapid drop-off as the PRD increases.

C. Maximizing Compression

One of the main goals of this research is to minimize signal bandwidth without affecting the ability to identify seizure information in the signal. As previously mentioned, an AUC percentage of more than 90% is considered very good performance for seizure detection. Therefore, 90% AUC percentage can be taken as the cut-off limit for the compression.

Referring again to Fig. 5, it can be seen that for JPEG2000, a 90% AUC percentage corresponds to a PRD of about 35%. From Fig. 2, the equivalent CR can be found. At 35% PRD, JPEG2000 achieves a CR of 40:1. Using SPIHT, a much higher PRD can be tolerated. The AUC percentage for SPIHT does not fall below 90% until the PRD is 47%. Examining this value, we see that SPIHT can compress to 120:1 before performance falls below the acceptable level.

Fig. 4 also shows the same EEG signal being compressed and reconstructed at (d) 40:1 CR for JPEG2000 and (e) 120:1 for SPIHT. From the figure, it can be seen that while some of the finer details of the original signal are missing, the reconstructed signals still represent the overall shape and structure quite accurately. This would account for the high ROC area, in spite of the high rate of compression.

D. Power Consumption

In order to justify lossy compression of EEG signals, it is important to identify the advantage of using it. If the data are to be kept for future review, reduction of the size of the data allows for more recordings to be stored on a given storage device. In the case of the data being transmitted wirelessly, the aim is to reduce the amount of data to be transmitted, thus reducing the time the antenna is active. Yates and Rodriguez-Villegas present a discussion on the key power tradeoffs in designing a wireless EEG headset, including data compression, battery, and antenna choice [44]. They concluded that compression prior to transmission could significantly improve battery life of a wireless headset as long as the complexity of the compression algorithm does not outweigh the reduction in data transmission.

TABLE I
ENERGY REQUIREMENTS TO TRANSMIT A FRAME OF EEG DATA WITH BLUETOOTH LE

Compression Ratio	1:1	7	9	50	60	120
nRF8001	0.54 mJ	0.07 mJ	60 µJ	10.8 µJ	9 µJ	4.5 µJ

In [24], Higgins *et al.* examine the effects of compressing EEG data using SPIHT and analyze the computational complexity of the operation. They conclude that the algorithm does not cause a significant load on the processor and, due to SPIHT being an embedded coder, the higher the compression level, the lower the load on the processor. For example, at a compression ratio of 10:1, the SPIHT algorithm resulted in a load of 0.055% on a 50-MHz Analog Devices Blackfin BF537 device [45], while at a compression ratio of 30:1, the load was even smaller, at 0.024%. In the case of JPEG2000, a number of researchers have proposed low-powered implementations of this algorithm [46]–[48], and it is widely used in digital cameras for image compression. The modifications made to the AC in this paper further reduce the computational complexity at the encoding stage, thus satisfying the requirements set forth in [44].

For wireless transmission of compressed or uncompressed EEG data, bluetooth low energy (LE) is a recently proposed, low-powered transmission protocol that can be considered. Here, we examine the expected power consumption for a typical commercial implementation of this protocol. From [49], it can be estimated that the Nordic nRF8001 Bluetooth LE transmitter has a power-per-bit expenditure of $\sim$33 nJ/b. Table I gives the energy required to transmit a single 4 s frame of EEG data. The compression levels in Table I match the operating points discussed earlier, and include the highest CR recorded in [24].

From Table I, it can be seen that reducing the size of the data greatly reduces the cost of transmitting the data. From [24], [45], and [50], it can be estimated that SPIHT consumes $\sim$15.9 μJ of energy to compress 1 frame on the BF537 processor at a CR of 50:1. Combining the total energy to compress and transmit the data at this CR gives approximately 26.7 μJ for compression and transmission. This corresponds to approximately 5% of the energy required to transmit the frame uncompressed. Even at a relatively low CR of 7:1, the energy to compress the data rises to $\sim$64 μJ, resulting in the total energy for compression and transmission of 134 μJ, equating to $\sim$25% of the energy required to transmit the frame uncompressed. Compression, therefore, results in a significant decrease in total energy expenditure.

V. CONCLUSION

This paper has presented and compared two lossy compression algorithms for use in seizure detection applications. A modified JPEG2000 algorithm and the SPIHT algorithm were used to compress and decompress signals from the EEG database provided by the University of Freiburg at varying levels of fidelity loss. The resulting reconstructed signals were passed through an automated seizure detection system (REACT) in order to determine what effect the loss of signal information has on the system's ability to classify seizures. Using these results, it was possible to determine the maximum amount of fidelity loss allowable for both algorithms and, by extension, the highest CR that can be achieved.

Both algorithms allowed for substantial savings in the amount of data required to be transmitted/saved for seizure detection. SPIHT sustains better seizure detection performance than JPEG2000 at higher rates of PRD. It also outperforms JPEG2000 in terms of PRD versus CR, both in terms of absolute values, and in relation to CR attained while maintaining seizure detection performance.

In cases where maximum compression is required (e.g., an AEEG device with automated seizure detection), SPIHT displays a clear advantage, achieving a 120:1 CR without impact on detection performance, compared to a CR of 60:1 for JPEG2000.

REFERENCES

[1] D. Hill, "Value of the EEG in diagnosis of epilepsy," *Br. Med. J.*, vol. 1, pp. 663–666, Mar. 1958.

[2] A. J. Casson, S. Smith, J. S. Duncan, and E. Rodriguez-Villegas, "Wearable EEG: What is it, why is it needed and what does it entail?" *Proc. IEEE*, vol. 2008, pp. 5867–5870, Aug. 2008.

[3] A. J. Casson and E. Rodriguez-Villegas, "Data reduction techniques to facilitate wireless and long term AEEG epilepsy monitoring," in *Proc. 3rd Int. IEEE/EMBS Conf. Neural Eng.*, May 2007, pp. 298–301.

[4] F. Vergari, V. Auteri, C. Corsi, and C. Lamberti, "A zigbee-based ECG transmission for a low cost solution in home care services delivery," *Mediterranean J. Pacing Electrophysiol*, [Online] http://www.mespe.net/en/newselem/

[5] C. Otto, A. Milenkovic, C. Sanders, and E. Jovanov, "System architecture of a wireless body area sensor network for ubiquitous health monitoring," *J. Mobile Multimedia*, vol. 1, no. 4, pp. 307–326, 2006.

[6] S. Faul, "Automated neonatal seizure detection," Ph.D. dissertation, Nat. Univ. Ireland, Cork, Ireland, 2007

[7] S. Faul, A. Temko, and W. Marnane, "Age-independent seizure detection," in *Proc. Annu. Conf. IEEE Eng. Med. Biol. Soc.*, 2009, pp. 6612–6615.

[8] R. P. McEvoy, S. Faul, and W. P. Marnane, "Ambulatory react: Real-time seizure detection with a DSP microprocessor," in *Proc. Annu. Conf. IEEE Eng. Med. Biol. Soc.*, 2010, pp. 2443–2446.

[9] M. D. Adams, *The JPEG-2000 Still Image Compression Standard*, Standards Contribution, ISO/IEC JTC 1/SC 29/WG 1N 2412, 2001

[10] A. Said and W. A. Pearlman, "A new fast and efficient image codec based on set partitioning in hierarchical trees," *IEEE Trans. Circuits Syst. Video Technol.*, vol. 6, no. 3, pp. 243–250, Jun. 1996.

[11] Univ. of Freiburg, Freibug, Germany (2011, Nov. 16). *EEG database—Seizure prediction Project Freiburg.* [Online]. Available: https://epilepsy.uni-freiburg.de/freiburg-seizure-prediction-project/eeg-database

[12] A. J. Casson, D. C. Yates, S. Patel, and E. Rodriguez-Villegas, "Algorithm for AEEG data selection leading to wireless and long term epilepsy monitoring," in *Proc. Annu. Conf. IEEE Eng. Med. Biol. Soc.*, Aug. 2007, vol. 2007, pp. 2456–2459.

[13] A. J. Casson and E. Rodriguez-Villegas, "On data reduction in EEG monitoring: Comparison between ambulatory and non-ambulatory recordings," in *Proc. Eng. Med. Biol. Soc.*, Aug. 2008, pp. 5885–5888.

[14] A. J. Casson and E. Rodriguez-Villegas, "Toward online data reduction for portable electroencephalography systems in epilepsy," *IEEE Trans. Biomed. Eng.*, vol. 56, no. 12, pp. 2816–2825, Dec. 2009.

[15] J. L. Cárdenas-Barrera, J. V. Lorenzo-Ginori, and E. Rodríguez-Valdivia, "A wavelet-packets based algorithm for EEG signal compression," *Med. Inf. Internet Med.*, vol. 29, no. 1, pp. 15–27, 2004.

[16] N. Sriraam, "Neural network based near-lossless compression of EEG signals with non uniform quantization," in *Proc. IEEE Eng. Med. Biol. Soc. Conf.*, 2007, vol. 2007, pp. 3236–3240.

[17] N. Sriraam and C. Eswaran, "Performance evaluation of neural network and linear predictors for near-lossless compression of EEG signals," *IEEE Trans. Inf. Technol. Biomed.*, vol. 12, no. 1, pp. 87–93, Jan. 2008.

[18] N. Sriraam, "Quality-on-demand compression of EEG signals for telemedicine applications using neural network predictors," *Int. J. Telemed. Appl.*, vol. 2011, 13 pp., 2011.

[19] Z. Lin, M. W. Hoffman, N. Schemm, W. D. Leon-Salas, and S. Balkir, "A CMOS image sensor for multi-level focal plane image decomposition," *IEEE Trans. Circuits Syst., I, Reg. Papers*, vol. 55, no. 9, pp. 2561–2572, Oct. 2008.

[20] M. Lanuzza, S. Perri, P. Corsonello, and G. Cocorullo, "An efficient wavelet image encoder for FPGA-based designs," in *Proc. IEEE Workshop Signal Process. Syst. Design Implementation*, 2005, pp. 652–656.

[21] Q. Lu, L. Du, and B. Hu, "Low-power JPEG2000 implementation on DSP-based camera node in wireless multimedia sensor networks," in *Proc. Int. Conf. Networks Secur., Wireless Commun. Trusted Comput.*, 2009, vol. 1, pp. 300–303.

[22] Y. Sun, H. Zhang, and G. Hu, "Real-time implementation of a new low-memory SPIHT image coding algorithm using DSP chip," *IEEE Trans. Image Process.*, vol. 11, no. 9, pp. 1112–1116, Sep. 2002.

[23] G. Higgins, S. Faul, R. P. McEvoy, B. McGinley, M. Glavin, W. P. Marnane, and E. Jones, "EEG compression using JPEG2000: How much loss is too much?," in *Proc. Annu. Conf. IEEE Eng. Med. Biol. Soc.*, Buenos Aires, Argentina, 2010, vol. 2010, pp. 614–617.

[24] G. Higgins, B. McGinley, N. Walsh, M. Glavin, and E. Jones, "Lossy compression of EEG signals using SPIHT," *Electron. Lett.*, vol. 47, pp. 1017–1018, 2011.

[25] K. Sayood, *Introduction to Data Compression*, 3rd ed. San Mateo, CA: Morgan Kaufmann, 2005.

[26] A. Moffat and A. Turpin, *Compression and Coding Algorithms*. New York: Springer, 2002.

[27] J. D. Villasenor, B. Belzer, and J. Liao, "Wavelet filter evaluation for image compression," *IEEE Trans. Image Process.*, vol. 4, no. 8, pp. 1053–1060, Aug. 1995.

[28] *Information Technology—JPEG 2000 Image Coding System—Part 1: Core Coding System*, Standard ISO/IEC 15444-1, 2000

[29] P. G. Howard, P. G. Howard, J. S. Vitter, and J. S. Vitter, "Analysis of arithmetic coding for data compression," *Inf. Process. Manage.*, vol. 28, pp. 749–763, 1992.

[30] I. H. Witten, R. M. Neal, and J. G. Cleary, "Arithmetic coding for data compression," *Commun. ACM*, vol. 30, no. 6, pp. 520–540, 1987.

[31] J. M. Shapiro, "Embedded image coding using zerotrees of wavelet coefficients," *IEEE Trans. Signal Process.*, vol. 41, no. 12, pp. 3445–3462, Dec. 1993.

[32] A. Temko *et al.* (2010). React: Real-time EEG analysis for event detection, in *Proc. Ist AMA-IEEE Med. Technol. Conf. Individualized Healthcare*. [Online]. Available: http://ama-ieee.embs.org/2010conf/overview/program/papers/

[33] A. Temko, R. P. McEvoy, D. Dwyer, S. Faul, G. Lightbody, and W. P. Marnane, "A method of analysing an electroencephalogram (EEG) signal, Patent Application No. 0906029.4," 2009.

[34] A. Temko, E. Thomas, G. Boylan, W. Marnane, and G. Lightbody, "An SVM-based system and its performance for detection of seizures in neonates," in *Proc. Annu. Conf. IEEE Eng. Med. Biol. Soc.*, 2009, pp. 2643–2646.

[35] A. Temko, E. M. Thomas, W. P. Marnane, G. Lightbody, and G. Boylan, "EEG-based neonatal seizure detection with support vector machines," *Clin. Neurophysiol.*, vol. 122, no. 3, pp. 464–473, Mar. 2011.

[36] A. Temko, E. M. Thomas, W. P. Marnane, G. Lightbody, and G. Boylan, "Performance assessment for EEG-based neonatal seizure detectors," *Clin. Neurophysiol.*, vol. 122, no. 3, pp. 474–482, Mar. 2011.

[37] B. Schelter, M. Winterhalder, T. Maiwald, A. Brandt, A. Schad, A. Schulze-Bonhage, and J. Timmer, "Testing statistical significance of multivariate time series analysis techniques for epileptic seizure prediction," *Chaos: Interdiscip. J. Nonlinear Sci.*, vol. 16, p. 013108, 2006.

[38] F. Gilliam, R. Kuzniecky, and E. Faught, "Ambulatory EEG monitoring," *J. Clin. Neurophysiol.*, vol. 16, no. 2, pp. 111–115, Mar. 1999.

[39] S. O'Regan, S. Faul, and W. Marnane, "Automatic detection of EEG artefacts arising from head movements," in *Proc. Annu. Conf. IEEE Eng. Med. Biol. Soc.*, 2010, pp. 6353–6356.

[40] L. Vigon, M. R. Saatchi, J. E. Mayhew, and R. Fernandes, "Quantitative evaluation of techniques for ocular artefact filtering of EEG waveforms," *IEE Proc.–Sci. Meas. Technol.*, vol. 147, no. 5, pp. 219–228, Sep. 2000.

[41] M. Divjak, D. Zazula, and A. Holobar, "Assessment of artefact suppression by ICA and spatial filtering on reduced sets of EEG signals," in *Proc. Annu. Conf. IEEE Eng. Med. Biol. Soc.*, Aug./Sep. 2011, pp. 4422–4425.

[42] D. Kelleher, A. Temko, S. O'Regan, D. Nash, B. McNamara, D. Costello, and W. P. Marnane, "Parallel artefact rejection for epileptiform activity detection in routine EEG," in *Proc. Annu. Conf. IEEE Eng. Med. Biol. Soc.*, Aug./Sep. 2011, pp. 7953–7956.

[43] H. Nolan, R. Whelan, and R. B. Reilly, "Faster: Fully automated statistical thresholding for EEG artifact rejection," *J. Neurosci. Methods*, vol. 192, no. 1, pp. 152–162, Sep. 2010.

[44] D. C. Yates and E. Rodriguez-Villegas, "A key power trade-off in wireless EEG headset design," in *Proc. 3rd Int. IEEE/EMBS Conf. Neural Eng.*, May 2007, pp. 453–456.

[45] (2012, Jun. 14). ADSP-BF537 | blackfin processor with embedded network connectivity | blackfin processors | processors and DSP | analog devices. [Online]. Available: http://www.analog.com/en/processors-dsp/blackfin/adsp-bf537/products/product.html

[46] G. Dimitroulakos, N. D. Zervas, N. Sklavos, and C. E. Goutis, "An efficient VLSI implementation for forward and inverse wavelet transform for JPEG2000," in *Proc. 14th Int. Conf. Digital Signal Process*, 2002, vol. 1, pp. 233–236.

[47] Y. Meng, L. Liu, L. Zhang, and Z. Wang, "A low power VLSI implementation for JPEG2000 codec," in *Proc. 6th Int. Conf. ASIC*, Oct. 2005, vol. 1, pp. 198–202.

[48] K. M. Varma, "Fast split arithmetic encoder architectures and perceptual coding methods for enhanced JPEG2000 performance," Ph.D. dissertation, Dept. Elect. Eng.,Virginia Polytechnic Institute and State University, Blacksburg, VA, 2006

[49] Nordic Semiconductor. (2012, Jun. 8). nRF8001, μblue, Bluetooth low energy. [Online]. Available: http://www.nordicsemi.com/eng/Products/Bluetooth-R-low-energy/nRF8001

[50] (2012, Jun. 15). Ee-298: Estimating power for Adsp-BF538/BF539 blackfin processors (rev 2, 07/2007)," [Online]. Available: http://www.analog.com/en/processors-dsp/blackfin/products/application-notes/resources/index.html

Authors' photographs and biographies not available at the time of publication.

Computers in Biology and Medicine 43 (2013) 661–669

Contents lists available at SciVerse ScienceDirect

Computers in Biology and Medicine

journal homepage: www.elsevier.com/locate/cbm

An evaluation of the effects of wavelet coefficient quantisation in transform based EEG compression

Garry Higgins*, Brian McGinley, Edward Jones, Martin Glavin

College of Engineering and Informatics, New Engineering Building, National University of Ireland, Galway, Galway, Ireland

ARTICLE INFO

Article history:
Received 18 April 2012
Accepted 14 February 2013

Keywords:
EEG
Compression
SPIHT
Quantisation
AEEG
Telemedicine

ABSTRACT

In recent years, there has been a growing interest in the compression of electroencephalographic (EEG) signals for telemedical and ambulatory EEG applications. Data compression is an important factor in these applications as a means of reducing the amount of data required for transmission. Allowing for a carefully controlled level of loss in the compression method can provide significant gains in data compression. Quantisation is easy to implement method of data reduction that requires little power expenditure. However, it is a relatively simple, non-invertible operation, and reducing the bit-level too far can result in the loss of too much information to reproduce the original signal to an appropriate fidelity. Other lossy compression methods allow for finer control over compression parameters, generally relying on discarding signal components the coder deems insignificant. SPIHT is a state of the art signal compression method based on the Discrete Wavelet Transform (DWT), originally designed for images but highly regarded as a general means of data compression. This paper compares the approaches of compression by changing the quantisation level of the DWT coefficients in SPIHT, with the standard thresholding method used in SPIHT, to evaluate the effects of each on EEG signals. The combination of increasing quantisation and the use of SPIHT as an entropy encoder has been shown to provide significantly improved results over using the standard SPIHT algorithm alone.

1. Introduction

Electroencephalography (EEG) has long been used as a tool in clinical settings for diagnosing a variety of neurological and physiological conditions. It involves measuring a person's neural activity by placing electrodes on the scalp and detecting the bio-electric activity caused by synchronised neuronal activity within the brain. Typically this is performed as an in-patient procedure, whereby the patient is monitored for an extended period of time in a clinical setting. This places the patient in a potentially unfamiliar environment which may cause anxiety or stress, and removes them from their natural environment, which may contain triggers for certain conditions. As an in-patient procedure, it also consumes clinical resources, which ultimately costs the health service in staff time and money.

One of the most common uses of EEG as a clinical tool is in the diagnosis of epilepsy. Epilepsy is a neurological condition that affects approximately 1% of the population [1,2], but is difficult to diagnose. The gold-standard diagnosis requires long-term EEG and video monitoring in an attempt to capture a seizure on both video and EEG telemetry [3]. However, there is still a chance that no epileptiform activity will be experienced within the period of evaluation. Although accurate figures for the general population are difficult to determine, one study has shown that for EEGs taken from 308 patients with epilepsy, 18% never exhibited epileptiform discharges over several months of recordings and only 55% displayed discharges during their first examination [4]. It is conceivable therefore, that a patient displaying potential signs of epilepsy, may display no seizure activity during a single in-patient monitoring session. Misdiagnosis is also a significant issue due to limitations in the data available to the clinician. Smith [5] reports that elongating the period of EEG observation would have the effect of reducing the number of false positives, and increasing the detection rate of epileptiform activity. Binnie and Stefan [6] report that long-term monitoring may be required in as many as 5% of people diagnosed with epilepsy, and 13–20% of adult tertiary referrals and up to 40% of child referrals with potential cases of epilepsy. Clearly, in these situations, long-term in-patient monitoring is less than ideal in terms of expense, resource allocation and patient inconvenience. This situation is exacerbated where the availability of trained clinicians with the skills to analyse long term EEG data for seizure activity is limited.

Recent years have seen an increased interest in Ambulatory EEG (AEEG) devices and telemedical applications [7–12]. In a recent survey of 17 neurologists in the UK, 88% said they thought AEEG recordings would be more common in the future, and 76%

* Corresponding author. Tel.: +353 91 492728.
E-mail address: g.higgins1@nuigalway.ie (H. Garry).

0010-4825/$ - see front matter © 2013 Elsevier Ltd. All rights reserved.
http://dx.doi.org/10.1016/j.compbiomed.2013.02.011

said it would be a "major improvement" to their practice if AEEG devices were available [8]. Although AEEG devices have been in existence since the 1960s [13,14], improvements in the efficiency of signal processing techniques, combined with increased capacity in modern batteries have made a practical implementation more feasible. Wireless communication however, still remains proportionally one of the largest consumers of power in the system [15]. For patients in remote areas, it can be problematic to provide skilled clinicians to analyse data. Telemedical systems can provide a means to monitor and diagnose potential epilepsy sufferers from remote locations [16–18]. Using an AEEG or remote EEG monitoring system would alleviate the demands placed on finite resources by allowing clinicians to review the data at their convenience, or use automated seizure detection to assist with diagnosis. Remote rural locations where these systems can be of the greatest benefit, are rarely serviced with high speed network connectivity, therefore attempting to transmit the raw, uncompressed signal is impractical. Any reduction in the quantity of the data to be transmitted would be a benefit.

In general, there are 2 types of data compression: lossless and lossy. Lossless compression maintains signal integrity while compressing and decompressing the data, but is generally severely limited in the Compression Ratio (CR) it can achieve. Currently the majority of EEG compression research focuses on this method. Lossy compression results in an imperfect representation of the original signal, because signal fidelity varies according to the parameters of the compression method. By allowing a measure of loss to be tolerated, far higher compression levels can be achieved. Careful selection of compression parameters can maximise CR while minimising the loss of important information contained within the signal.

This paper aims to examine the effects of compression by comparing two lossy approaches:

- Set Partitioning in Hierarchical Trees (SPIHT) compression, with loss introduced through SPIHT's thresholding and embedded encoding features.
- Progressive lossy quantisation of the wavelet coefficients with SPIHT being employed losslessly as an entropy encoder.

Both schemes can provide a wide range of compression ratios. This paper examines the impact of quantisation's rounding method as opposed to SPIHT's coefficient thresholding method as factors of compression in order to maximise compression gains.

The rest of the paper is arranged as follows: Section 2 outlines the research methodology used in this work and how this work fits into EEG compression research. The dataset used is described and the data compression algorithms are outlined. Additionally, the metrics used for evaluating the results are given. Section 3 presents the results obtained from the compression tests. Section 4 analyses these results and evaluates the validity of the conclusions reached from them, and compares the results found here with results from similar research elsewhere. Section 5 gives the conclusions of the paper and proposes potential future work.

2. Research methodology

2.1. Epileptiform EEG database

The epileptiform EEG data used in this research was provided as part of the Seizure Prediction Project by the University of Freiburg, Germany [19]. The database contains EEG data recorded during pre-surgical monitoring. It contains seizure and non-seizure data for 21 patients ranging in age from 13 to 50. The dataset was chosen due to its public availability and to limit the number of artefacts present due to recordings being made through intracranial electrodes. The 6-channel EEG used in the recordings, is similar to the number of channels likely to be used in an AEEG device [20].

2.2. Compression

2.2.1. Background

Biomedical signal compression techniques can be broadly divided into three categories: (1) Direct Data (2) Transform based compression and (3) Other compression methods [21,22]. Direct Data methods are generally time domain based approach that exploits redundancies in signal data to increase compression. Compression efficiency is therefore limited by the fact that EEG is not sparse in the time domain. Memon et al. present an evaluation of a number of direct data compression techniques in [23]. In it they note that traditional direct data techniques do not work well on EEG signals due to the lack of reoccurring, exact patterns.

Methods in category (3) include compression methods such as non-linear prediction, neural network based compression and subband coding (other than those used in transform based approaches). Sriraam et al. present a number of recent papers on EEG compression using neural networks [24,25]. In both papers, the authors make use of predictors as part of an approach to give near-lossless compression of EEG data. This is combined with quantisation and entropy encoding schemes to maximise compression gains. In [26], Bazán-Prieto et al. present an EEG compression technique based on cosine modulated filter banks, with 7 bit quantisation. They test their algorithm on two EEG databases; the CHB-MIT Scalp EEG Database and the MIT-BIH Polysomnographic Database [27]. It is noted in [22] that despite the similarity between the subband decomposition employed by their algorithm and those frequently employed by transform based compression, it is not in actuality a transform method.

Transform-based compression includes methods that transform the time domain signal into the frequency, or other domain prior to compression. Examples of these transform operations include the Fourier Transform (FT) and Wavelet Transform (WT) which exploit signal sparsity in a particular domain [28,29]. The research presented by Cárdenas-Barrera et al. in [28] is an important paper in the field of EEG compression. It is the first paper to propose an upper limit to the level of fidelity loss allowable in EEG compression, based on retaining the majority of the signals energy. In this work they examine lossy compression approaches based on wavelet and wavelet packet transforms using the MIT-BIH Polysomnographic Database [27]. In [30], Daou and Labeau present a 2-D SPIHT based EEG compression methodology using EEG data obtained from Montreal Neurological Institute. They propose a pre-processing technique to exploit the correlation between EEG channels to maximise compression and employ two transform operations: a DWT and Discrete Cosine Transform (DCT).

The research presented in the present paper falls into category (2). This paper contributes to the area of transform-based encoding by evaluating the impact of reduced quantisation bit-rates on DWT coefficients, prior to entropy encoding. Section 4.2 provides a comparison between the results of this algorithm and other works of lossy EEG compression.

2.2.2. Discrete Wavelet Transform (DWT)

This section provides a brief overview of the DWT which is employed as a pre-processing step to the compression approaches investigated in this paper. DWT is commonly used in compression

algorithms due to its ability to represent signals in both the time and frequency domain. The DWT decomposes a signal into a set of basis functions known as wavelets [31,32]. The initial wavelet, also known as the mother wavelet (ψ), is used to construct the other wavelets by means of dilation and shifting. Dilation is achieved by multiplying the function's time orientation n by a scaling factor 2^m, where $m \in Z$. Shifting in time is done by $k \in Z$. Therefore, the wavelet decomposition is defined by

$$x(n) = \sum_m \sum_k c_{m,k}(\psi(2^m n - k)), \quad m,k \epsilon Z \tag{1}$$

where the scale m relates to the wavelet's dilation. Basis functions associated with large scales extract low-frequency information from the signal, while small scales extract high-frequency or fine-detail components. The DWT coefficients $c_{m,k}$ are defined as the inner product of the original signal and the selected basis functions:

$$c_{m,k} = \langle x(n), \psi_{m,k}(n) \rangle \tag{2}$$

These coefficients provide an alternative representation of the original signal, giving good localisation of the signal's energy components from both a time and frequency perspective. In this application the CDF 9/7 biorthogonal DWT was used [33,34] at a 10 level decomposition. This mother wavelet was chosen due to its widespread use in compression research, including SPIHT compression of biomedical signals [35]. The high-level of wavelet decomposition extracts the dominant low-frequency components of the signal. This improves SPIHTs compression efficiency by allowing the construction of "higher" zero-trees while encoding. This ability to construct large zero-trees is in agreement with empirical results which reveal that a 10 level decomposition provides best compression gains and reconstruction capability, with low levels of fidelity loss.

2.2.3. Quantisation

Quantisation is a nonlinear and noninvertible method of mapping a large, finite sequence of numbers, $x(n)$, onto a smaller scale, $\hat{x}(n)$. Quantisation occurs in digital signal processing where signals are sampled and converted into a digital format. The range $x(n)$ is divided into a number of equal intervals and then each interval is mapped to a codeword. It is worth noting that the codeword refers only to the interval and not to the original value. All input values are then expressed in terms of the interval they fall between.

The decoding process attempts to convert the $\hat{x}(n)$ sequence back to the original scale. However, due to the codeword referring to the interval only, the decoder cannot know the exact value of the original signal. For this reason, the decoded sequence, $x'(n)$, will not be an exact reconstruction of the original sequence, $x(n)$. The larger the number of intervals, the closer the decoded sequence will be to the original. However, with a smaller number of intervals, the number of bits needed to represent the encoded sequence diminishes. The quantisation bit-rates used in this paper ranged from 1 to 16 bits. 16 bits was chosen as the highest resolution as it is the quantisation level used during the raw capture of the EEG signals. Quantisation was performed on the wavelet coefficients in order to reduce the range of the coefficients being passed to the SPIHT encoder.

2.2.4. Set Partitioning in Hierarchical Trees

Initially proposed by Said and Pearlman in [36], Set Partitioning in Hierarchical Trees (SPIHT) is a compression method originally designed for image compression that has since been applied to many other application areas [35,37,38]. Its core principles are derived from the Embedded Zerotree Wavelet (EZW) coder proposed by Shapiro in [39] by exploiting the fact that wavelet coefficients in different sub-bands have a temporal relationship with one another. As with the EZW algorithm, SPIHT arranges the bits in order of significance, with the most significant bits being encoded first. Therefore, if the encoding or transmission is interrupted at any point, the signal can be reconstructed to a level of fidelity appropriate to the number of bits received. This means that SPIHT allows for direct control of the CR of the signal being encoded.

In this paper, the data was compressed with CRs from the set $c=\{1, 2, 5, 6, 7, 10, 30, 35, 40, 55, 110, 160, 200\}$. For $c=1$, SPIHT operates in a lossless manner, where the input sequence prior to compression is identical to the output sequence after the data has been decompressed. When SPIHT operates at CRs higher than this, it compresses the signal by discarding all coefficients below the selected threshold. For example, for $c=4$, only 25% of the original bit length is saved.

2.2.5. Approaches to compression

The DWT, Quantisation and SPIHT components were used to test different approaches to lossy compression. Compression involves the original signals undergoing a DWT operation followed by Quantisation, before being encoded using SPIHT. Two different variations in this methodology were used: First, the traditional SPIHT approach where the desired CR was selected prior to compression and was achieved by terminating encoding at the desired bit-length. For this approach, the quantisation level of the DWT coefficients was set at 16 bits. This was done to isolate the compressive effects to that of SPIHT's bit-ordering/discarding. This approach was dubbed "Standard SPIHT". In the second approach, the number of bits available to the quantizer was varied and the resulting coefficients encoded by SPIHT in lossless mode. In this approach, SPIHT was used as an entropy coder to gain maximum compressive gains from the lower bit-rates. This approach was taken to isolate the effects of varying the quantisation level in order to examine its specific effects. This approach was dubbed "QSPIHT".

2.3. Performance metrics

Two performance metrics were used for evaluating the performance of the compression algorithms.

- **Percentage Root-mean squared Distortion (PRD)** is a standard metric for measuring the distortion between 2 signals. It is defined as

$$\mathrm{PRD} = \left(\frac{\|x - \hat{x}\|}{\|x - \bar{x}\|}\right) \times 100 \tag{3}$$

  where x is the original signal, $\hat{x}$ is the reconstructed signal, $\bar{x}$ is the mean of the signal and $\|.\|$ represents the Euclidean and l^2 norm.
  Previous research has already investigated the effects of PRD on EEG signals and proposed limits to ensure no impact on diagnostically relevant information. Cárdenas-Barrera et al. proposes a PRD limit of 7% to ensure 99.5% of the signals energy is retained [28]. Higgins et al. however, determined that a much higher PRD (30%) can be tolerated while still maintaining seizure information [40], [41]. This is further verified in [29] where an automated seizure detection algorithm is used to verify these PRD limits. These 7% and 30% PRD limits were chosen as the operating points in this research to provide a reference point for potential real-world applications such as clinical review and automated seizure detection.
- **Compression Ratio (CR)** is defined as the ratio of the size of the compressed signal in relation to that of the original signal,

and is given by the formula

$$CR = \frac{L.r}{\hat{b}} \quad (4)$$

where L is the length of the input signal in samples, r is the original quantisation (bit resolution) of each original sample and $\hat{b}$ is the number of bits representing the compressed signal.

In order to determine the CRs of the compression methods, the overall length of the compressed databases was used. The cumulative number of bits for each frame was recorded and the total number of bits for the whole database was compared to the size of the uncompressed data to give a true CR for each compression method.

Two further metrics were used to evaluate the validity of the compression results:

- The **Power Spectral Density (PSD)** is a method of analysing the contribution of each frequency to the overall signal power. It describes how the power of a time series is distributed with frequency. The PSD of the signals after compression was plotted against the PSD of the original signals to evaluate the impact of the lossy compression on the energy of the signal. For this research the Welch method of PSD estimation was applied to the signals being analysed [42]. A segment length of 64 with a 50% overlap using the Hamming windowing method and 64 length window was used.
- Finally, the **Cumulative Density Function (CDF)** is a measure of probability distribution of a random variable. Given a continuous random variable X, the CDF is denoted as a function $F(x)$, and is defined for a number x by

$$F(x) = P(X \leq x) = \int_0^x f(s)ds \quad (5)$$

That is, for a given value x, $F(x)$ gives the probability that observed value of X will be less than or equal to x. The CDF was used to examine the likelihood of a compressed frame having a PRD at or below a specific value when the given compression parameters are applied.

Unlike other bioelectric signals, such as ECG [43], no metric exists to evaluate fidelity loss in EEG signals in regards diagnostically relevant information. PRD was chosen for this research due to its widespread use to analyse quality degradation in lossy EEG compression [26,28,29]. In this research, PSD analysis is added to verify the results inferred by the PRD values.

3. Results

3.1. Standard SPIHT compression

For this approach, the quantisation level was fixed at 16 bits. The signals were compressed with SPIHT at a range of lossy compression settings, ranging from CRs of 2 to 200, and then decompressed. The PRD of each frame was calculated and then the mean and standard deviation over the whole database was determined. Table 1 presents the results of this work. It can be seen that at the lowest compression level (CR=2), the PRDs are very small, suggesting an insignificant loss in fidelity between the original and reconstructed signal.

As previously stated, two PRD limits are proposed for use in this research. The 7% and 30% limits were used as lower and higher cut-off points for seizure detection applications [28,40,41]. These limits were therefore selected as operating points for comparative reasons. It can be seen from Table 1 that a CR setting of 5 (CR5) gives a PRD of 5.99%, which lies within the 7% cut-off limit. Looking at the 30% limit, it can be seen that a CR setting of 35 (CR35) gives a PRD of 29.26%.

Table 1
Results for standard SPIHT compression.

Expected CR	Actual CR	Average PRD (%)	Standard deviation (%)
200	202.36	63.49	20.67
160	160.75	58.63	20.29
110	110.87	50.78	19.73
55	55.38	36.97	19.08
40	40.29	31.40	18.92
35	35.24	29.26	18.85
30	30.24	26.90	18.50
10	10.25	12.29	11.02
7	7.26	8.94	8.97
6	6.26	7.67	7.95
5	5.26	5.99	6.18
2	2.28	0.52	0.34

Table 2
Results for QSPIHT compression.

Bit level	QSPIHT CR	Average PRD (%)	Standard deviation (%)
1	613.20	68.15	13.18
2	260.13	50.09	15.43
3	128.78	35.04	15.23
4	70.88	23.66	13.88
5	40.14	15.58	12.11
6	22.39	9.89	9.56
7	13.05	6.09	7.00
8	8.14	3.67	5.09
9	5.51	2.18	3.66
10	4.11	1.32	2.89
11	3.27	0.83	2.49
12	2.74	0.56	2.34
13	2.36	0.42	2.29
14	2.09	0.34	2.28
15	1.88	0.31	2.27

The final column gives the standard deviation of the PRD results. At the proposed settings, the standard deviation is ± 6.18 and ± 18.85. This suggests that while the average PRD results fall within the limits, it is obvious that some frames can be well above the desired limits. Further analysis of these results is therefore required and is provided in Section 4.1 of this paper.

3.2. QSPIHT compression

For this section, the database was compressed by quantising the data in the range of 1–15 bits, and compressed using SPIHT in lossless mode. Table 2 gives the CRs for the database after SPIHT compression has been applied. The PRD values were recorded for each frame and then averaged over the whole database at each quantisation level. Table 2 gives the average PRD and standard deviation at each bit-rate.

Looking at the results, it can be seen that while the PRD initially increases slowly, the rate of increase gets larger as the quantisation level approaches 1 bit. Taking the initial 7% PRD limit, it can be seen that at 7 bit quantisation (Q7) the PRD is 6.09%. For the 30% PRD limit, far lower quantisation levels can be tolerated. In this situation, 4 bit quantisation (Q4) is required to bring it below the 30% cut-off point, giving an average PRD of 23.66%.

Again the standard deviation is given in the last column of the table. For the suggested limits of 7% and 30% PRD is ± 7.00 and ± 13.88 respectively. Further analysis of the distribution of the results is therefore required and provided in Section 4.1 of this paper.

3.3. Comparison

In order to evaluate the performance of each approach, it is necessary to look at the PRD achieved by each at any given CR. Fig. 1 gives a plot of the CR vs. PRD for both methods. While the CRs for the standard SPIHT approach are known prior to compression, the exact CRs for the QSPIHT approach can only be determined after compression has taken place. Fig. 2 gives a magnified view of Fig. 1 from 0% to 10% PRD. Looking at Fig. 2 it can be seen that both approaches initially have very similar PRD and CR values. This is to be expected as at this point both approaches have little loss in signal fidelity, keeping CRs low. As the compression rate increases, the curves diverge. It is clear from the graph that QSPIHT out-performs Standard SPIHT compression in terms of PRD at a given CR. While the largest gains are at the higher CRs, these results fall outside the upper limits of loss imposed and are therefore irrelevant in the context of this research. Below the 30% limit, the QSPIHT approach still provides an advantage. At 30% PRD, the QSPIHT approach gives a CR of just over 100, while the Standard SPIHT approach gives a CR of approximately 40.

Within the 7% PRD limit, the advantage of the quantisation approach is still substantial. The 7 bit quantisation limit, found in the above section to fall below this cut-off point, gives a CR of 13.05. At 7% PRD, Standard SPIHT gives a CR of approximately 6.

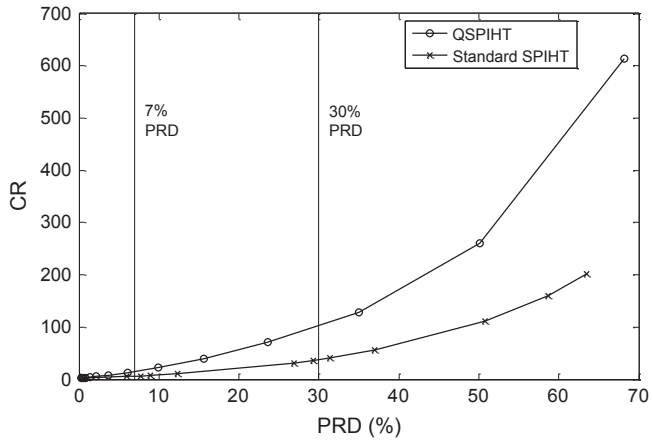

Fig. 1. Plot of PRD vs. CR for Standard and QSPIHT approach.

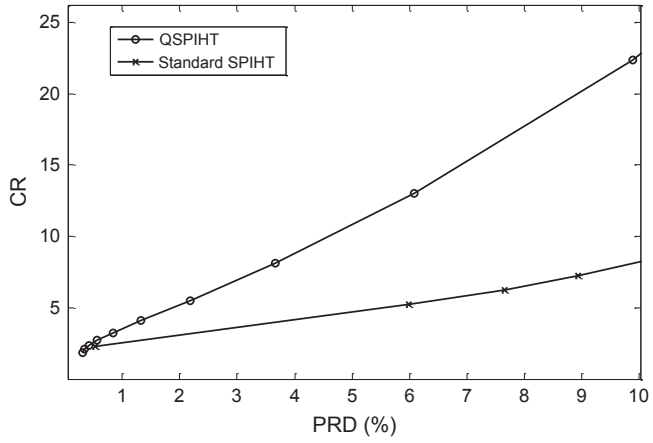

Fig. 2. Plot of PRD vs. CR for PRDs up to 10%.

4. Further evaluation of validity of results

4.1. Analysis

In order to analyse the distribution of the PRD results at the proposed compression settings, the Cumulative Density Function (CDF) for the resulting frames was calculated and plotted. Fig. 3 shows the CDF of the QSPIHT and Standard SPIHT approaches at Q7 and CR5 respectively for the 7% PRD limit. Looking at Fig. 3 it can be seen that the CDF of both approaches are very similar. Both rise rapidly until the probability goes above 0.9, where a shallower increase can be observed. This is to be expected as the (relatively) low compression settings maintain most of the signal fidelity. Examining the 7% PRD ($x=7$), it can be seen that the probability of a given frame having a PRD of 7% or less for both approaches is 0.8 or 80%.

Fig. 4 shows the CDF of both algorithms at the proposed 30% PRD settings (Q4 and CR35). Again both CDFs follow a similar distribution. Standard SPIHT starts higher than QSPIHT, implying a higher proportion of frames with PRDs below 10%. Above this however, QSPIHT rises faster than Standard SPIHT, implying the QSPIHT approach gives lower PRDs than Standard SPIHT in this range. At 30% PRD ($x=30$) there is a 0.8 or 80% chance for QSPIHT and approximately 0.75 or 75% chance for Standard SPIHT that a given frame will have a PRD equal to or lower than the cut-off.

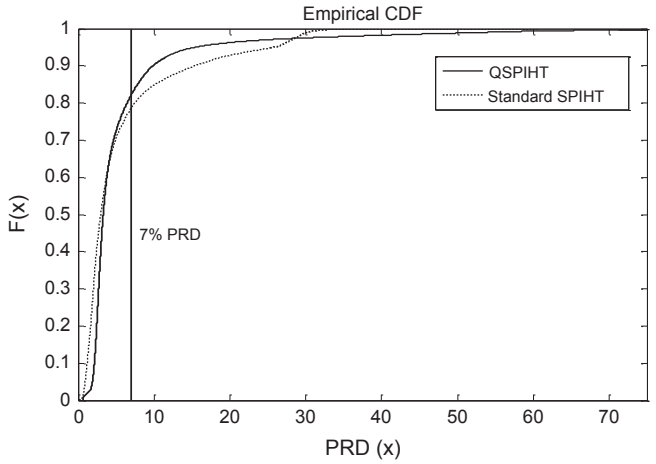

Fig. 3. Cumulative distribution function of PRD results per frame at proposed 7% PRD settings.

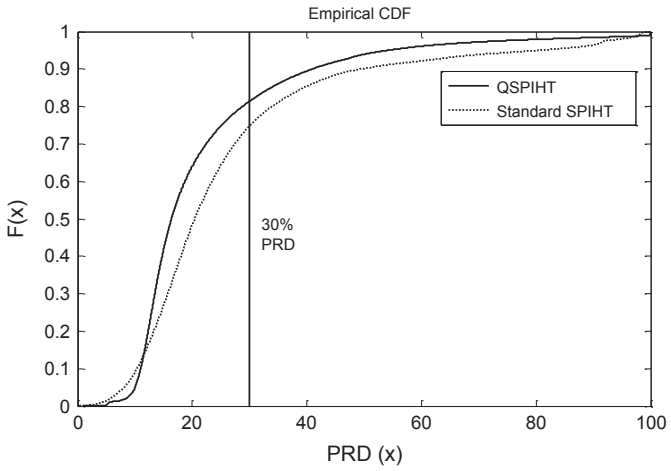

Fig. 4. Cumulative distribution function of PRD results per frame at proposed 30% PRD settings.

Since PRD is a measure of the level of difference between two signals, and not by definition an objective evaluation of the impact of the loss of diagnostically relevant information in the signal, it should not be used as the sole metric to evaluate the performance of the algorithms. To do this, a visual inspection and PSD analysis was performed on a selection of reconstructed files whose PRDs were close to the above limits. Figs. 5 and 6 give the PSDs of original signal and those of the QSPIHT and Standard SPIHT approaches at the 30% and 7% cut-off PRDs, given in Plots (i–ii) in each figure. Fig. 5 is a randomly chosen EEG signals containing no seizure information, while Fig. 6 was chosen to contain periods of seizure data. The parameters found to give optimum results in the section above were used to select the signals for comparison. Specifically, these were CR35 and Q4 at 30% PRD and CR5 and Q7 at 7% PRD for Standard SPIHT and QSPIHT respectively. Performance was judged on how closely the PSD of the reconstructed signals visually matched that of the original signal, i.e. how well the energy is maintained in the signal after lossy compression.

Generally all 4 reconstructed signals maintain a PSD close to that of the original signal, particularly in the case of the low PRD signals. Fig. 5 shows the greatest amount of variation in the signals PSDs with all PSDs being very similar in Fig. 6. Plot (i) shows Standard SPIHT at CR35. The greatest variation in original and reconstructed signals PSDs can be seen here, with the reconstructed signals power being generally slightly lower than the original. Plot (i) also shows QSPIHT at Q4. Here the PSD is closer to that of the original signal, although some variation is still visible. Plot (ii) shows Standard SPIHT at CR5. Again an improvement can be seen in the reconstructed signals PSD but some loss in fidelity is still evident. Finally, Plot (ii) also displays QSPIHT at Q7. Here almost no variation in PSD between the original and reconstructed signals is visible, suggesting almost no loss in signal information during compression.

A visual inspection was also performed on the signals. Fig. 7 shows a sample of the database with (i) the original EEG signal, and the signal compressed with (ii) QSPIHT at Q4 and (iii) Standard SPIHT at CR5. This signal gives CRs of 10 and 5 and PRDs of 3 and 2 respectively. Visually, these three signals are nearly identical, suggesting very high retention of signal integrity. Fig. 8 shows a plot of (i) the same original EEG signal, and the corresponding sample compressed with (ii) QSPIHT at Q4 and (iii) Standard SPIHT at CR35. At these settings, these algorithms give a CR of 42 and 35 and PRD of 14% and 17% respectively. At this higher level of loss, some visual discrepancies can be seen. These higher levels of compression cause a smoothing effect on the signals due to the loss of finer detail coefficients. While some of the finer details are lost in the compression, the general shape of the signal is very well maintained. This again suggests the majority of the signal information is maintained at this compression level.

The similarities, visually and in the PSDs, of the original and reconstructed signals after compression lends credence to the choice of the 7% and 30% PRDs as operating points, as most of the signals power is preserved at each compression level. When QSPIHTs superior PSD results are combined with the compression results from Sections 3.1 and 3.2 above, a clear advantage in increasing quantisation level to improve CR performance can be seen.

4.2. Comparison with other work

A direct comparison with other EEG compression research is difficult due to the variety of EEG databases and performance evaluation metrics used. In comparison to other biomedical signal research, there is a relatively small amount of research being done in the area of EEG compression. In order to address some of these difficulties, a publicly available EEG database was selected for testing [19] and results were reported using the PRD metric given in (3) as it is not influenced by the signal mean. It is possible to make general comparisons when CR and PRD results are reported by comparing with those of Fig. 1. It should be noted that an alternative definition of PRD, employed by [24,28,30], does not remove the signal mean prior to calculation. This inclusion of the mean (DC bias) can create an artificially low PRD, whereby the mean of the signal is maintained, while important signal information is lost. Without adjusting for the signal mean in PRD calculations, the results can be up to 4 times better (lower PRD for a given CR) than if the definition employed in this paper is

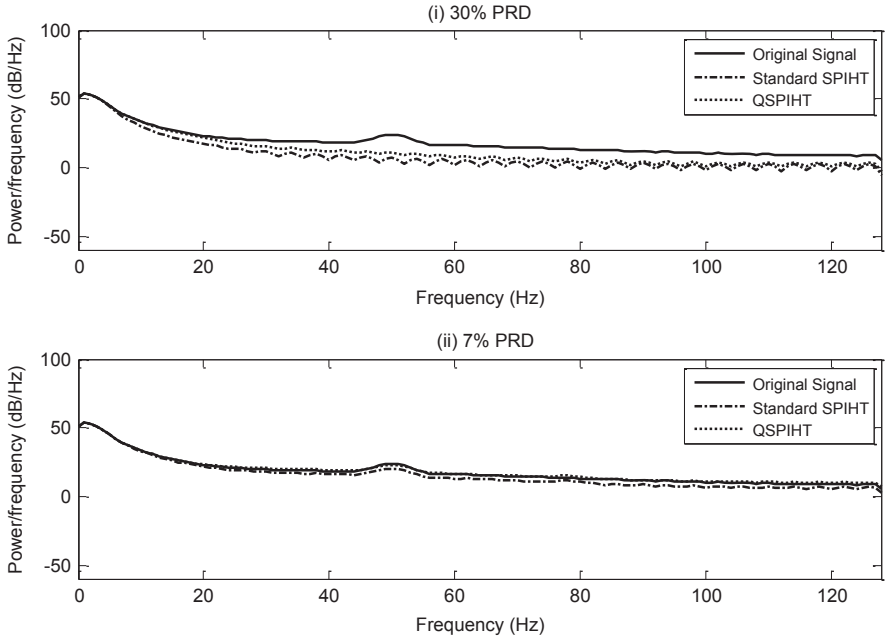

Fig. 5. Welch Power Spectral Density (PSD) of non-seizure EEG sample.

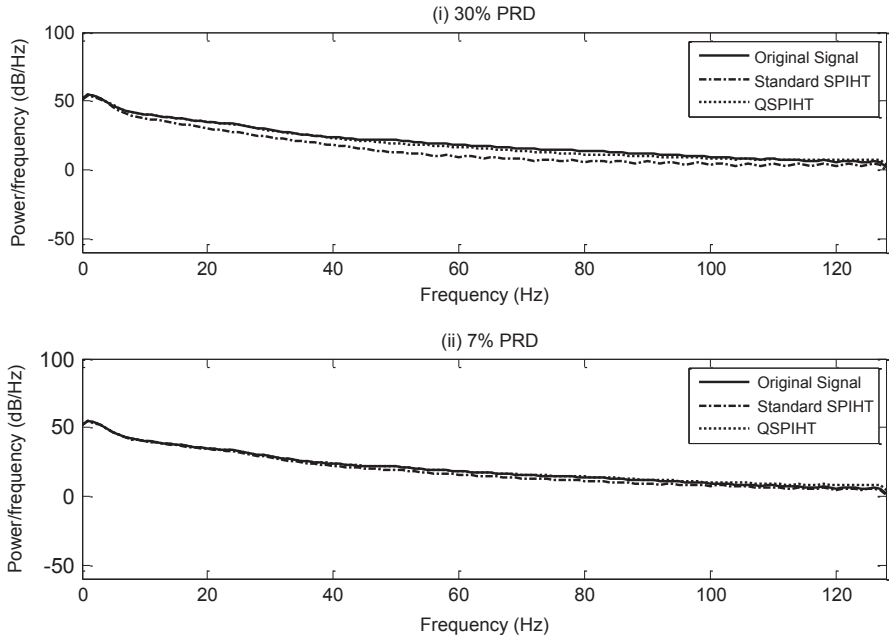

Fig. 6. Welch Power Spectral Density (PSD) of EEG sample containing seizure.

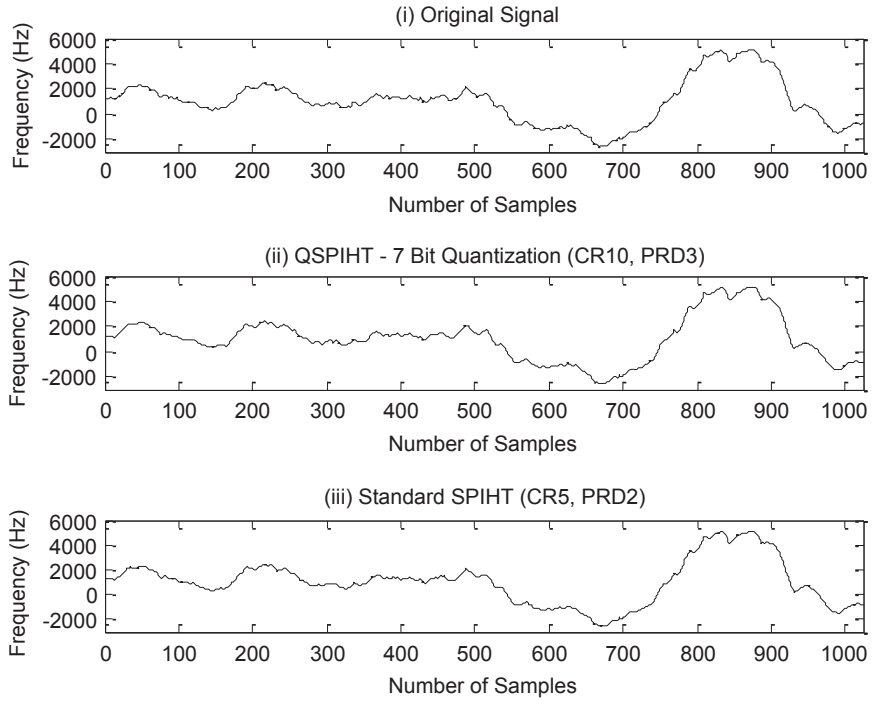

Fig. 7. Plot of sample EEG signal. (i) Original EEG signal, (ii) signal compressed with QSPIHT at Q7 and (iii) standard SPIHT at CR5.

used [26]. In the case of [26,28], QSPIHT was applied to the same databases to aid comparison. Table 3 gives the results of QSPIHT run on these databases for bit-levels 4–9.

For transform based compression, Cárdenas-Barrera reported an average PRD of 9.54% and CR of 7.79; while at 7 bit quantisation the average CR is 5.68 with an average PRD of 6.02% in [28]. Table 3 gives the corresponding results for QSPIHT. The database used was the MIT-BIH Polysomnographic database. At Q7, a CR of 9.5 at a PRD of 6.93% is achieved. It is interesting to note the advantage of using SPIHT as an entropy encoder, increasing the CRs from 7.79 to 13.021 and 5.68 to 9.5024 for 6 and 7 bit quantisation respectively.

Daou and Labeau present a 2-D SPIHT based EEG compression methodology in [30]. Improved compression performance in comparison to 1-D SPIHT and a number of other algorithms were reported for PRDs lower than 30%. The results found here suggest that the addition of a quantisation block, with an appropriate bit-level, prior to SPIHT encoding may provide improved compression results with minimal impact on fidelity.

An alternative approach to compression is presented in [26]. Bazán-Prieto et al. report achieving a CR of 5.97 at 4.61% PRD and 11.23 CR at 10.45% PRD for the CHB-MIT database. On the same database, QSPIHT gave a CR of 5.33 at 3.08% PRD and 13.42 CR at 10% PRD. This was achieved at Q7 and Q5 respectively. For the

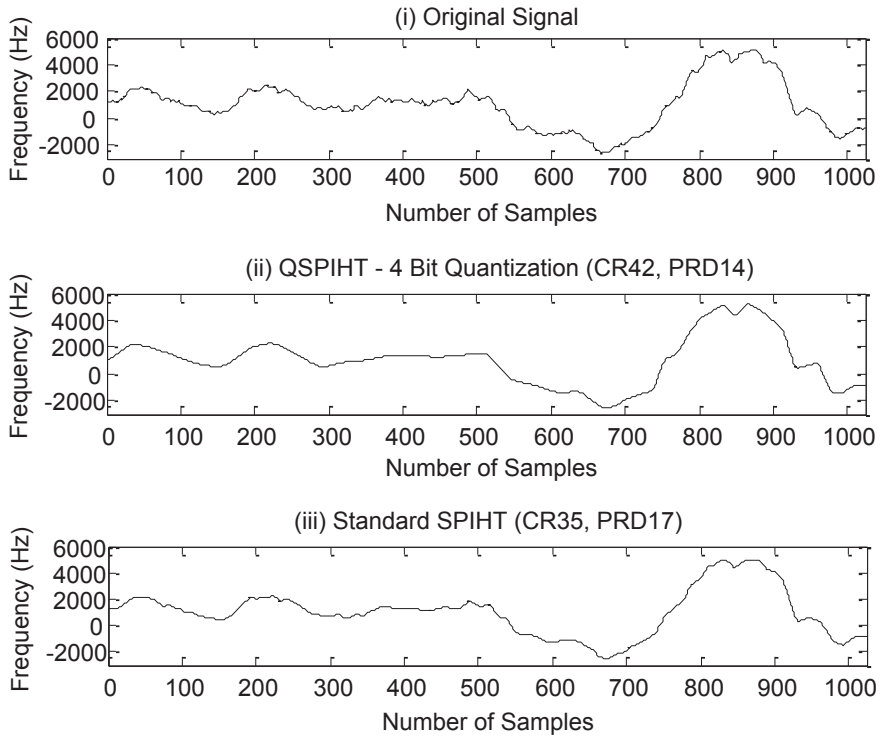

Fig. 8. Plot of sample EEG signal. (i) Original EEG Signal, (ii) signal compressed with QSPIHT at Q4 and (iii) standard SPIHT at CR35.

Table 3
CR and PRD results for QSPIHT run on MIT-BIH polysomnographic and CHB-MIT scalp EEG databases [27].

Bit level	MIT-BIH polysomnographic		CHB-MIT scalp EEG	
	CR	PRD (%)	CR	PRD (%)
4	34.4721	29.8875	24.3321	16.5954
5	20.0354	19.2435	13.4155	10.0279
6	13.0210	11.8092	8.0243	5.7098
7	9.5024	6.9341	5.3314	3.0815
8	7.3393	4.0791	3.9292	1.6105
9	3.7265	2.5436	3.1403	0.8410

MIT-BIH Polysomnographic database, a CR of 4.11 is reported at 3.79% PRD and 8.21 CR at 10.26% PRD. QSPIHT achieved a CR of 3.73 at a 2.54% PRD and 13.02 CR at 11.81% PRD. This was achieved at Q9 and Q6 respectively.

In [24], Sriraam reports CRs of approximately 5:1 with PRDs no higher than 5%, using a proprietary database. This result is similar to those of the Standard SPIHT approach used here, where CR and PRD have a close to linear relationship. QSPIHT may offer improvements on these results.

5. Summary and conclusions

This paper has examined two methods of EEG compression based on reducing data length by: (i) ordering the coefficients into hierarchical trees and then discarding those that fall below the threshold value and (ii) rounding coefficients to integer values using varying levels of quantisation and losslessly compressing them. This was done by applying the SPIHT algorithm at a variety of compression levels in the first approach and varying the quantisation level for the second. Two limits of signal loss were used to evaluate the compression algorithms performance against each other in relation to real-world applications. It was found that (ii) achieved higher CRs at a given PRD than (i). At a 7% PRD, (ii) achieved a CR of 13.05 while (i) achieved 6. At 30% PRD, (ii) achieved a CR of 100 compared to 40 with (i). The validity of these results was evaluated by comparing the information contained in the signals after they had been decompressed, with that of the original signal. It was found that the reconstructed signals maintain the energy spectrum of the original signal well, particularly at low PRDs. Furthermore, it was found that the PSD of data compressed using (ii) was closer to that of the original signals than (i). This suggests that (ii) achieves higher CRs than (i) while maintaining better data fidelity. Thus, it appears to be more beneficial to the integrity of the EEG data to use a compression method that represents all signal coefficients, even in a reduced form, rather than one that simply discards coefficients.

This work may be extended by applying the results found here to the design of an EEG compression algorithm that makes use of higher quantisation levels as the basis of compression. Combining higher quantisation levels with other methods of data compression may offer a means of further increasing CRs without undue impact on the EEG signals. While SPIHT is used here in lossless mode, the results may be improved by combining higher quantisation levels, with a measure of lossy compression. Alternatively, a coder other than SPIHT could be used post-quantisation if a requirement such as ultra-low power consumption is required. Furthermore, the quantisation method used here was a standard, uniform quantisation method. Implementing a more advanced quantisation method may yield higher CRs or improve signal integrity at a given CR.

Conflict of interest statement

None declared.

Acknowledgements

The authors would like to acknowledge the Albert-Ludwigs-Universität, Freiburg, Germany, for allowing access to their adult EEG database.

This work was supported by Science Foundation Ireland under Strategic Research Cluster SFI/07/SRC/I1169.

References

[1] A. Neligan, L. Sander, The incidence and prevalence of epilepsy [Online]. Available from: 〈http://www.epilepsysociety.org.uk/Forprofessionals/Articles-1/Introduction〉, 2005.
[2] A.J. Fowle, C.D. Binnie, Uses and abuses of the EEG in epilepsy, Epilepsia 41 (2000) S10–S18, Mar.
[3] E. Waterhouse, New horizons in ambulatory electroencephalography, IEEE Eng. Med. Biol. Mag. 22 (3) (2003) 74.
[4] C.A. Marsan, L. Zivin, Factors related to the occurrence of typical paroxysmal abnormalities in the EEG records of epileptic patients, Epilepsia 11 (4) (1970) 361–381.
[5] S.J.M. Smith, EEG in the diagnosis, classification, and management of patients with epilepsy, J. Neurol. Neurosurg. Psychiatry 76 (2) (2005) ii2–ii7, Jun.
[6] C.D. Binnie, H. Stefan, Modern electroencephalography: its role in epilepsy management, Clin. Neurophysiol. 110 (10) (1999) 1671–1697 Oct.
[7] A.J. Casson, E. Rodriguez-Villegas, Data reduction techniques to facilitate wireless and long term AEEG epilepsy monitoring, in: Proceedings of the 3rd International IEEE/EMBS Conference on Neural Engineering, 2007, pp. 298–301.
[8] A.J. Casson, S. Smith, J.S. Duncan, and E. Rodriguez-Villegas, Wearable EEG: what is it, why is it needed and what does it entail? in: Proceedings of the IEEE conference on Engineering in Medicine and Biology Society, vol. 2008, pp. 5867–5870, 2008.
[9] D. Gopikrishna, A. Makur, I. Bangalore, A high performance scheme for EEG compression using a multichannel model, Lect. Notes Comput. Sci. (2002) 443–451.
[10] S. Ktata, K. Ouni, N. Ellouze, A novel compression algorithm for electrocardiogram signals based on wavelet transform and SPIHT, Int. J. Signal Process. 5 (3) (2009).
[11] R.P. McEvoy, S. Faul, W.P. Marnane, Ambulatory REACT: Real-time seizure detection with a DSP microprocessor, in: proceedings of the Annual Conference of the IEEE Engineering in Medicine and Biology Society (EMBC), 2010, pp. 2443–2446.
[12] A. Avila, R. Santoyo, S.O. Martinez, Hardware/software implementation of the EEG signal compression module for an ambulatory monitoring subsystem, in: Proceedings of the 6th International Caribbean Conference on Devices, Circuits and Systems, 2006, pp. 125–129.
[13] A. Kamp, Eight channel EEG telemetry, in: Symposium on the EEG in Relation to Space Travel, American Electroencephalographic Society, Atlantic City, NJ, 1962.
[14] J. Ives, J. Woods, 4-Channel 24 h cassette recorder for long-term EEG monitoring of ambulatory patients, Electroencephalogr. Clin. Neurophysiol. 39 (1) (Jul. 1975) 88–92.
[15] C. Otto, A. Milenkovic, C. Sanders, E. Jovanov, System architecture of a wireless body area sensor network for ubiquitous health monitoring, J. Mobile Multimedia 1 (4) (2006) 307–326.
[16] F. Vaz, O. Pacheco, A.M. da Silva, A Telemedicine Application For EEG Signal Transmission, in: Proceedings of the Annual International Conference of the IEEE Engineering in Medicine and Biology Society, 1991, vol. 13, pp. 466–467.
[17] C.E. Elger, W. Burr, Advances in telecommunications concerning epilepsy, Epilepsia 41 (S5) (2000) S9–S12, May.
[18] E. Jovanov, D. Starc˘ević, A. Samardz˘ić, A. Marsh, Z. Obrenović, EEG analysis in a telemedical virtual world, Future Gener. Comput. Syst. 15 (2) (1999) 255–263, Mar..
[19] EEG Database—Seizure Prediction in Freiburg, Germany [Online]. Available from: 〈https://epilepsy.uni-freiburg.de/freiburg-seizure-prediction-project/eeg-database〉 (accessed 16.11.11.).
[20] F. Gilliam, R. Kuzniecky, E. Faught, Ambulatory EEG monitoring, J. Clin. Neurophysiol. 16 (2) (1999) 111–115, Mar..
[21] A.E. Cetin, H. Köymen, Compression of digital biomedical signals, in: D. Joseph (Ed.), The Biomedical Engineering Handbook, second ed.,CRC Press LLC, Bronzino, Boca Raton, 2000.
[22] M. Blanco-Velasco, F. Cruz-Roldán, F. López-Ferreras, Á. Bravo-Santos, D. Martínez-Muñoz, A low computational complexity algorithm for ECG signal compression, Med. Eng. Phys. 26 (7) (2004) 553–568.
[23] N. Memon, Xuan Kong, J. Cinkler, Context-based lossless and near-lossless compression of EEG signals, IEEE Trans. Inf. Technol. Biomed. 3 (3) (1999) 231–238.
[24] N. Sriraam, Quality-on-demand compression of EEG signals for telemedicine applications using neural network predictors, Int. J. Telemed. Appl. 2011 (2011) 13.
[25] N. Sriraam, C. Eswaran, Performance evaluation of neural network and linear predictors for near-lossless compression of EEG signals, IEEE Trans. Inf. Technol. Biomed. 12 (1) (2008) 87–93.
[26] C. Bazán-Prieto, M. Blanco-Velasco, J. Cárdenas-Barrera, F. Cruz-Roldán, Retained energy-based coding for EEG signals, Med. Eng. Phys. 34 (7) (2012) 892–899.
[27] A.L. Goldberger, L.A.N. Amaral, L. Glass, J.M. Hausdorff, P.C. Ivanov, R.G. Mark, J.E. Mietus, G.B. Moody, C.-K. Peng, H.E. Stanley, PhysioBank, PhysioToolkit, and PhysioNet components of a new research resource for complex physiologic signals, Circulation 101 (23) (2000) e215–e220, Jun..
[28] J.L. Cárdenas-Barrera, J.V. Lorenzo-Ginori, E. Rodríguez-Valdivia, A wavelet-packets based algorithm for EEG signal compression, Med. Inf. Internet Med. 29 (1) (2004) 15–27.
[29] G. Higgins, B. McGinley, S. Faul, R.P. McEvoy, M. Glavin, W. Marnane, E. Jones, The effects of lossy compression on diagnostically relevant seizure information in EEG signals, IEEE Trans. Inf. Technol. Biomed. 99 (2012) 1.
[30] H. Daou, F. Labeau, Pre-processing of multi-channel EEG for improved compression performance using SPIHT, in: Proceedings of the 2012 Annual International Conference of the IEEE Engineering in Medicine and Biology Society (EMBC), 2012, pp. 2232–2235.
[31] K. Sayood, Introduction to Data Compression, third ed., MorganKaufmann, Morgan Kaufmann Publishers, 500 Sansome Street, Suite 400, San Francisco, CA 94111, 2005.
[32] A. Moffat, A. Turpin, Compression and Coding Algorithms, Springer, Kluwer Academic Publishers Group, Distribution Centre, Post Office Box 322, 3300 AH Dordrecht, The Netherlands, 2002.
[33] I. Daubechies, Ten Lectures on Wavelets, first ed., SIAM: Society for Industrial and Applied Mathematics, Society for Industrial and Applied Mathematics, 3600 Market Street, 6th Floor Philadelphia, PA 19104-2688, USA, 1992.
[34] A. Cohen, I. Daubechies, J. Feauveau, Biorthogonal bases of compactly supported wavelets, Commun. Pure Appl. Math. 45 (5) (Jun. 1992) 485–560.
[35] Zhitao Lu, Dong Youn Kim, W.A. Pearlman, Wavelet compression of ECG signals by the set partitioning in hierarchical trees algorithm, IEEE Trans. Biomed. Eng. 47 (7) (2000) 849–856.
[36] A. Said, W.A. Pearlman, A new fast and efficient image codec based on set partitioning in hierarchical trees, IEEE Trans. Circuits Syst. Video Technol. 6 (1996) 243–250.
[37] M. Pooyan, A. Taheri, M. Moazami-Goudarzi, I. Saboori, Wavelet compression of ECG signals using SPIHT algorithm, Int. J. Signal Process. 1 (3) (2004) 4.
[38] M. Raad, A. Mertins, From lossy to lossless audio coding using SPIHT, in: Proceedings of the 5th International Conference on Digital Audio Effects, 2002, pp. 245–250.
[39] J.M. Shapiro, Embedded image coding using zerotrees of wavelet coefficients, IEEE Trans. Signal Process. 41 (1993) 12.
[40] G. Higgins, S. Faul, R.P. McEvoy, B. McGinley, M. Glavin, W.P. Marnane, E. Jones, EEG Compression Using JPEG2000: How much loss is too much?', in: Proceedings of the Annual Conference of the IEEE Engineering in Medicine and Biology Society (EMBC), Buenos Aires, Argentina, 2010, vol. 2010, pp. 614–617.
[41] G. Higgins, B. McGinley, N. Walsh, M. Glavin, E. Jones, Lossy compression of EEG signals using SPIHT, Electron. Lett. 47 (18) (2011) 1017–1018.
[42] P. Welch, The use of fast Fourier transform for the estimation of power spectra: a method based on time averaging over short, modified periodograms, IEEE Trans. Audio Electroacoust. 15 (2) (1967) 70–73, Jun..
[43] Y. Zigel, A. Cohen, A. Katz, The weighted diagnostic distortion(WDD) measure for ECG signal compression, IEEE Trans. Biomed. Eng. 47 (11) (2000) 1422–1430.